A DOUBLE DWELL FREQUENCY SYNCHRONIZATION SCHEME FOR OFDM SYSTEMS

By

Nour Ali Kousa

A Thesis Presented to the Faculty of the
American University of Sharjah
College of Engineering
in Partial Fulfillment
of the Requirements
for the Degree of

Master of Science in
Electrical Engineering

Sharjah, United Arab Emirates
January 2015

Approval Signatures

We, the undersigned, approve the Master's Thesis of Nour Ali Kousa

Thesis Title: A DOUBLE DWELL FREQUENCY SYNCHRONIZATION SCHEME FOR OFDM SYSTEMS

Signature	**Date of Signature** (dd/mm/yyyy)
_____	_____
Dr. Mohamed El-Tarhuni Professor, Department of Electrical Engineering Thesis Advisor	
_____	_____
Dr. Mohmoud H. Ismail Visiting Associate Professor, Department of Electrical Engineering Thesis Committee Member	
_____	_____
Dr. Rana Ejaz Ahmed Associate Professor, Department of Computer Engineering Thesis Committee Member	
_____	_____
Dr. Naser Qaddoumi Interim Electrical Department Head	
_____	_____
Dr. Mohamed El-Tarhuni Associate Dean, College of Engineering	
_____	_____
Dr. Leland Blank Dean, College of Engineering	
_____	_____
Dr. Khaled Assaleh Director of Graduate Studies	

Acknowledgements

I would like to express my sincere appreciation and my truthful thanks to my advisor, Professor Mohamed El-Tarhuni. Without his advice and guidance this work would not have been completed. A true mentor, he remains a figure of inspiration and I feel fortunate to have completed my thesis with him. Although he was my only advisor, he was always available to assist and guide during this thesis.

I gratefully acknowledge the help and support provided by all the professors and lab instructors in the Electrical Engineering department at AUS.

Finally, I would like to thank my family and friends for all their love, support, and patience throughout my life.

To my husband, son, and daughter

You are my life

Abstract

Orthogonal Frequency Division Multiplexing (OFDM) is being used in many recent communication systems to cope with the demand for high data rate applications. It provides a significant improvement in the bandwidth efficiency with simple equalization at the receiver. ODFM systems provide high immunity against multipath fading and inter symbol interference (ISI) since the high data rate stream is divided among narrow overlapping but orthogonal subcarriers. However, OFDM requires accurate timing and frequency synchronization to preserve the orthogonality between subcarriers and maintain acceptable performance. Achieving accurate synchronization is a challenging task in multicarrier systems such as OFDM. It is noticed that frequency synchronization is more critical in OFDM than timing synchronization since a small frequency offset can destroy the orthogonality among the subcarriers causing inter-carrier interference (ICI), which results in serious performance degradation. In this thesis, the effect of frequency offset on OFDM system performance is investigated and a new synchronization scheme based on the Double Dwell System (DDS) is proposed. In DDS, the frequency offset estimation is carried over two stages: a coarse estimate is obtained over the first stage followed by a fine estimate in the second stage. The system performance is evaluated in terms of the mean square error (MSE) and symbol error rate (SER) and is compared to the conventional Single Dwell System (SDS). Simulation results show a significant performance improvement in the proposed method over SDS. Other results are presented in this thesis such as interference impact, pilot symbol design, optimization of search window and step size, and mitigation of fading effects.

Search Terms- OFDM, Synchronization, Double Dwell System, Carrier Frequency Offset, Inter Carrier Interference, Mean Square Error, and Symbol Error Rate.

Table of Contents

List of Figures

Abbreviations

AWGN	-	Additive White Gaussian Noise
CFO	-	Carrier Frequency Offset
CP	-	Cyclic Prefix
CRLB	-	Cramer Reo Lower Bound
DDS	-	Double Dwell System
DFT	-	Discrete Fourier Transform
FFT	-	Fast Fourier Transform
ICI	-	Inter Carrier Interference
IFFT	-	Inverse Fast Fourier Transform
ISI	-	Inter Symbol Interference
ML	-	Maximum likelihood
MSE	-	Mean Square Error
OFDM	-	Orthogonal Frequency Division Multiplexing
PAPR	-	Peak to Average Power Ratio
SDS	-	Single Dwell System
SER	-	Symbol Error Rate
SIR	-	Signal to Interference power Ratio
SNR	-	Signal to Noise Ratio

Chapter 1: Introduction

1.1. Orthogonal Frequency Division Multiplexing

Orthogonal Frequency Division Multiplexing (OFDM) has received significant interest in the last few years due to its major advantages over other transmission techniques. In OFDM, the total available bandwidth is divided into a number of overlapping but orthogonal subcarriers. Each subcarrier carries a smaller amount of data, which provides immunity to multipath fading and inter symbol interference (ISI) in which a frequency selective fading channel will appear as a flat fading channel. This is considered as the main advantage of OFDM systems since it results in simple equalization in the receiver while having higher data rate transmission and spectrum efficiency.

The concept of OFDM dates back to 1960s when the first OFDM system was proposed by Chang in 1966 [1]. However, due to implementation complexity, the applications of the OFDM systems were mainly limited to military communications. In 1971, Weinstein and Ebert proposed an OFDM system based on Fast Fourier Transform (FFT) and Inverse Fast Fourier Transform (IFFT) operations, which significantly reduced the implementation complexity of the system. Since then and due to the increasing demand for better bandwidth efficiency and higher data throughput, OFDM systems started to receive more attenuation and more practical research has been carried out to improve the system capabilities. OFDM became popular for practical applications in the beginning of the 1990s when the need for higher data rate mobile radio systems was of prime interest.

Because of subcarriers orthogonality, OFDM provides a significant improvement in bandwidth efficiency over classical parallel data transmission. The subcarriers in OFDM systems are overlapping resulting in almost a 50% saving in bandwidth when compared to classical FDM systems. OFDM is implemented using FFT/IFFT, which significantly simplifies the computation requirements of the process from N^2 for conventional parallel data transmission using a Discrete Fourier Transform (DFT) to $N \log_{10} N$, where N is the number of subcarriers used [2]. The time domain OFDM symbol has a special structure that includes a cyclic prefix (CP), which helps in mitigating the effect of delay spread caused by multipath fading channels. A CP of length N_g samples is added for each OFDM symbol by copying the

last N_g samples to the beginning of the symbol. Another feature that is easily exploited in OFDM is the use of adaptive modulation and coding according to the estimated channel conditions. Each subcarrier can be modulated and encoded independently to avoid transmission on subcarriers under deep fading conditions or high interference levels; resulting in significant improvement in the bit error probability, especially for fast frequency selective fading channels [3].

OFDM has emerged as an attractive technique in many recent high speed communication systems such as [4]:

- Fourth Generation Long Term Evolution (4G LTE)
- Digital Subscriber Line (DSL) and Asymmetric DSL (ADSL) modems
- Digital Audio Broadcasting (DAB) radio and Digital Video Broadcasting (DVB)
- Power line communications
- High Definition television (HDTV) broadcasting
- Wireless Networking standard (WLAN-IEEE 802.11a)
- WiMax standard (IEEE802.16)

1.2. Issues with OFDM Systems

Although OFDM is a very attractive system for mobile radio applications, it has some challenges to overcome in order to achieve optimum performance. The most challenging issue is that OFDM is very sensitive to time and frequency synchronization errors. Any frequency shift between the transmitter and the receiver results in a loss of subcarrier orthogonality leading to inter-carrier interference (ICI) and causing significant performance degradation. It has been noted that the frequency offset should not exceed 1% of the subcarrier spacing to maintain negligible Signal-to-Noise Ratio (SNR) degradation of about 0.1 dB [2].

Another issue with OFDM is that the addition of a cyclic prefix causes extra loss in the transmission efficiency since no user data is transmitted in this interval. This will reduce the actual bit rate for data transmission and hence, reduce the spectral efficiency. Normally, the CP is limited to a maximum of 25% of the OFDM symbol duration in order to minimize the loss in SNR.

Another disadvantage of the OFDM system is its large dynamic range. An OFDM signal consists of many randomly modulated signals that may be added up in phase producing a signal with large peaks, and at other times add destructively producing small peaks resulting in a large Peak-to-Average Power Ratio (PAPR). PAPR reduces the power amplifier efficiency by pushing it into saturation and increases the complexity of the analog-to-digital/digital-to-analog converter.

Phase noise is another problem associated with OFDM transmission [5]. Phase noise is a direct consequence of frequency deviation between the transmitter and the receiver oscillators. Any practical oscillators cannot generate carriers at exactly the same frequency and hence, introduces ICI. A rule of thumb for negligible SNR degradation (less than 0.1 dB) was reported in [2] where the -3 dB phase noise bandwidth had to be around 0.1% to 0.01 % of the subcarrier spacing.

1.3. Thesis Contribution

The main objectives of this thesis can be summarized as follows:

- Investigate the effect of frequency synchronization on OFDM system performance
- Design a synchronization algorithm to estimate and correct frequency offset errors
- Optimize different design parameters to enhance the system performance
- Examine the effect of the number of pilot subcarriers and the choice of the best pilot sequence that reduces the mean square error

The proposed frequency synchronization scheme is based on Double Dwell Synchronization in which a two-stage search is performed to provide an initial coarse estimate of the carrier offset followed by a much finer estimate to improve the accuracy. The proposed system is evaluated via MATLAB simulations. Simulation results shows that DDS is able to track and correct a small fractional offsets for a wide range with high accuracy and minimized complexity for both AWGN and flat fading channel conditions.

1.4. Thesis Organization

The rest of the thesis is organized as follows: Chapter 2 includes background about OFDM systems and related synchronization issues and presents some of the existing frequency synchronization schemes available in the literature. Chapter 3 presents the proposed frequency synchronization scheme and the mathematical model of the OFDM system under consideration. In Chapter 4, the performance of the proposed scheme is evaluated via simulation for AWGN, and for fading channel in Chapter 5, respectively. Chapter 6 concludes the thesis and presents suggestions for future work.

Chapter 2: Background and Literature Review

In this chapter, the basics of the OFDM system are described in Section 2.1. The channel model is presented in Section 2.2, while the choice of OFDM system design parameters like number of subcarriers, length of the cyclic prefix and modulation level per subcarrier is reviewed in Section 2.3. Section 2.4 illustrates the synchronization issues in OFDM systems and presents some of the existing frequency synchronization schemes in the literature.

2.1. OFDM Basics

The basic principle of OFDM is to divide a high data rate stream into a number of lower data rate streams sent in parallel over a number of orthogonal subcarriers. The reduction in the data rate results in longer symbol duration for each subcarrier, hence, converting a frequency selective channel into many parallel flat fading channels, which reduces the effect of ISI and enhances the BER. The separation between adjacent subcarriers should be equal to the reciprocal of the symbol duration to maintain orthogonality and avoid interferences. Figure 1 shows the overlapping spectrum in OFDM systems and Figure 2 demonstrates the improvement achieved in bandwidth efficiency in OFDM systems compared to conventional FDM schemes.

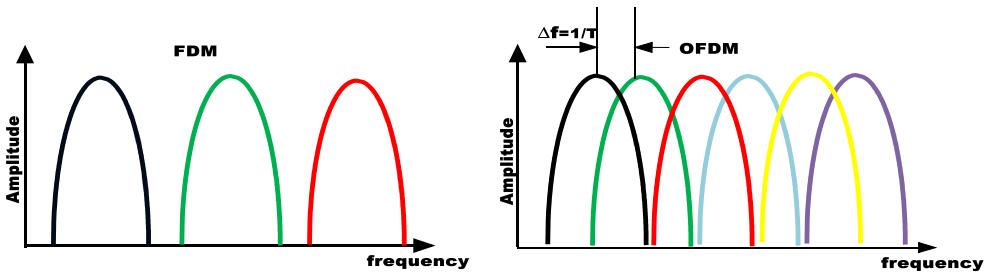

Figure 1: Overlapping Spectrum of OFDM system

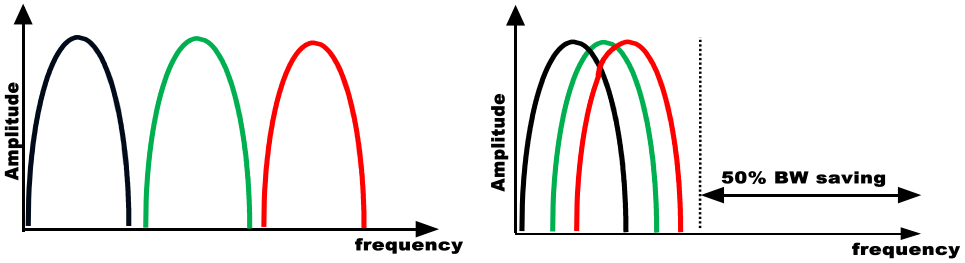

Figure 2: Comparison of FDM and OFDM Schemes

The addition of the guard time in OFDM system ensures elimination of ISI. This is implemented in OFDM by cyclically extending the symbol where the last part of each OFDM symbol is copied and added to the beginning of the symbol as shown in Figure 3. This arrangement ensures that orthogonality among subcarriers is maintained, thus preventing ICI. The length of the cyclic prefix should be longer than the expected maximum delay spread (T_{ds}) caused by the channel (i.e. $T_g > T_{ds}$).

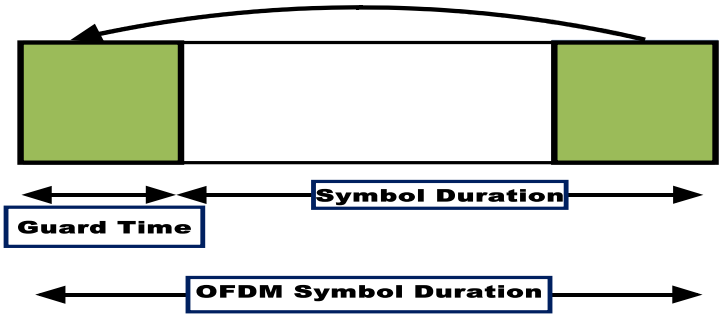

Figure 3: OFDM symbol structure

2.1.1. Orthogonality in OFDM Systems

Orthogonality among subcarriers in an OFDM system is a very important feature that differentiates OFDM from ordinary FDM systems. It prevents the subcarriers from interfering with each other although they overlap in frequency [6]. Therefore, orthogonality should always be preserved for all subcarriers at all times. For this to be achieved:

i. The subcarrier spacing Δf should equal to or multiple of the reciprocal of the symbol period T, such that $\Delta f = \frac{1}{T}$
ii. Each subcarrier contains an integer number of cycles within the symbol period (T)
iii. There is a perfect frequency synchronization between the transmitter and the receiver

Figure 4 shows an example of an OFDM signal frequency spectrum in which at the maximum of each subcarrier all other subcarriers cross zero hence, eliminating interference among adjacent subcarriers and preserving orthogonality. Figure 5 shows the inter carrier interference caused by a small frequency offset destroying the

orthogonality among adjacent subcarriers. The symbol boundaries and optimum timing instance to start detecting each symbol is of significant importance to ensure orthogonality.

The effect of the FFT window location is also important to ensure orthogonality. The FFT window should contain an integer number of cycles. However, any shift will obliterate this property causing phase rotation in the symbol location that will also destroy orthogonality.

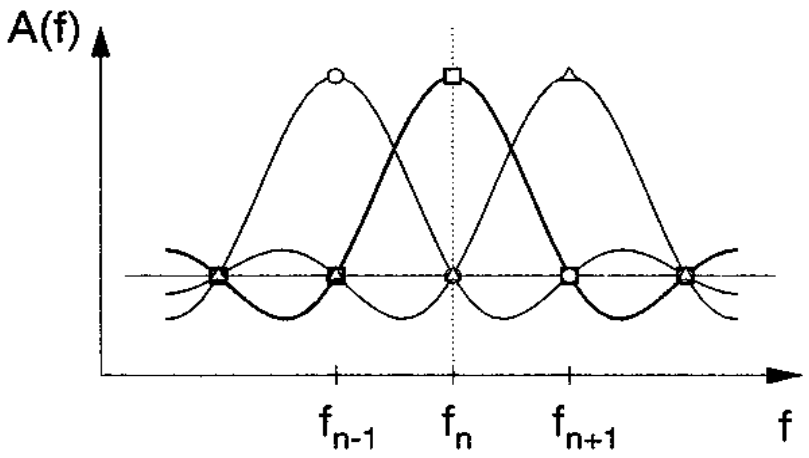

Figure 4: OFDM spectrum and orthogonality principle [7]

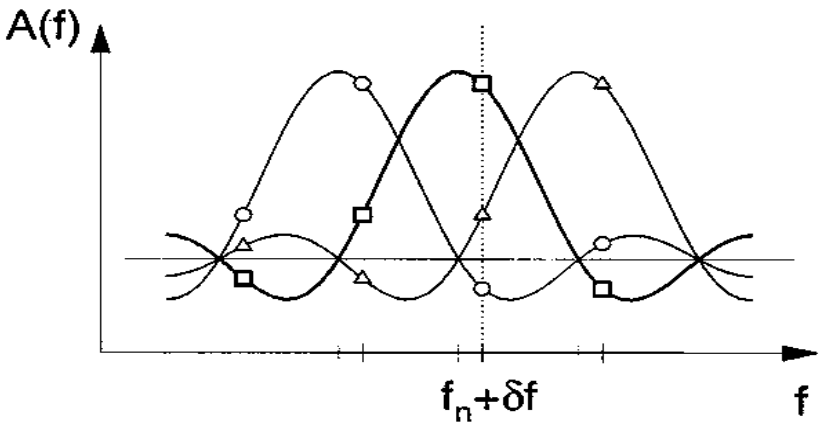

Figure 5: Effect of frequency offset in OFDM system [7]

2.1.2. Single Carrier versus Multi Carrier Modulation Scheme

Multicarrier transmission is used to overcome the effect of multipath propagation and ISI on the transmitted signal, which is a major concern in wideband single carrier transmission. In multicarrier systems, the same signal may be sent over the available number of subcarriers, which provides signal diversity or the signal is divided into a number subcarriers and each subcarrier carries different data, which enhances the spectral efficiency [8]. OFDM is a type of multicarrier systems.

In single carrier transmission, the information is sent serially over the communication channel. If the data rate is high, ISI will appear between adjacent symbols due to multipath fading causing significant degradation in the system performance. A complex linear and nonlinear equalizer is needed at the receiver side to mitigate these effects [9]. On the other hand, in multicarrier transmission, data is sent in parallel over the several subcarriers and each subcarrier carries a smaller amount of data such that the frequency response of the channel will be approximately flat over each subcarrier; this provides great immunity against ISI and multipath fading and, therefore, a simple equalizer can compensate for the channel effects. Raised cosine pulse shaping is usually required in FDM systems to reduce out of band emissions, but due to the optimal spacing between subcarriers in OFDM systems the need for such pulse shaping is relaxed [10].

Additionally, in the single carrier case, more interference will happen as the data rate increases above the coherence bandwidth of the channel ($\frac{1}{T_s} > B_c$) where T_s is the symbol time, B_c is the coherence bandwidth of the channel but for multicarrier transmission and because of the addition of the factor N (number of used subcarrier), the symbol rate of each subcarrier could be made less than the coherence bandwidth of the channel $\left(\frac{1}{N*T_s} < B_c\right)$, and hence reduces the chance for interference.

2.1.3. OFDM System Block Diagram

The general block diagram of an OFDM system is shown in Figure 6. The user data sequence, modeled as a randomly generated sequence, is modulated using one of the modulation schemes such as Quadrature Amplitude Modulation (QAM) or Phase Shift Keying (PSK). Adaptive modulation, where each subcarrier uses a different

modulation level, can be used in OFDM to improve system performance. Serial to parallel (S/P) conversion is needed to distribute the high speed data input across the subcarriers. IFFT is then performed to get the time domain signal. The signal is then converted back from parallel to serial stream and a cyclic prefix is added to the beginning of each OFDM symbol before it is up converted and transmitted over the channel. At the receiver, the opposite operations are performed with one extra block which is the synchronization circuit that is responsible for correcting any time or frequency offsets while all other blocks are performing similar functions to those at the transmitter side.

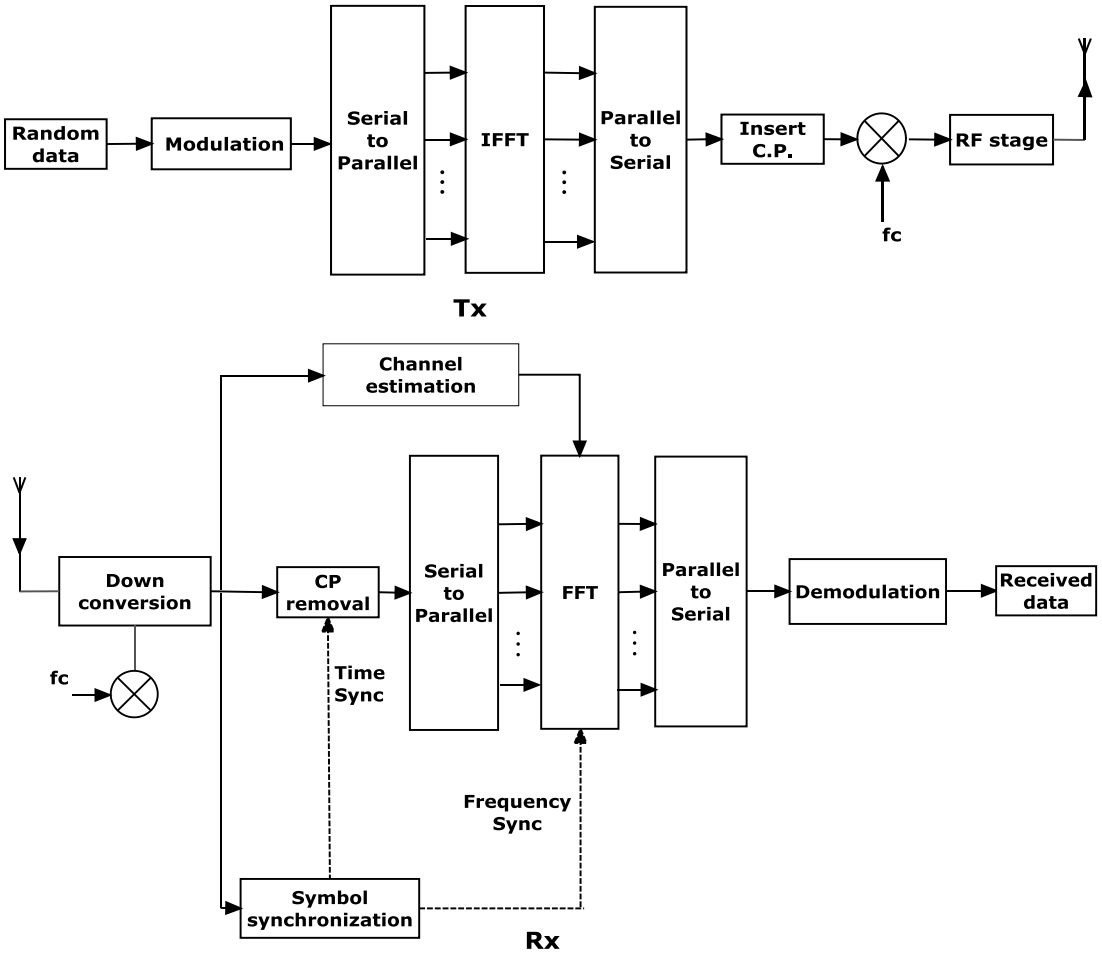

Figure 6: OFDM general block diagram

2.1.4. FFT and IFFT in OFDM Systems

The main purpose of FFT/IFFT is to transfer a function from the time domain to the frequency domain or vice versa. The length of the FFT/IFFT defines the total number of subcarriers used in the system for data transmission, pilot transmission, or null

subcarriers used for guard band implementation. For example, in IEEE 802.11 standard, the FFT/IFFT size is 64 (which indicates the total number of subcarriers in the system) out of which 48 subcarriers are utilized for data transmission, 4 are pilot subcarriers, while the remaining 12 subcarriers are not used (nulls) [11]. Different approaches for FFT/IFFT algorithms are available in the literature, but the Cooley and Tukey (CT), based on the butterfly algorithm, is the most popular algorithm that is commonly used in OFDM systems [12].

The FFT/IFFT is an efficient and fast way to compute the DFT/IDFT. In DFT/IDFT the signal is multiplied with a series of sinusoids of different frequencies. However, the efficient implantation of FFT/IFFT in OFDM systems in which duplicated terms are removed reduces the number of mathematical operations. The use of FFT in OFDM systems greatly reduces the computational requirements to $N \log_2 N$ compared to N^2 in the case of conventional DFT based systems. Considering a 32 subcarriers system, 1024 multiplications are needed using DFT, while only 160 (32×5) are needed for FFT. This difference increases as the number of subcarriers increases [11]. Figure 7 shows the simplification achieved in the system when FFT/IFFT is employed, demonstrating that the IFFT block eliminates the need for individual multipliers.

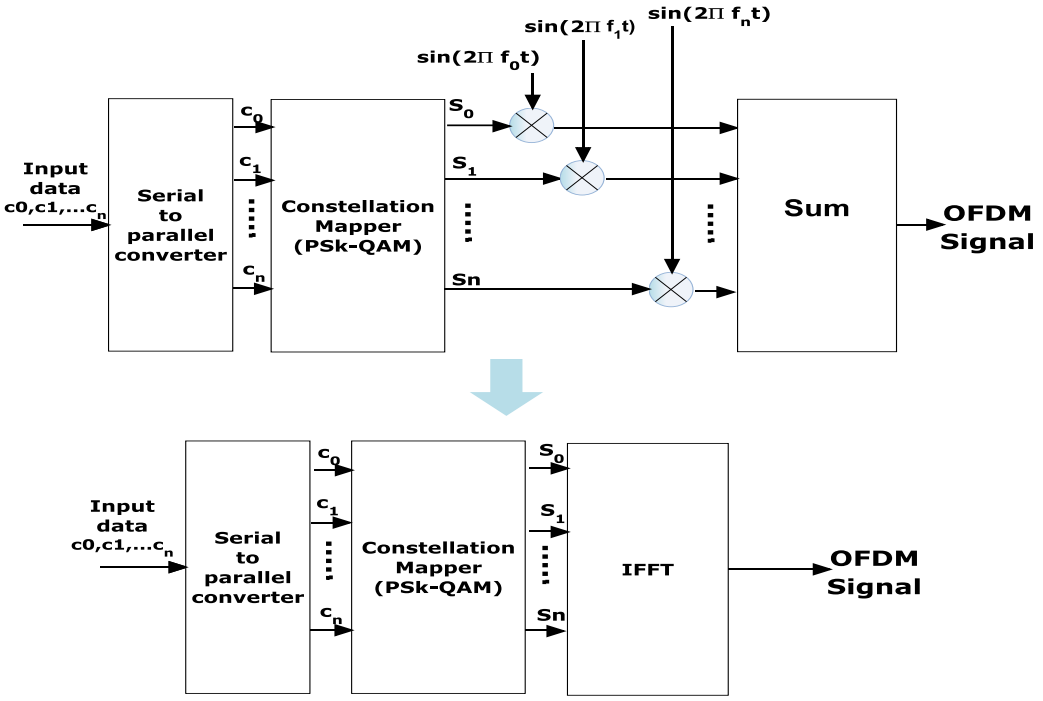

Figure 7: IFFT implantation in OFDM systems

2.2. Channel Modeling

The received signal strength is usually affected by two factors, namely multipath propagation and fading. A received signal is the summation of all the electromagnetic waves that were reflected, diffracted, or scattered due to the obstacles in the propagation environment. Those added multipath components may enhance or degrade the signal strength as they are received with different amplitudes, phases, and delays, leading to what is known as the multipath fading as shown in Figure 8. Fading causes large degradation to the received signal strength and might result in intersymbol interference (ISI).

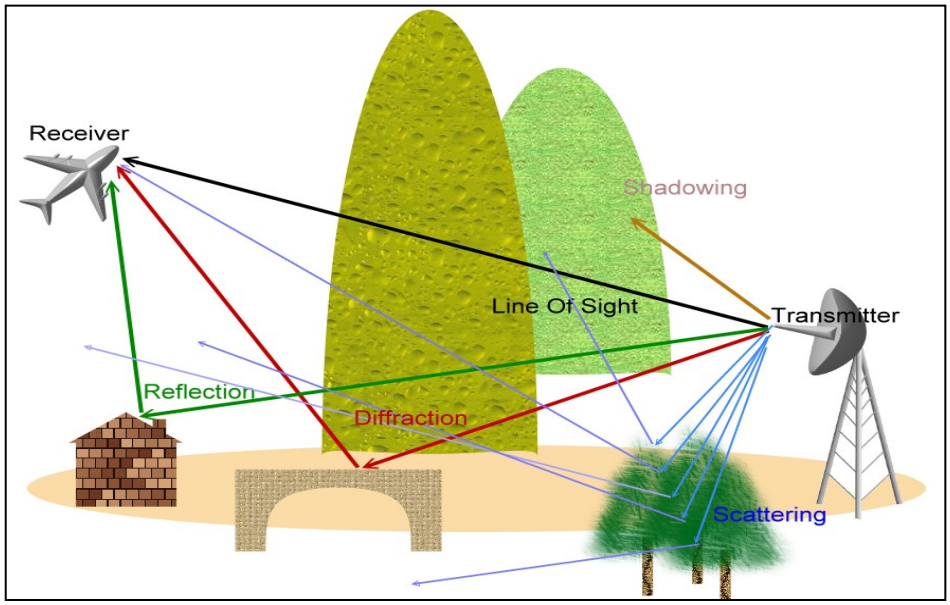

Figure 8: Multipath propagation [13]

The reflected components may enhance or degrade the received signal strength depending on whether they add constructively or destructively. Furthermore, in the case of a moving receiver and/or transmitter, the signal is greatly affected by the Doppler shifts, which results in a shift in the frequency components of the signal. The maximum Doppler frequency is determined by the mobility of the transmitter and receiver and is given by:

$$f_{dmax} = \frac{v.f_c}{c}$$

where v is the speed of the terminals in (m/s), f_c is the carrier frequency in (Hz) and c is the speed of light in (m/s).

Fading may be classified according to the channel delay spread and the symbol duration into flat fading or frequency selective fading. If the channel delay spread is greater than the symbol period, then the received signal experiences frequency selective fading channel conditions, while if the symbol period is less than the delay spread, the received signal undergoes flat fading (frequency non-selective fading) conditions. Another way is to consider the coherence bandwidth of the channel and the signal bandwidth. The received signal undergoes frequency flat fading if the signal bandwidth is less than the coherence bandwidth of the channel, whereas the received signal experiences a frequency selective fading channel condition when the signal bandwidth is greater than the coherence bandwidth of the channel.

The two most popular channel models for the received signal amplitude are Rayleigh and Rician fading. They are differentiated based on the existence or absence of the line of sight (LOS) component. In the Rician fading channel, the signal consists of the summation of reflected components and a LOS component. Meanwhile, in a Rayleigh channel, the received signal is made up of only reflected components.

Fading is commonly mitigated by means of diversity. Diversity involves the transmission of the same signal through different independent fading channels, which helps in reducing the probability of losing the signal due to deep fades and, hence, enhancing the Bit Error Rate (BER) performance. Diversity may be applied spatially, temporally, or in frequency, based on the status of the channel and the allowed bandwidth.

The main advantage of using OFDM systems is in improving the system performance under fading channel conditions. The way the data is distributed in OFDM systems ensures that the symbol duration is always much larger than the expected delay spread of the channel and thus converts a frequency selective fading channel into many parallel flat fading channels, which simplifies the receiver structure and the equalization needed [5]. In single carrier narrow band FDM systems, a single deep fade may cause entire failure of the communication link, whereas in multicarrier OFDM systems, such deep fades will only affect a small number of subcarriers as shown in Figure 9.

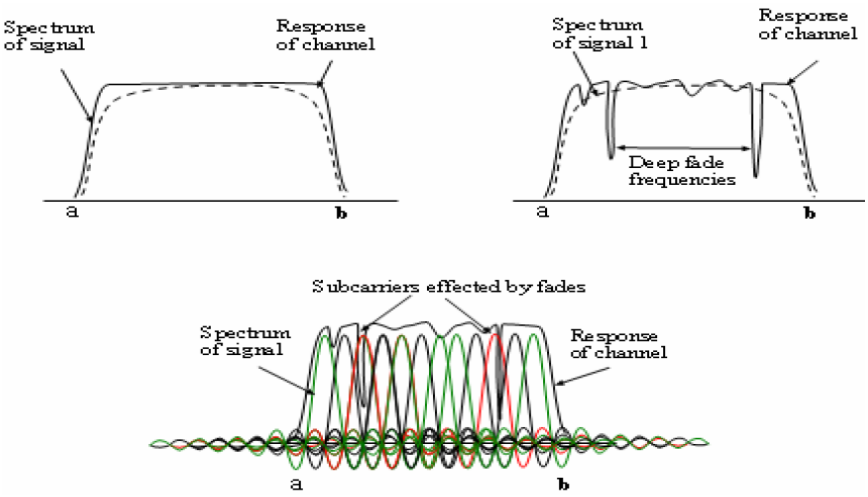

Figure 9: Fading effect in single and multicarrier systems [9]

2.3. Design Requirements for OFDM Systems

For proper design of an OFDM system, the following parameters need to be considered [14]:

i. Transmission efficiency (Bit rate)
ii. Available bandwidth
iii. Power efficiency
iv. Delay spread of the channel

The choice among these parameters involves some trade off decisions, but the following provides general guidelines for designing an OFDM system:

- **Cyclic Prefix (CP):**

To avoid ISI, the length of the cyclic prefix (guard time) should be longer than the expected maximum delay spread of the channel. As a rule of thumb, the CP length should be two to four times the expected delay spread of the channel [15] [16].

- **OFDM Symbol Duration:**

The symbol duration should be much longer than the guard time length. A practical design choice is to set the symbol duration five times (or more) longer than the guard time to avoid excessive signal-to-noise ratio (SNR) loss.

- **Number of Subcarriers:**

The number of subcarriers determines the data rate and the complexity of the system. A higher number of subcarrier implies higher implementation complexity and higher sensitivity to frequency and phase offset [17]. To ensure orthogonality among subcarriers, the subcarrier spacing should be equal to the inverse of the symbol duration. The number of subcarriers is then determined by dividing the available bandwidth by the subcarrier spacing.

- **Modulation and Coding Techniques:**

Once the transmission data rate is known, a combination of modulation and coding schemes are selected to achieve the required bit error probability. Quadrature Amplitude Modulation (QAM) is the most widely used modulation technique in OFDM systems.

2.4. Synchronization Issues in OFDM Systems

Synchronization in wireless communications systems is extremely important and is of even more importance for multicarrier systems such as OFDM. This is because in those systems the bandwidth of each sub channel is only a small fraction of the total available bandwidth, and a small synchronization error (carrier offset error) will damage the orthogonality among the subcarriers and yield a large degradation in performance [18]. Therefore, a very precise carrier frequency offset (CFO) estimator is needed in OFDM systems in order for the receiver to successfully detect the transmitted data.

Two main synchronization tasks need to be performed; namely time synchronization and frequency synchronization. In time synchronization, the symbol boundaries and the best sampling instant are determined to reduce ICI and ISI. On the other hand, frequency synchronization deals with estimation and correction of the carrier frequency offset where the receiver needs to track the frequency and the phase of the received signal with the locally generated signal at the receiver. However, because of multipath fading and interference, synchronization tasks and especially frequency synchronization become very challenging. The addition of the cyclic prefix in OFDM facilitates the timing synchronization [19] [20] as it gives the system some margin to complete the synchronization. On the other hand, a small frequency offset

may produce a large degradation in system performance. The main purpose of this thesis is to propose a new frequency synchronization algorithm and optimize different design parameters to enhance the performance of the OFDM systems.

2.4.1. Carrier Frequency Offset

Carrier frequency offset can be due to the difference between the transmitter and receiver frequencies caused by local oscillator drifts [21]. In any wireless communication system, the transmitted signal is modulated into a carrier frequency, as shown in Figure 10, to which the receiver is expected to tune such that it synchronizes with the received signal. However, the receiver frequency can never exactly match the frequency of the transmitter due to noise, instability, and frequency drifts causing frequency offset. Frequency offset can also be due to the relative motion between the communicating terminals, known as Doppler shift. The higher the Doppler frequency shift is, the more the frequency offset in the system, causing more ICI and more performance degradation. Carrier frequency offset must be much smaller than the subcarrier spacing, and because of the large number of modulated subcarriers, is extremely critical and needs extra attention. Frequency offset is usually modeled as a complex sinusoidal multiplied by the received signal [22].

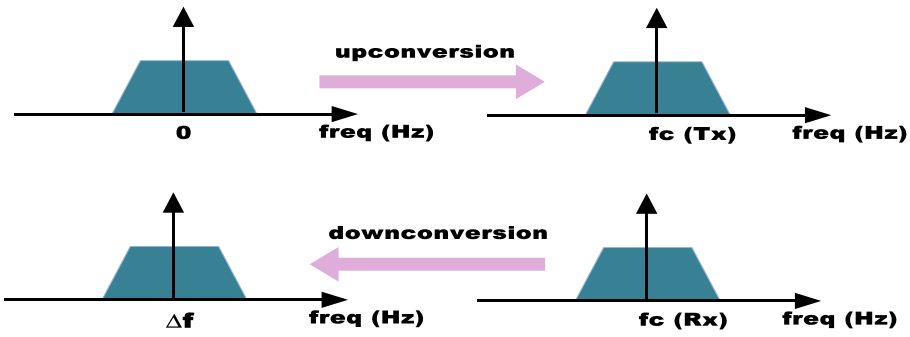

Figure 10: Baseband/pass band conversion of signal frequency

Frequency offset is commonly divided into an integer part, which is a multiple of the subcarrier spacing, and a fractional part which is less than half of the subcarrier spacing. The integer part will only cause shifts in the indices of the subcarrier without affecting their orthogonality, while the fractional part will cause signal attenuation and ICI [17] [20] [23].

A number of methods have been proposed in the literature to decrease the system sensitivity to frequency offset, such as windowing of the transmitted signal or self-cancellation schemes. However, these methods require extra overhead, which decreases the bandwidth efficiency [20] [23]. In this work, a conventional OFDM system is considered without the use of windowing or self-cancellation.

Frequency offset estimation can be divided into two main categories; namely pilot-aided or blind synchronization. In pilot-aided synchronization, a known training pattern is transmitted on a regular basis allowing the receiver to estimate the carrier frequency and correct the offset. This method provides high estimation accuracy with low computational requirements, but reduces the bandwidth efficiency. On the other hand, only the user data is transmitted in the blind synchronization schemes (also known as non-pilot aided estimation). These schemes require intensive computation to achieve an acceptable accuracy but might be a better candidate when data throughput is more critical [24]. The estimation range of blind synchronization is very narrow [25], which is the main drawback of non-pilot aided synchronization. Hence, the pilot-aided approach is the most used frequency offset estimation scheme in most of the industry standards and, hence, will be the main focus of this thesis.

In pilot-aided frequency offset estimation, the number of subcarriers used as pilots and the way they are distributed are factors that influence the estimator's computational complexity and accuracy. The distribution of the training symbols can be classified into two main categories as shown in Figure 11 [26].

A. Block-type: For a certain period, all subcarriers are used as pilots.
B. Comb-type: In each symbol, specific numbers of subcarriers are reserved for pilot transmission. A special case of the comb type is when the entire training pilots are inserted at the beginning of the symbol known as preamble.

The training pilots can be a random sequence, or specially designed sequence like m-sequence or Zadoff-Chu sequence.

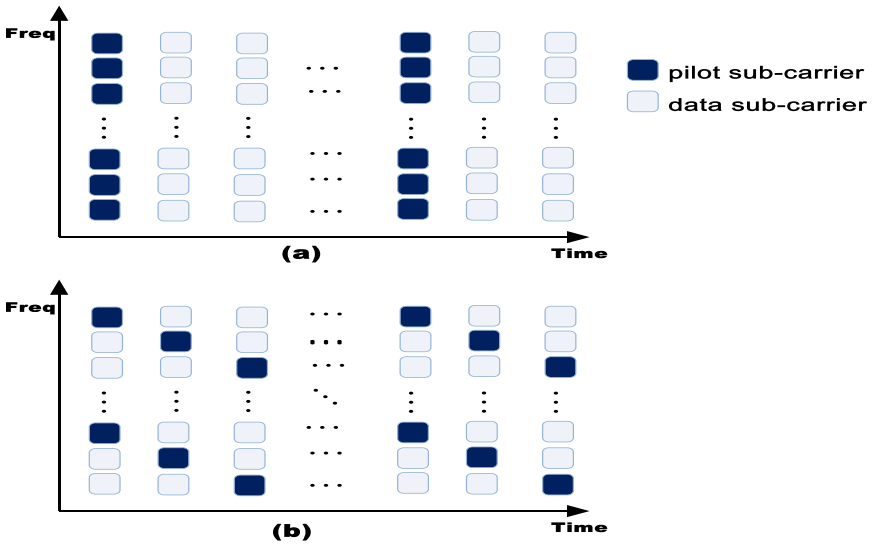

Figure 11: Carrier distribution on OFDM symbols: (a) Block type (b) Comb type

A maximum length sequence (m-sequence) is a binary sequence generated using a linear feedback shift register (LFSR) and exclusive OR (XOR) gates. It is widely used in many communication systems such as spread spectrum applications, radar technology and for many other measurement purposes because of its good auto correlation properties with minimum out of phase values.

The m-sequence can be generated by linearly combining the binary elements of the shift register to generate a longer sequence [27]. The generated sequence will have a length of $2^N - 1$, where N is the number of stages in the shift register. The initial state of the shift register can be randomly initialized but cannot be all zeros. The generated sequence is also called a pseudo noise (PN) sequence because it resembles a random noise yet can be arithmetically reproduced. For example, Figure 12 shows a 3 stages shift register used to generate an m-sequence of length 7 $(2^3 - 1)$ [28]. A variation of m-codes can be used to generate other codes with different cross and auto correlation properties like Gold sequences and Kassami sequences.

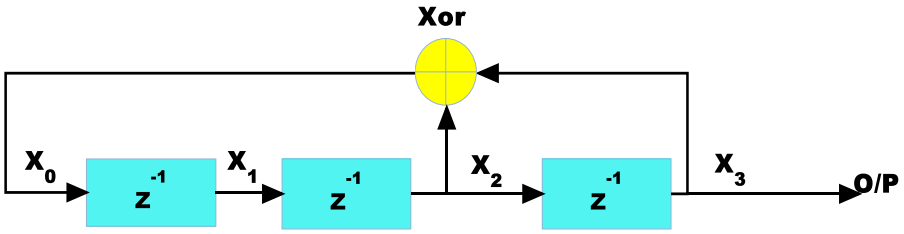

Figure 12: m-sequence generation using LFSR

The Zadoff-Chu (ZC) sequence is a complex-valued sequence with constant amplitude and zero out of phase auto correlation values (CAZAC). A ZC code has good auto and cross correlation properties, which are needed to ensure reliable communications, and establish timing synchronization [29]. The low cross correlations property of ZC reduces inter cell interference. ZC is used in many applications in LTE systems such as the primary synchronization sequence, uplink reference signal, and random access channel [30].

2.4.2. Pilot-Aided Synchronization Methods

In this section, we will discuss different carrier frequency offset estimation methods proposed in the literature. The focus will be on pilot-aided methods as it is mostly implemented in many standards; yet, some blind synchronization estimation methods are briefly discussed.

A maximum likelihood (ML) CFO estimator based on sending two identical training symbols is presented in [31]. By comparing the phase of the repeated symbols at the receiver side, the carrier frequency offset can be estimated since any phase difference will be due to carrier offset only. The estimation range is limited to half of the subcarrier spacing, but an acquisition solution was developed to widen the estimation range to more than half of the subcarrier spacing in which the training pilots are given a shorter period and the subcarriers are separated by a larger value.

In [32], the Schmidle and Cox Algorithm (SCA) is presented. It uses two training symbols. The first training symbol has two identical parts in time domain that contain pilots at even subcarriers and nulls at odd subcarriers and is used for symbol timing and initial frequency offset estimation of less than half of the subcarrier offset. The other symbol contains a pseudo noise sequence and is added to enhance the frequency estimation and to widen the estimation range.

In [33], Morelli and Mengali (M&M) presented an improved frequency offset estimator, which is an extension of the SCA algorithm (ESCA). It uses one training symbol only (rather than two as in SCA). This training symbol has $L > 2$ identical parts and the estimation of the frequency offset is done by observing the identical parts of the training symbol. The training symbols are generated from a PN sequence at frequencies multiple of L/T, and zero on the rest. The Best Linear Unbiased

Estimator (BLUE) is then used for frequency estimation. The estimation range can extend to $L/2$ of the subcarrier spacing with improved accuracy. Another similar method based on the BLUE principle is proposed in [34]. This method uses the same training symbol as the M&M method but with a different approximation method for calculating the covariance matrix.

A comparison between the SCA scheme [32] and the M&M scheme [33] is presented in [35] along with a modification of the SCA algorithm and a least square (LS) frequency offset estimation scheme. The modified SCA algorithm requires one training symbol only with less computational requirements. The LS estimation is done by estimating the slope of the phase angle of the received training sequence. The sensitivity to quantization of the arg function (argument of the complex number) is presented and quantified for the three algorithms (LS, M&M, and SCA). The authors prove that the LS algorithm is least affected by such errors (quantization errors).

Frequency offset estimation using one training symbol is proposed in [36], where offset estimation is performed using null subcarriers in all odd subcarriers and a specially designed sequence, such as almost perfect autocorrelation sequence or the modified m-sequence, is transmitted on even subcarriers. The odd subcarriers are used for fractional offset estimation and the even subcarriers are used for integer frequency offset estimation. It is shown that an estimation range proportional to the inverse of the sampling duration can be attained.

In [37], a maximum likelihood frequency estimator is introduced in which the received signal is correlated with a set of sinusoids that are generated at the receiver side to maximize the correlation output. It is shown that the choice of the number of searched offsets (k) can affect the computations needed, where a larger value of k involves more computational operations. The spacing between the searching frequencies is also investigated showing that large spacing may reduce the accuracy of the estimator, whereas a smaller value may reduce the estimation range. Hence there is a tradeoff between the needed accuracy and the required estimation range.

Two methods for estimating the integer CFO based on the ML approach are presented in [38] and [39], where the fractional offset is assumed to be known. In [38], a joint estimate of the integer CFO and channel impulse response (CIR) is achieved under Rayleigh fading channel conditions. Pilot subcarriers are used for CIR

estimation from which the integer CFO is estimated. On the other hand, in [39] the estimation is achieved based on correlating two consecutive OFDM symbols in the frequency domain. The authors consider estimation of CFO based on transmission of known pilot subcarriers or using the user data only without adding pilots. An approximation of the ML is also derived for the AWGN channel to reduce the estimation complexity.

The work presented in [40] discusses the design of a preamble made up of j repetitive slots for CFO estimation in OFDM symbols. The objective of this work is to optimize the preamble design (the number of repetitive slots) under different channel conditions using the Cramer Rao Bound. The authors show that the acquisition range increases with j and is given by $(-{}^{j}/_{2}\ ,\ {}^{j}/_{2})$.

A simple FFT-based estimation method is proposed in [25] using one training symbol. The estimation is performed in two steps, where coarse and fine searches are performed; the actual frequency offset is the sum of the two values obtained in the two searches. The results are evaluated in terms of MSE and are compared with the method in [32].

Another method for CFO estimation in frequency domain assuming perfect timing synchronization is suggested in [41]. The estimation is done by observing the pilot subcarrier frequencies at the transmitter and the receiver where any shift in the received pilot frequencies will be caused by the CFO. It is proposed to separately estimate the frequency of each subcarrier and combine all the results by calculating the mean value. The estimation is again divided into two stages, where the coarse estimate is obtained from the DFT calculation to bring the offset to within half of the subcarrier spacing, followed by the fine estimate to iteratively estimate the remaining fractional offset.

A joint timing and frequency synchronization algorithm using training symbols with special phase rotational relationship is presented in [42]. The training symbols do not have time domain repeatability, as in all the previously discussed methods, but rather a training symbol with a special phase rotation is used. The derivation of this algorithm is based on the assumption that adjacent channels

experience the same fading, which affects the accuracy of this method in frequency selective fading channels.

Another method for joint timing and frequency synchronization algorithm in OFDM is presented in [43] considering AWGN and then extended to multipath fading in [44]. A single symbol preamble that is divided into two identical parts composed of m-sequences is utilized. The correlation is performed in two stages. In the first stage, a coarse estimate is performed using sliding correlation over the whole OFDM symbol, in this step a plateau is obtained indicating the start of the frame giving an initial estimate of the frequency offset. The next correlation stage is performed over a smaller interval around the obtained plateau. However, to get the training symbol length as that of the actual data symbol, a cyclic prefix with a different number of samples is added to the training symbols, which may complicate the process of recovering the original data and removing the cyclic prefix at the receiver.

The work in this thesis is an extension to the work in [45], to allow for using any pilot signal structure as opposed to the pilot signal used in [45], which was restricted to be a sinusoidal signal. Furthermore, we optimize the correlation window for the first and second stages of the algorithm in order to find the best combination for minimizing the MSE. The impact of interference and the design of the pilot symbols are also addressed in this thesis.

2.4.3. Blind Synchronization Methods

Blind synchronization usually depends on the structure of the OFDM symbol where the cyclic prefix is used to determine the frequency offset. Other methods are also available in the literature. In this section, brief descriptions of some blind synchronization schemes are provided.

The cyclic prefix inserted at the beginning of each OFDM symbol contains a copy of the last part of the symbol. Hence, the timing offset can be estimated by correlating each symbol with a delayed version. Then the frequency offset can be estimated from the phase of the maximum correlation by dividing this phase over $(2\pi T)$. A maximum offset of half the subcarrier spacing can be estimated by this method [2]. Another approach for joint time and frequency synchronization based on a maximum likelihood estimator using the cyclic prefix is suggested in [22]. In [46] a CP is used for the OFDM system under a time variant long echo fading channel.

Blind synchronization using null subcarriers at distinct spacing is presented in [47]. A cost function is derived by placing the null subcarrier at specific frequencies, and the minimum of this cost function gives a direct estimate of the CFO.

In [48], the CFO is estimated in two stages where the integer part of the offset is first obtained and corrected, followed by a fine search for fractional offset estimation. The performance is compared with the derived Cramer-Rao Lower Bound (CRLB). The estimation is done with the aid of null subcarriers at specific locations determined based on modified Fibonacci series.

In [19], a joint symbol timing and frequency offset estimation is proposed by measuring the interference at the output of the FFT block when timing or frequency offset exists since any offset will destroy the orthogonality between subcarriers leading to more interference. The idea is to compare the output of the FFT in case of offset occurrence with the ideal case when the offset is zero. A cost function is to be minimized with respect to both the symbol time and the frequency offset leading to a joint estimate for time and frequency errors. A two dimensional search is applied, which complicates the searching process.

Chapter 3: Mathematical Model and Proposed Scheme

Frequency synchronization is one of the most challenging issues in OFDM systems. Accurate frequency estimation is a critical task that needs to be accurately achieved to ensure reliable communication. In this chapter, the mathematical model of the OFDM system under consideration is first presented, followed by the proposed frequency synchronization scheme. The effect of different design parameters is investigated to optimize the estimation.

3.1. Mathematical Model

As mentioned earlier, the user data is first converted from serial to parallel and applied to a digital modulator block (e.g., QAM). Let the output of the modulator be the data sequence $\{C_0,C_1,C_2,\dots C_{N-1}\}$ where N is the total number of subcarriers. The OFDM transmitted signal after performing the IFFT is given by:

$$c_n = \frac{1}{N}\sum_{k=0}^{N-1} C_k \, e^{j2\pi kn/N} \,, \tag{1}$$

where $n = 0,1,\dots,N-1$ represents the sample number.

A cyclic prefix (CP) of length N_g is then added for each OFDM symbol by copying the last N_g samples of the IFFT block output to the beginning of the OFDM symbol to form $\{C_{N-N_g-1}, C_{N-N_g},\cdots, C_{N-1}, C_0,C_1,C_2,\dots C_{N-1}\}$. The length of the CP is chosen to be longer than the maximum expected delay spread of the channel in order to mitigate the effect of multipath propagation. Thus, the total length of the transmitted signal is $N_T = N + N_g$ samples.

The general model for a dispersive radio channel can be expressed as:

$$h(t) = \sum_{j=1}^{L} \alpha_j(t).\delta(t-\tau_j) \,, \tag{2}$$

where $\alpha_j(t)$ is the path gain, τ_j is the j^{th} path delay, and L is the total number of multipath components.

Frequency offset is introduced to the received signal and it is modeled as a complex sinusoid. Thus, the OFDM signal after passing through the communication channel is given by:

$$r_n = h_n * (c_n \; e^{\mathrm{j}2\pi\frac{\varepsilon n}{N_T}}) + w_n \tag{3}$$

with $n = 0,1,\ldots,N_T - 1$ and ε is the normalized frequency offset such that $\varepsilon = \frac{\Delta f_\varepsilon}{\Delta f}$ where Δf_ε is the frequency offset in Hz and Δf is the subcarrier spacing defined as $\Delta f = \frac{1}{T}$, h_n is the channel impulse response, w_n is the Additive White Gaussian Noise (AWGN) with zero-mean and variance σ^2, and "$*$" is the convolution operation.

An estimate of the frequency offset $\hat{\varepsilon}$ is first obtained as will be discussed in the following section. Then, the estimated value is used for offset correction by multiplying the received signal with the complex conjugate of the introduced sinusoids as follows:

$$v_n = r_n.\; e^{-\mathrm{j}2\pi\hat{\varepsilon}n/N_T} \;\; , \; n = 0,1,\cdots N_T \, , \tag{4}$$

Next, the cyclic prefix is removed after the serial to parallel conversion. The FFT is then performed to get the frequency domain sequence. Channel correction for the fading channel is performed in the frequency domain by dividing by the channel path gains (α). The signal is then passed to the demodulator block to recover the original sequence.

3.2. Proposed Double Dwell Frequency Synchronization Scheme

The proposed frequency offset synchronization is based on the Double Dwell System (DDS), where the frequency estimation is carried over two stages as shown in Figure 13.

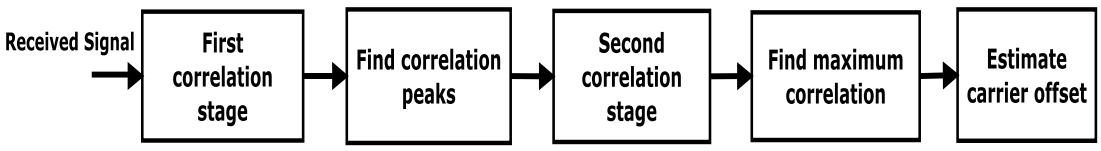

Figure 13: Block diagram of the proposed scheme

In the first stage, a coarse search over the range of possible offsets is performed to get an initial rough estimate of the offset. Searching is conducted over a large range of offsets, ε_{r1}, with a large step size in order to quickly scan the uncertainty range. Defining the number of performed correlations as N_1 and the normalized searching range as ε_{r1}, then the step size (β_1) for searching of the first stage correlations can be calculated using:

$$\beta_1 = \frac{2\,\varepsilon_{r1}}{N_1}, \tag{5}$$

The results of the first stage are then used to perform a second search with a smaller step size (fine search) over a much smaller range determined as the frequency offsets between the two highest correlation peaks obtained in the first stage. A sample of the correlation function obtained from the first stage is shown in Figure 14, where the actual normalized offset was set to 1.35 and the correlation was done over a normalized frequency offset range of 5 at a step size of 0.2. The highest peak, which represents the first stage estimate of the offset is observed at an offset of 1.4 and the two adjacent peaks are observed at 1.2 and 1.6. Since the correlation value at 1.2 is found to be higher than the correlation value at 1.6, the second stage search will be performed between 1.2 and 1.4 offsets using a much smaller step over a much smaller range of 0.2 (difference between 1.4 and 1.2).

In extreme cases where the correlation peak is located at the edge of the estimation range, the second searching stage will be specified by the peak and the adjacent value as shown in Figure 15 for an offset value of 2 where the second stage correlation will be performed between 1.8 and 2.

The first correlation stage is performed by multiplying the received signal with a reference complex exponential for every possible offset ε_i within that search range ε_{r1} and averaging over N_T samples to get:

$$R_i = \frac{1}{N_T}\left|\sum_{n=0}^{N_T-1} r_n x_n^*\, \zeta_i\right|, \tag{7}$$

where $i = 1,2,\ldots N_1$ and x_n^* is the complex conjugate of the known pilot data used at the n^{th} subcarrier at the transmitter and ζ_i is defined as $(e^{-j2\pi\varepsilon_i\frac{n}{N_T}})$,details about

pilots symbol design will be provided in section 5.5. The maximum of the magnitude of the correlation function is obtained as follows:

$$R_{im} = \max(R_i), \quad i = 1,2,\cdots,N_1 \tag{7}$$

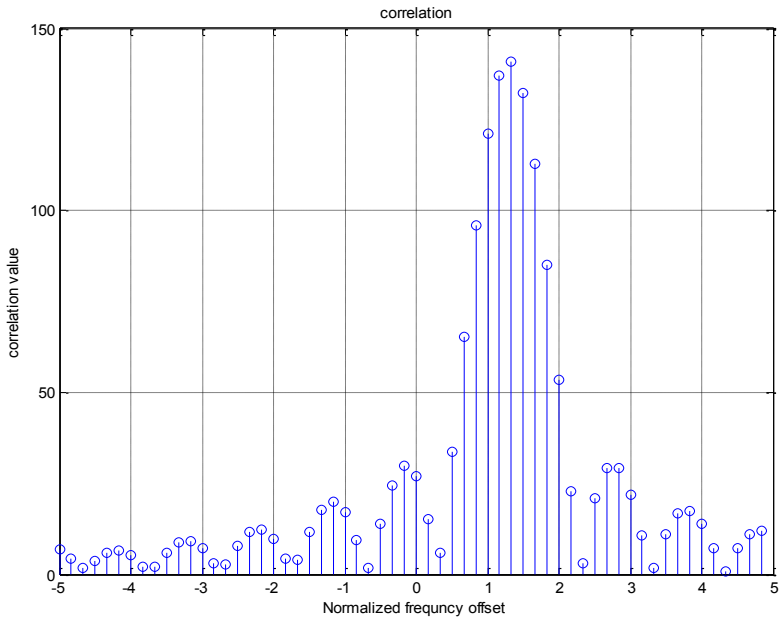

Figure 14: Sample of the first stage correlation function

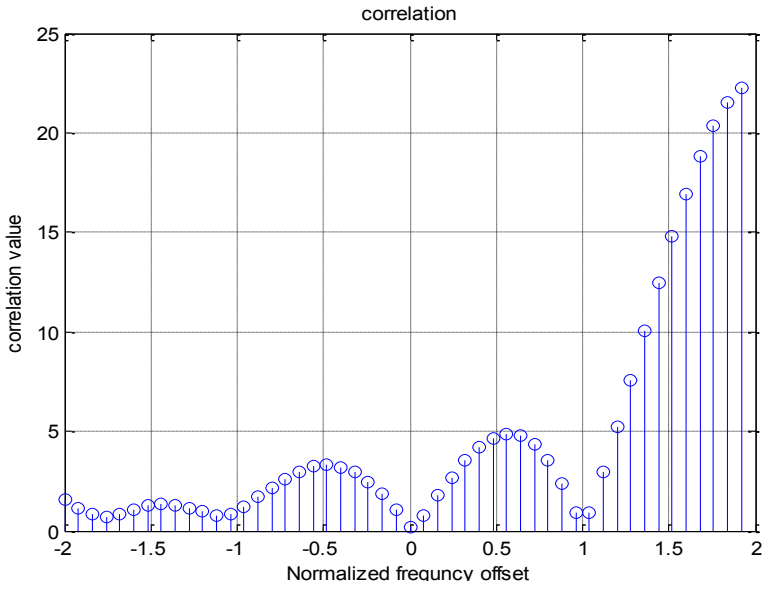

Figure 15: Example of the correlation function in extreme cases

After identifying the maximum value, the index of the first stage offset is obtained from which the adjacent peaks are compared to start the second searching stage. The procedure for CFO estimation can be illustrated as shown in Figure 16.

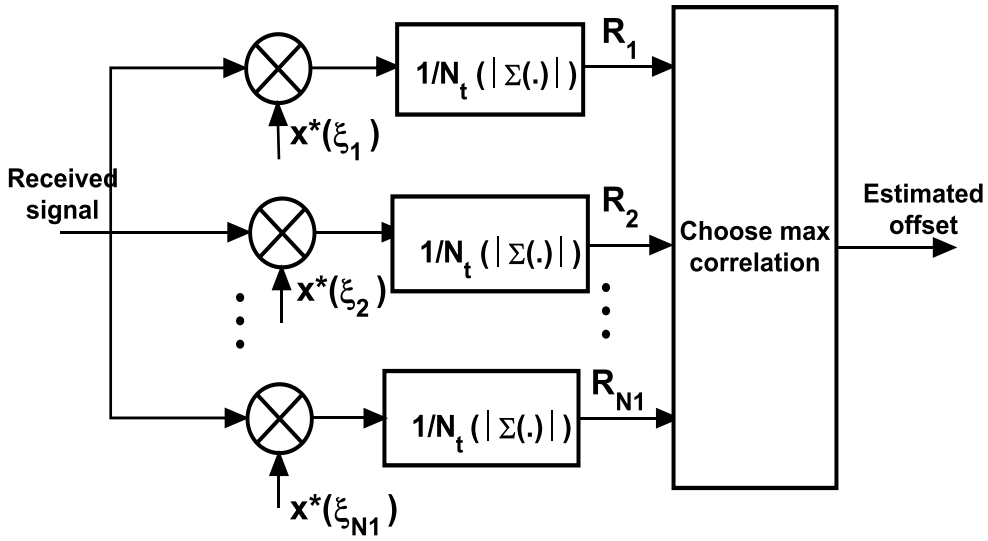

Figure 16: First stage correlation for frequency estimation

To improve the reliability of identifying the location of the correlation peaks at the first stage, the correlation results for each offset are averaged over a number of OFDM symbols (Q times), to obtain:

$$R_{ia} = \frac{1}{Q}\sum_{q=1}^{Q}|R_i(q)|\,, \tag{8}$$

Averaging is more important for the fading channels as it helps to reduce the effect of deep fades and improve the estimation accuracy. Figure 17 shows the proposed scheme for fading channel. Note that the averaging will also be beneficial in AWGN since it results in more reduction of the noise variance.

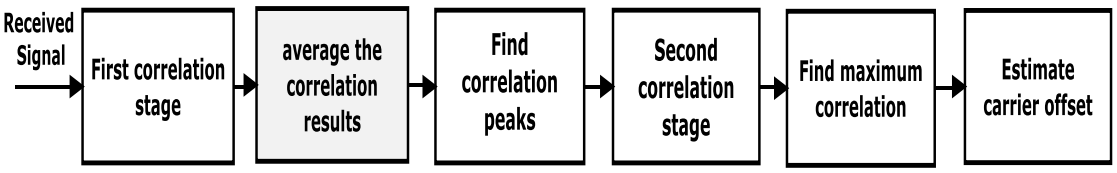

Figure 17: Block diagram of proposed scheme in fading channel

The second correlation stage is done using an expression similar to (6). However, the range of the second stage $\boldsymbol{\varepsilon_{r2}}$, will be specified by the maximum two peaks found on the first correlation stage and is limited to $\boldsymbol{\beta_1}$(The spacing between

the offsets in the first stage). The number of offsets searched during the second stage is N_2 searched at a smaller step size β_2 which can be calculated using:

$$\beta_2 = \frac{\varepsilon_{r2}}{N_2} \tag{9}$$

where $\varepsilon_{r2} = \beta_1$, which is the spacing between the correlation peaks from the first search stage

As a result, the second search stage will be more focused and hence, provides more accurate estimation. Note that the total number of performed correlations $N_{tot} = N_1 + N_2$. It is important to remark that for conventional Single Dwell System (SDS) N_{tot} correlations are performed using a fixed step size, while for the proposed Double Dwell System (DDS), N_{tot} correlations are also performed but over two stages with two different step sizes. Thus, the proposed DDS has the same complexity as that of the SDS but with higher accuracy.

Carrier offset correction is done based on the final offset estimate ($\hat{\varepsilon}$) obtained from the location of the peak correlation from the second stage. The corrected signal is then processed to demodulate the transmitted data.

The carrier offset estimator performance is evaluated by computing the Mean Square Error (MSE) between the estimated offset and the actual offset over N_c simulation runs as follows:

$$MSE = \frac{1}{N_c}\sum_{m=0}^{N_c-1}[\hat{\varepsilon}(m) - \varepsilon]^2 \tag{10}$$

where $\hat{\varepsilon}(m)$ represents the estimated offset during the m^{th} simulation run. The accuracy of the proposed carrier offset estimator is affected by a number of parameters such as the number of subcarriers used, the total number of performed correlations (M), the number of performed correlation in each stage (M_1 and M_2), Estimation range (ER), and the averaging window (Q). The effect of each of these parameters is investigated through simulations and the results for AWGN and fading channel are presented in Chapter 4 and Chapter 5, respectively.

Chapter 4: Performance Evaluation of Proposed Double-Dwell Scheme in AWGN

In this chapter, a detailed evaluation of the DDS performance using extensive Matlab simulations is presented. The performance is evaluated under AWGN channel conditions and compared to the conventional SDS. Simulations are performed in different steps as follows:

i. Simulating the basic OFDM system blocks with no frequency offset.
ii. Performance of OFDM system in the presence of frequency offset.
iii. Frequency synchronization using a conventional Single Dwell System.
iv. Frequency synchronization using the proposed Double Dwell System.

Simulations are performed using Binary phase shift keying (BPSK) as the modulation scheme. The length of the IFFT/FFT defines the total number of subcarriers in the system, which is initially set to 32 (other values are also examined). A cyclic prefix duration equals 10% of the OFDM symbol duration is used. An AWGN channel model is used in these simulations with the signal-to-noise ratio (SNR) varying from 0 to 10 dB and simulations are repeated 1000 times for each SNR value. The effect of all simulation parameters is investigated to optimize system performance and show the gain achieved using the DDS.

4.1. Simulating the Basic OFDM System Blocks

Simulations are first done to implement the basic OFDM system blocks, to investigate the function of each block, and to study the overall system operation assuming perfect synchronization. The transmitter is simulated by passing the randomly generated sequence to the modulator, converting the serial stream to parallel, applying IFFT, and adding the cyclic prefix. A sample of the generated OFDM transmitted time-domain signal is shown in Figure 18. The symbol error rate (SER) is evaluated as a function of the SNR as shown in Figure 19. The results show a perfect match between simulated and theoretical SER, which is the same as BER for BPSK, indicating the accuracy of the simulation model.

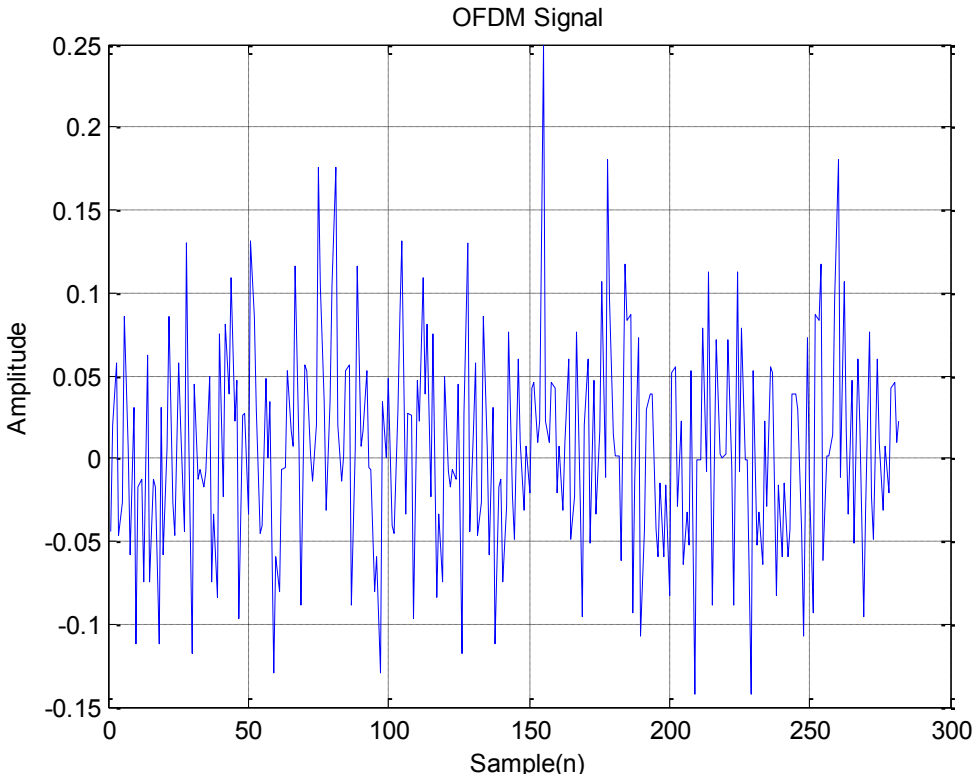

Figure 18: Example of an OFDM signal

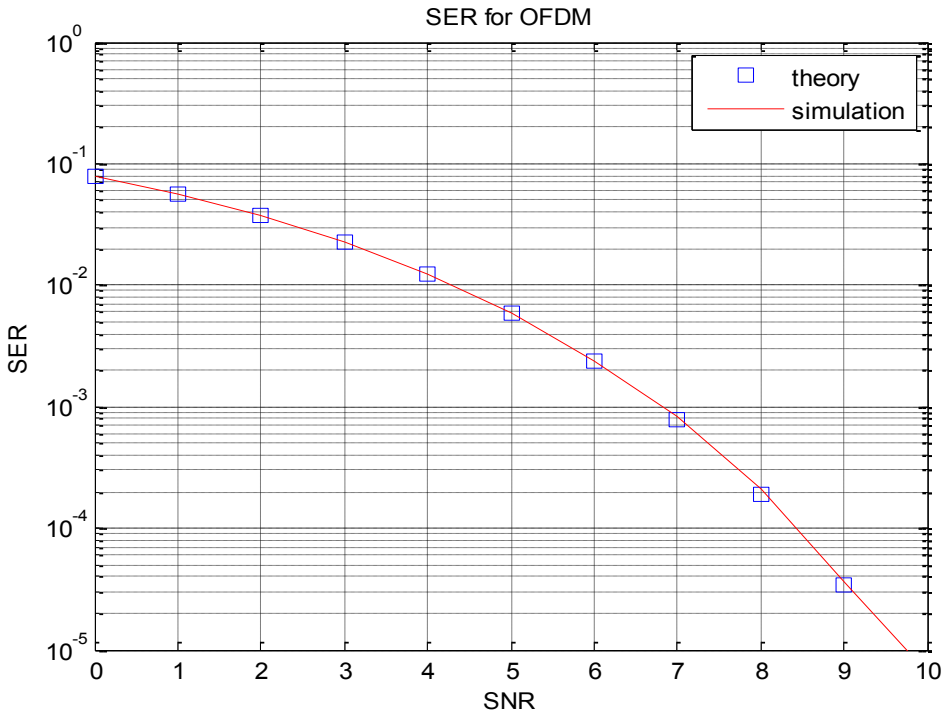

Figure 19: Comparison of simulated and theoretical SER with perfect synchronization

4.2. OFDM Performance in Presence of Frequency Offset

To demonstrate the impact of frequency synchronization errors, a frequency offset is introduced at the received signal without any correction at the receiver side. Figure 20 shows the SER performance for different offset values. It is clear that the larger the frequency offset the higher the SER degradation. For example, to achieve a SER of (10^{-4}), 9 dB of SNR is needed at zero frequency offset, while 16 dB is needed to achieve the same SER for a normalized offset value of 0.2. Hence, about 8 dB more is needed and the degradation is even higher for higher offset values. The system will be totally useless (50% SER) for a normalized offset greater than $\pm$ 0.3. Thus, accurate estimation and correction of frequency errors is essential to avoid such losses and maintain acceptable performance.

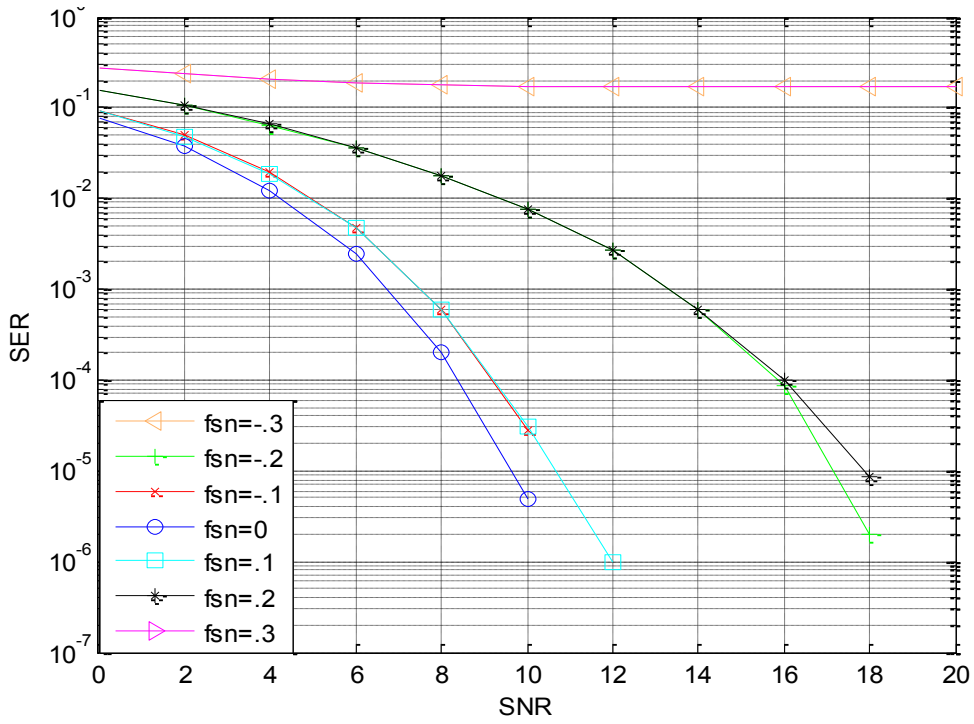

Figure 20: Impact of frequency offset error on symbol error rate

The SER performance is also evaluated with respect to the normalized frequency offset for different SNR values as shown in Figure 21. It is noticed that higher SNR values are required to compensate for higher offset values to get the same SER performance.

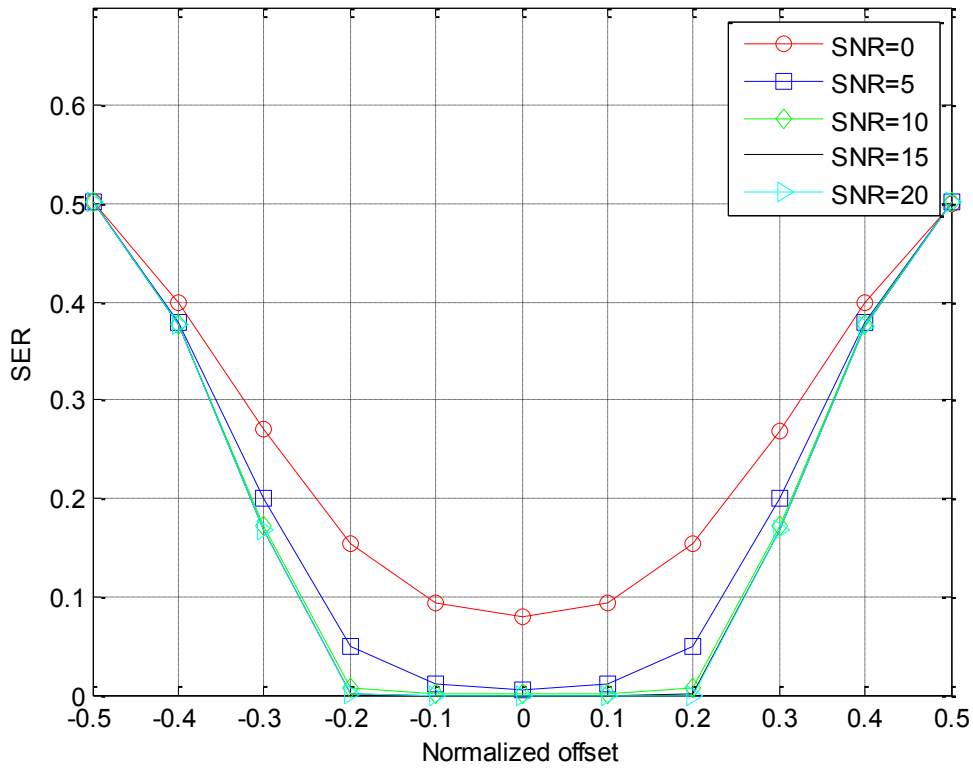

Figure 21: SER vs. normalized offset for different SNR values

4.3. Frequency Synchronization

Frequency offset synchronization is performed for OFDM to compensate for the introduced offset. The synchronization is based on comparing both the introduced offset with a range of offsets at the receiver using a simple correlator with known training patterns sent over all subcarriers. The estimated offset value is used to correct and compensate for the introduced offset. The difference between the introduced and the estimated offsets is used to evaluate the mean-square error (MSE) for a range of SNR for both SDS and DDS.

Simulations are performed with the experiment repeated 1000 times for each SNR value. The experiments are repeated for both the SDS and DDS to evaluate their performance using different testing parameters such as total number of subcarriers, required estimation ranges, and total number of performed searches. The effect of each parameter is studied to show its impact on the estimation accuracy.

4.3.1. Single Dwell System (SDS)

In SDS, a fixed step size is used to search a range of frequency offsets. The received signal is correlated with each possible offset over a number of samples equals the FFT size (32 samples). The offset that results in the maximum magnitude at the correlator output is used as the frequency offset estimate. Figure 22 shows the MSE for SDS under AWGN conditions, where the actual normalized offset is set to 0.15. It is noticed that the MSE decreases as the SNR increases but will reach a constant value after which the estimation accuracy does not improve even when SNR is very large. This is because the SDS uses a fixed step size. The correlation function for a search range from -10 to $+10$ is shown in Figure 23 when the actual normalized offset value is 0.15. It is clear that the peak of the correlation function is located close to the desired value. The SER for an OFDM system using BPSK when using the actual and the estimated offsets is shown in Figure 24. It is clear that the performance did not degrade since the offset is being corrected by the SDS.

Simulations are then run to study the impact of the number of subcarriers used on the system as shown in Figure 25. The MSE is simulated for 64, 128, and 256 subcarriers. It is noticed that with a smaller number of subcarriers, larger SNR values are needed to achieve the same MSE. For instance, to achieve MSE of (10^{-4}), the required SNR is 5.5 dB for 256 subcarriers while 8.5 dB is needed when the number of subcarriers is reduced to 128, and even higher SNR value is required when the number of subcarriers is reduced to 64. This is expected since increasing the number of subcarrier means increasing the correlation period and giving the system more time to improve the estimation accuracy. Figure 26 illustrates the SER performance for the different cases and it is noticed that there is no major difference in performance for different number of subcarriers.

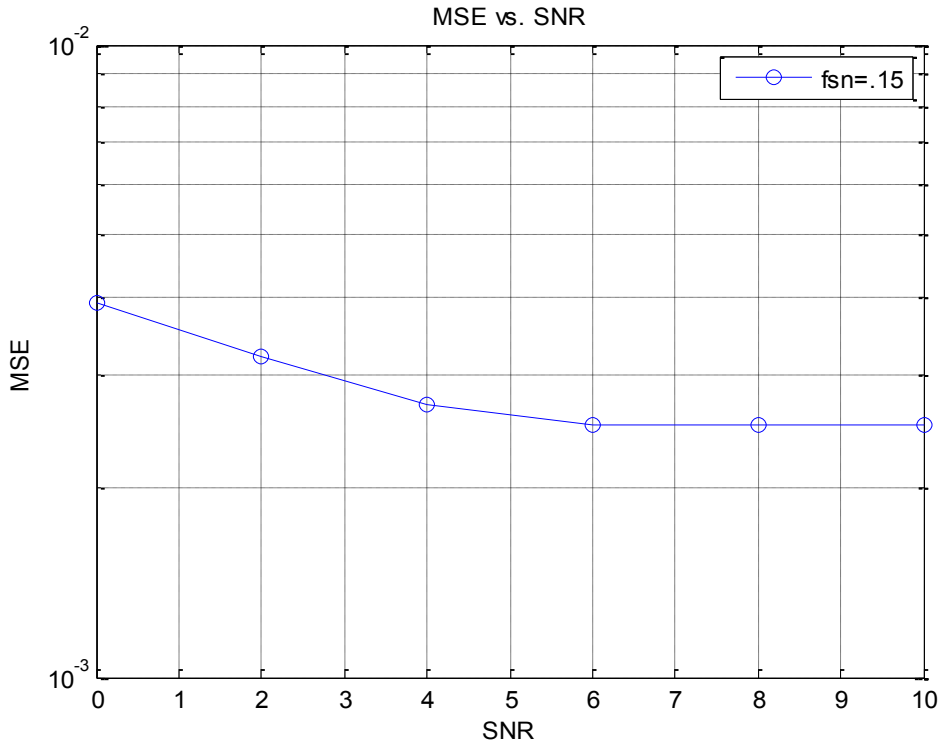

Figure 22: MSE Performance for SDS in AWGN

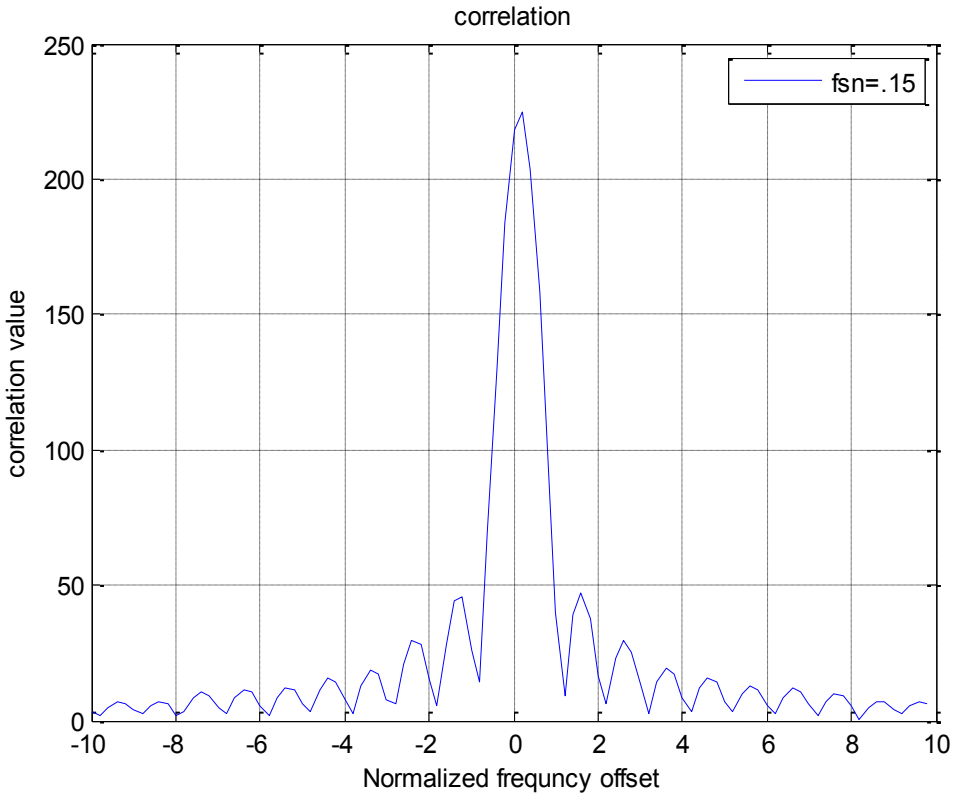

Figure 23: Correlation output of SDS

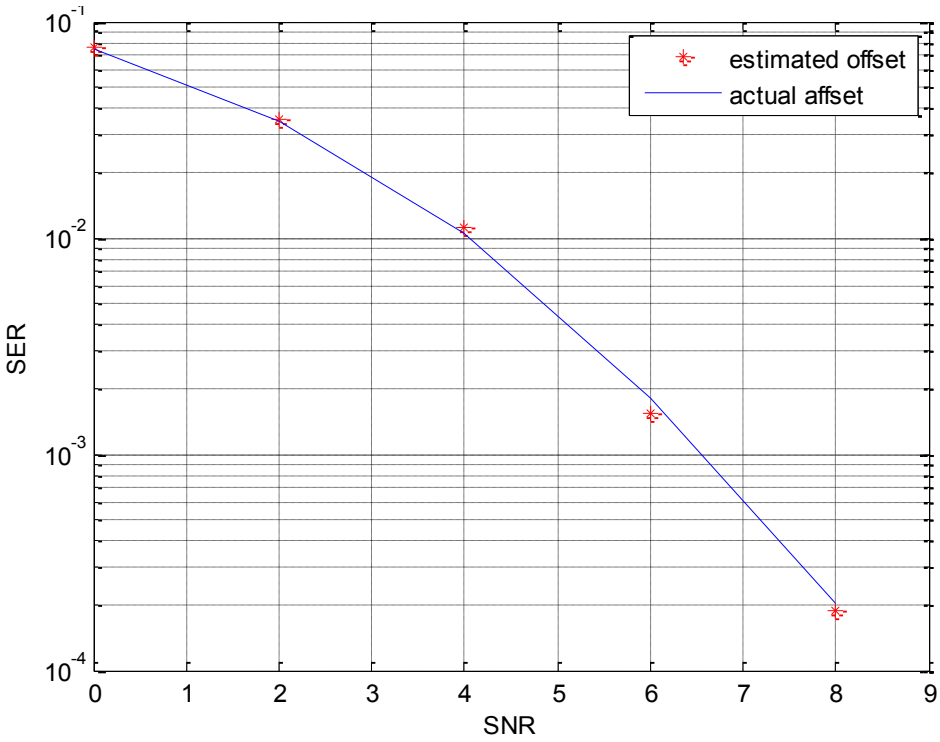

Figure 24: Simulation and theoretical SER performance for SDS

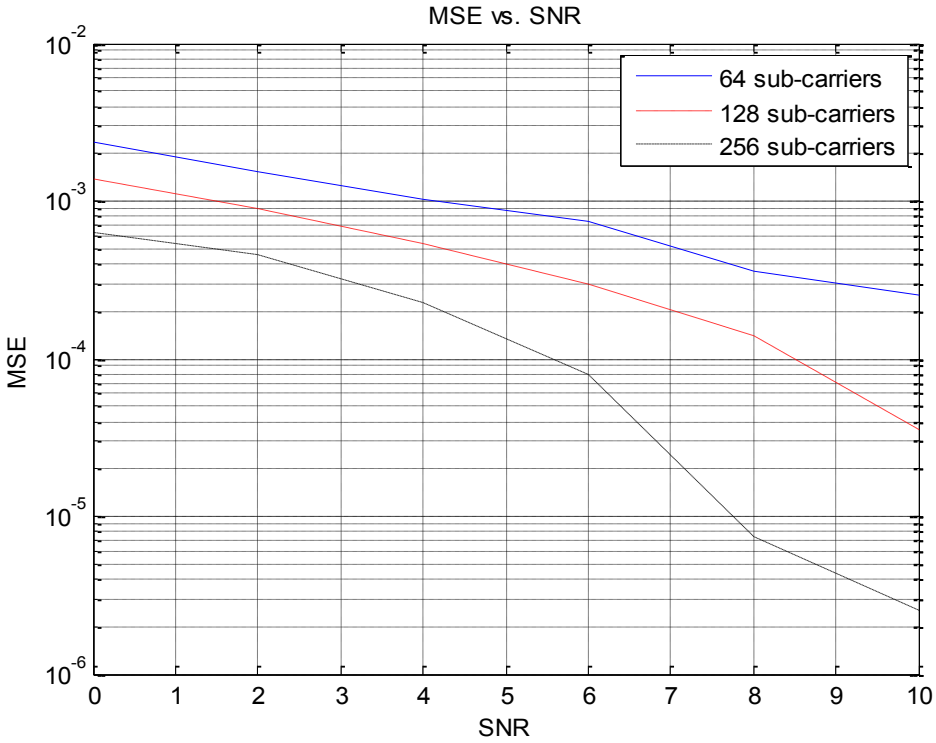

Figure 25: MSE Performance for different number of subcarriers

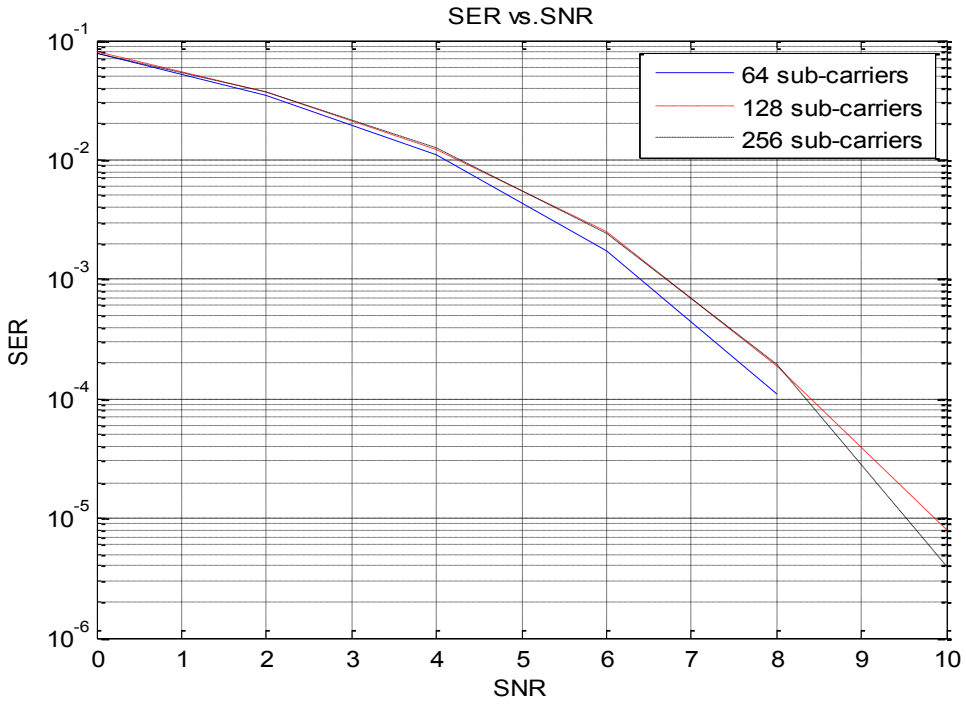

Figure 26: SER performance for SDS with different number of subcarriers

In the previous cases, the estimation range (ER) was assumed to be large enough such that the actual offset is within the searching range. However, we show next the performance for different offset values assuming the following two scenarios:

- The offset is within the estimation range
- The offset is outside the estimation range

In the first case, as the offset value is within the estimation range, it can be detected and compensated for without causing any degradation. In the second case, in which the introduced offset is outside the specified range, there is no way to get accurate estimation and there will be residual errors. These errors will increase as the offset increases outside the estimation range.

Simulations are run for estimation range of -1 to $+1$ and the offset values are set to 0.3, 1.1 and 1.8 with other parameters fixed as before. The results obtained are shown in Figure 27 indicating that the MSE has a large degradation for f_{sn} =1.8 since it lies outside the estimation range. On the other hand, very accurate estimation is achieved for f_{sn} =0.3. It is noted that the correlation does not give one distinct peak when the offset is outside the estimation range as shown is Figure 28. Figure 29

shows significant degradation in the SER especially when the offset is outside the estimation range.

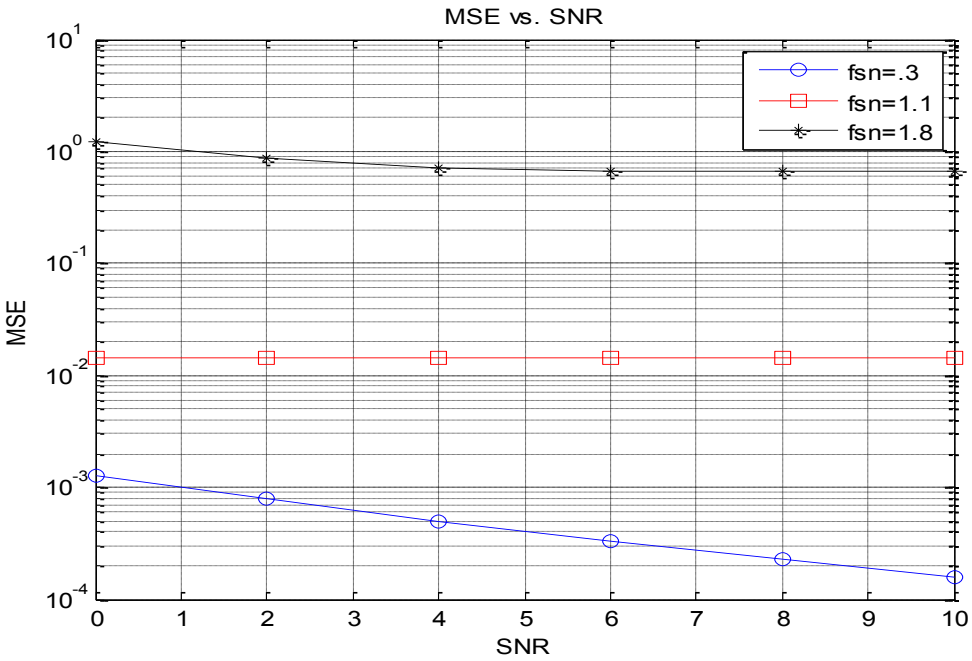

Figure 27: MSE performance for SDS with offset inside or outside the estimation range

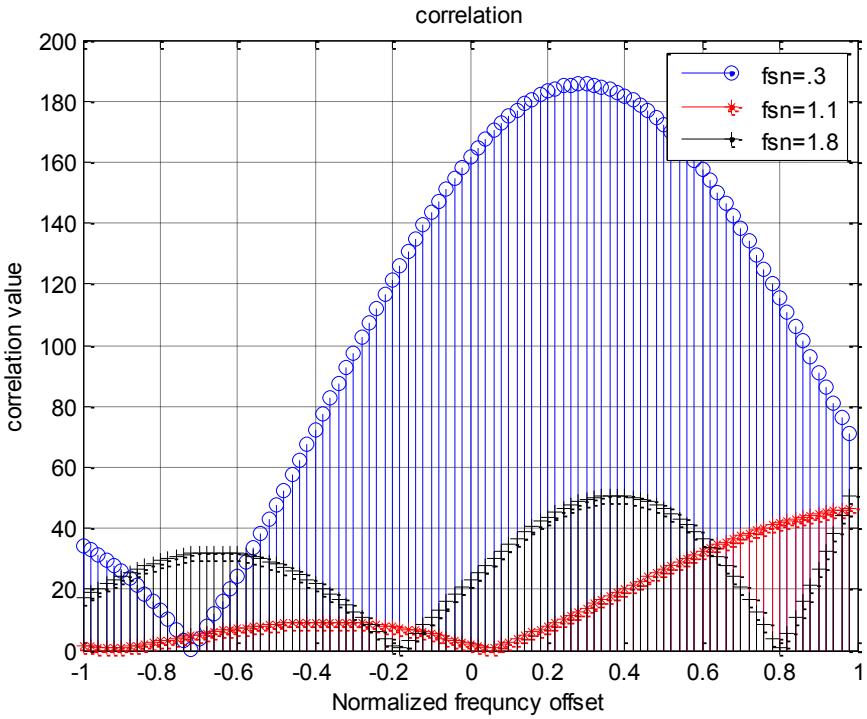

Figure 28: Correlation function result for different offset values

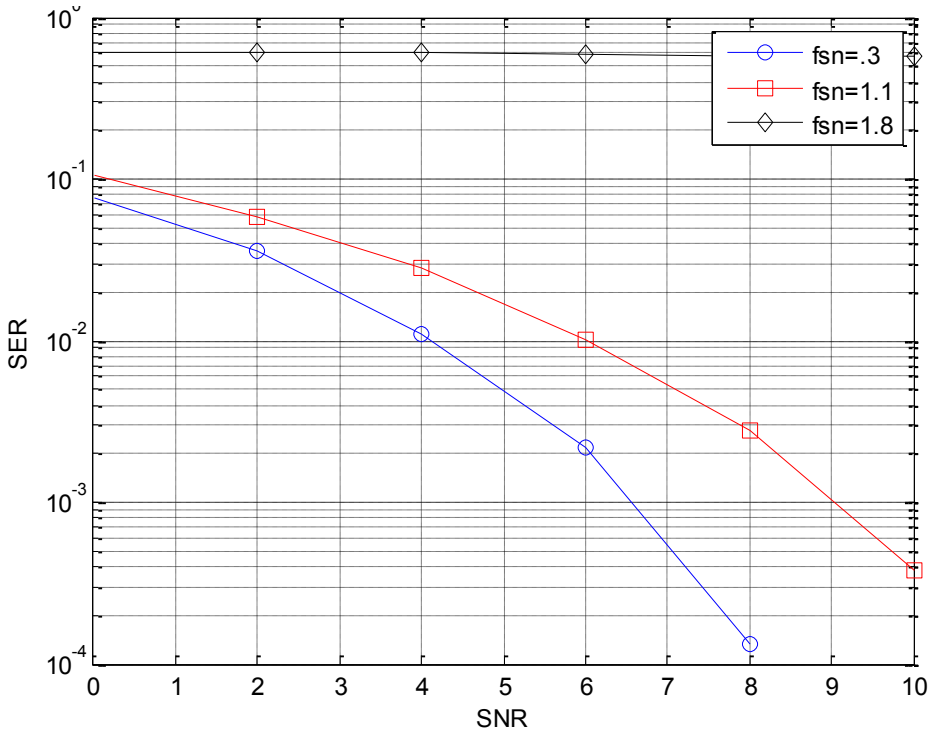

Figure 29: SER performance for SDS with offset inside or outside the estimation range

Further, simulations are run for different estimation ranges ($i.e., ER =$ 10 and 2) while fixing the offset value and the total number of performed searches (correlations). It is important to note that increasing the estimation range without changing the number of correlations increases the searching step size, which results in more degradation. Hence, the choice of the estimation range is critical as it affects the searching step size and the estimation accuracy. Figure 30 illustrates the MSE obtained for the two cases of ER showing degradation by an order of magnitude in the MSE when the ER increases from 2 to 10. Figure 31 shows the correlation results obtained for the two ranges. It is noticed that the peaks of the smaller range will be concentrated around the correct offset leading to better performance. Finally, the SER performance is shown in Figure 32 with the smaller estimation range resulting in a slightly better performance.

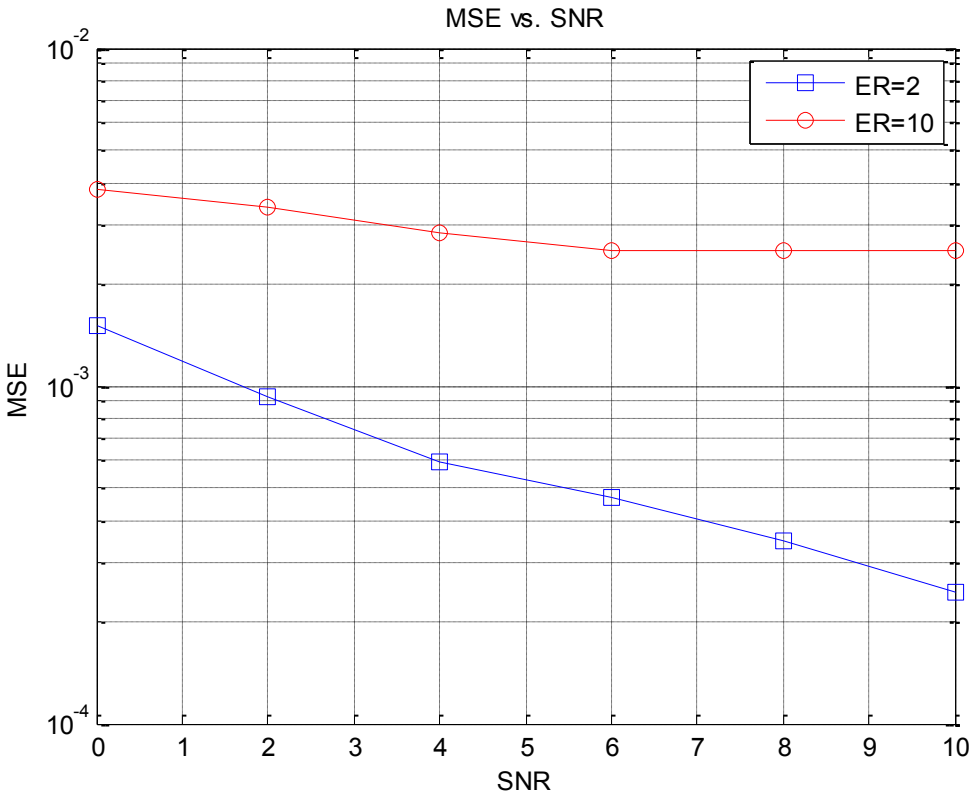

Figure 30: MSE degradation for SDS with different estimation range

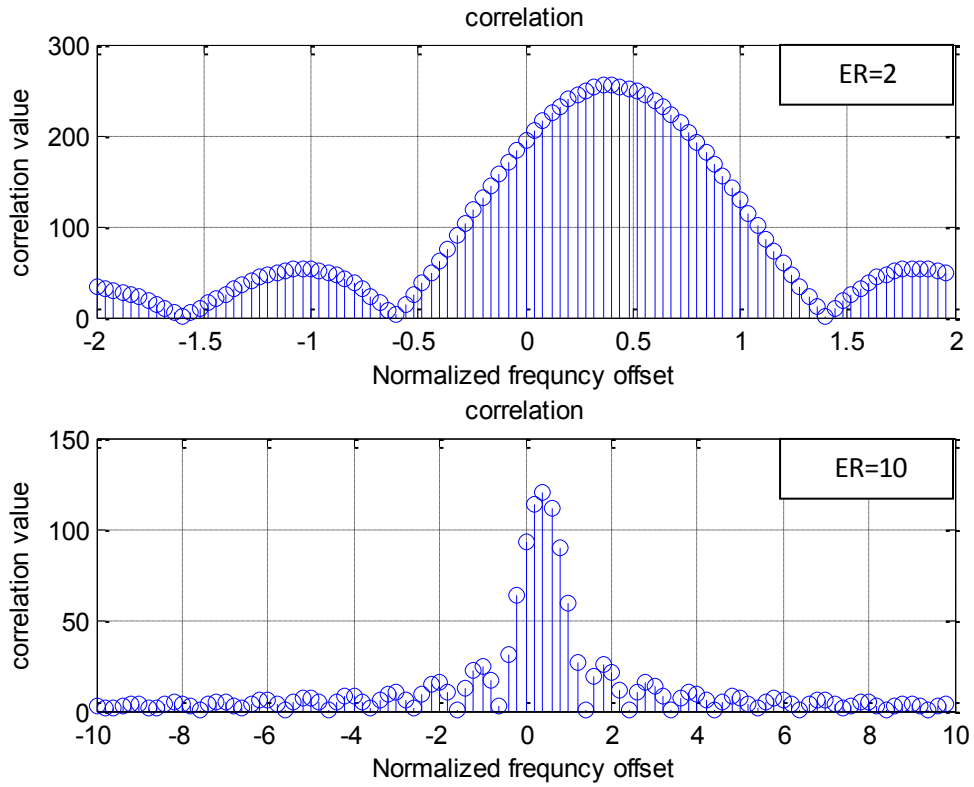

Figure 31: Correlation function for SDS with different estimation range

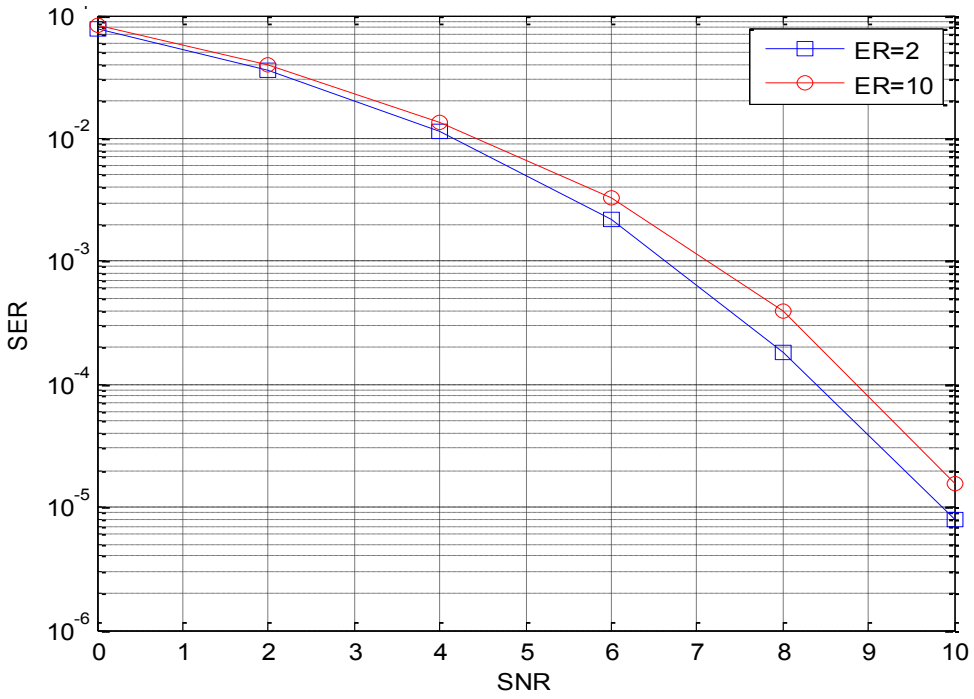

Figure 32: SER for SDS with different estimation range

4.3.2. Double-Dwell System (DDS)

As mentioned earlier, the proposed DDS finds the correlation peak and the two adjacent peaks obtained from the first searching stage. Then, a second correlation stage is started where the searching window of the second stage is limited to the frequency offsets that have the two peak values. In this stage, a fine estimation with a much smaller searching window and step size is performed to get the final estimated frequency offset value that will be used to correct the frequency error in the received signal.

Simulations are run for the DDS using the following parameters: f_{sn}=0.35, *ER=10* and N_{tot}=100 total correlations. The same simulations are conducted for the SDS as explained in the previous section in order to compare the performance of the proposed DDS and conventional SDS schemes. The results show a significant improvement in the MSE performance when using the DDS compared to the SDS as shown in Figure 33. This improvement is obtained without any increase in the complexity since the number of total correlations is the same for both schemes. It is noticed that the SER performance does not change significantly for both systems as shown in Figure 34 since we have a small residual frequency error after correction. However, by increasing the total number of performed correlations from 100 to 1000,

the SDS shows significant improvement by almost one order of magnitude with a performance close to that of the DDS as shown in Figure 35. This is because increasing the total number of correlations results in a smaller step that improves the accuracy of the SDS but at the expense of higher complexity and more delay until the offset estimation is obtained. Note that the DDS with 100 correlations achieves the same performance as the SDS with 1000 correlations.

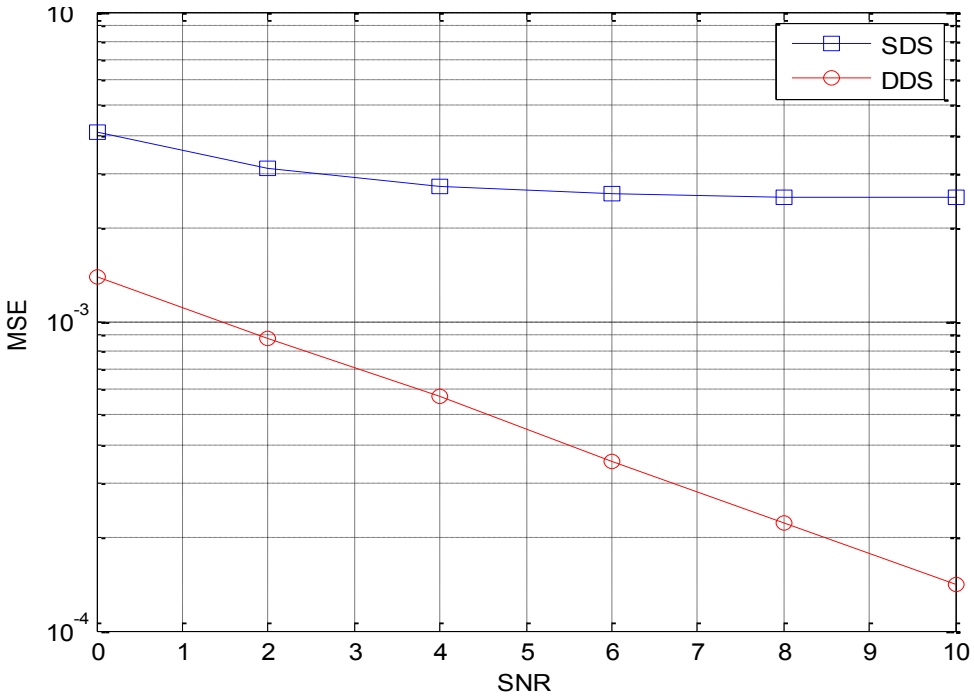

Figure 33: MSE performance for SDS and DDS with 100 correlations in AWGN

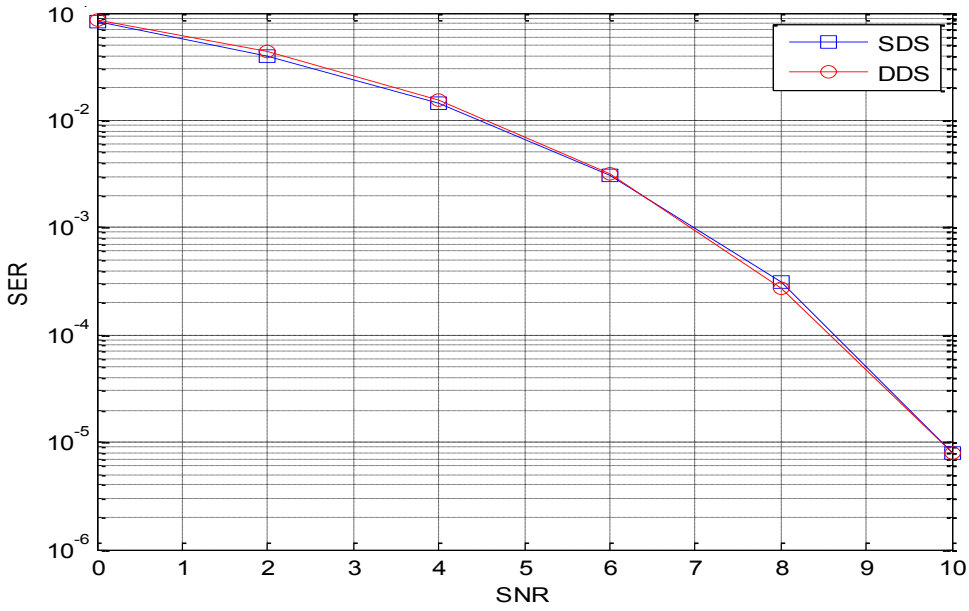

Figure 34: SER performance for SDS and DDS with 100 correlations in AWGN

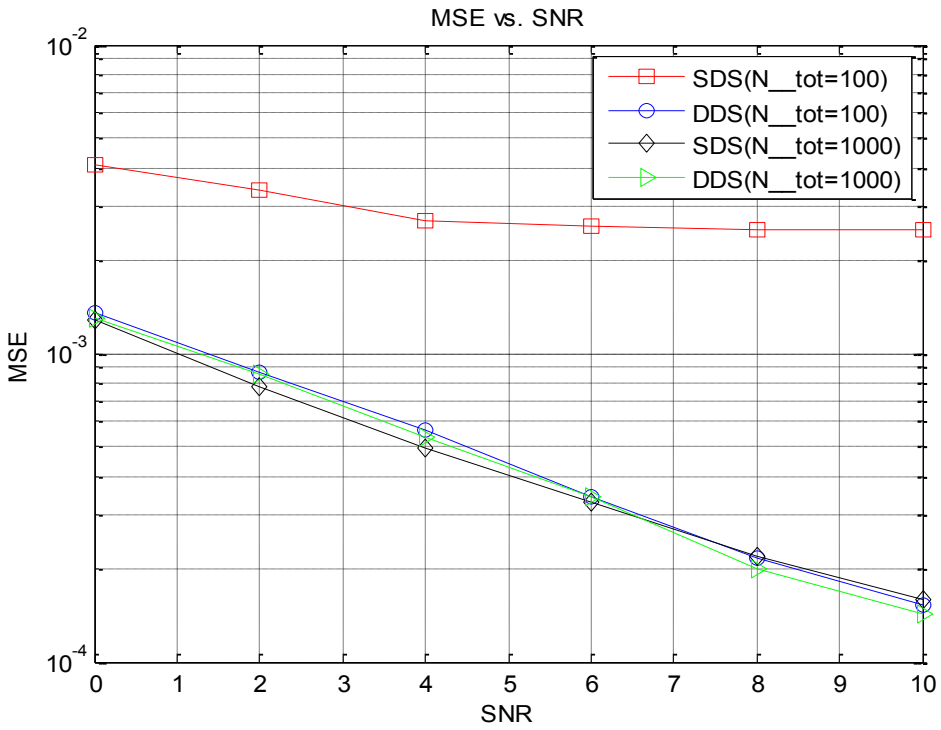

Figure 35: Impact of number of correlations on MSE performance for SDS and DDS

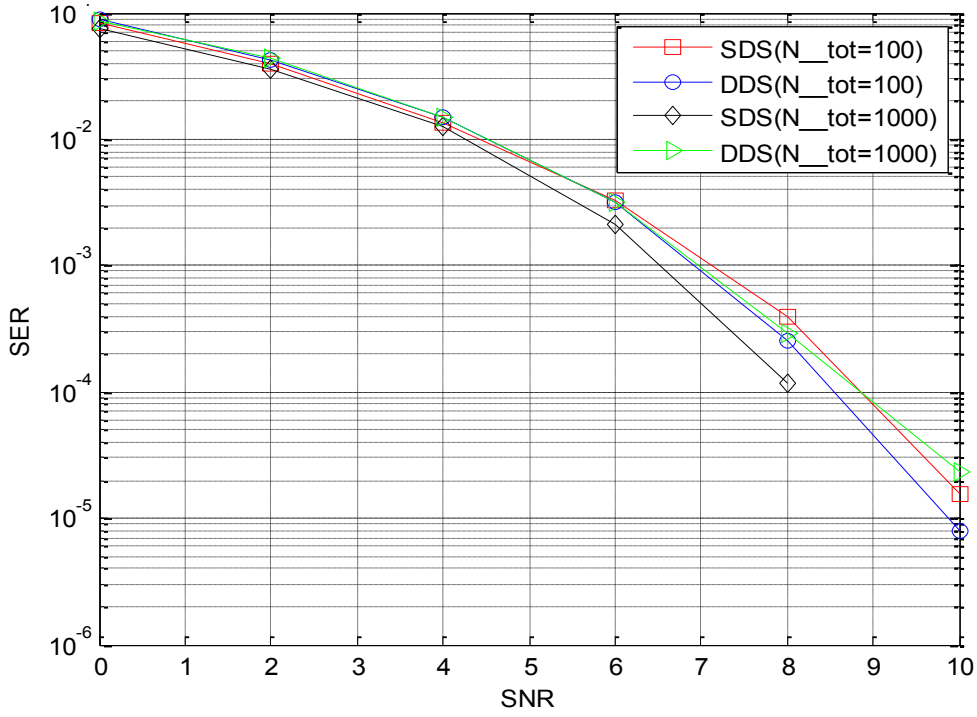

Figure 36: Impact of number of correlations on SER performance for SDS and DDS

4.4. CRLB for AWGN Channel

The Cramer Rao Lower Bound (CRLB) provides a theoretical upper bound on the estimator accuracy of any estimator as measured by the MSE. For the frequency estimation problem in AWGN, the CRLB is evaluated using [49]:

$$\mathrm{CRLB} = \frac{3.\mathrm{SNR}^{-1}}{2\pi^2.\mathrm{N}.(1-\frac{1}{\mathrm{N}^2})}$$

where SNR is the signal to noise ratio and N is the number of subcarriers. The performance of the proposed DDS is compared to the CRLB in Figure 37 for different values of subcarriers. It is noted that the proposed scheme achieves the CRLB as the number of the subcarriers increases as shown in Figure 37.

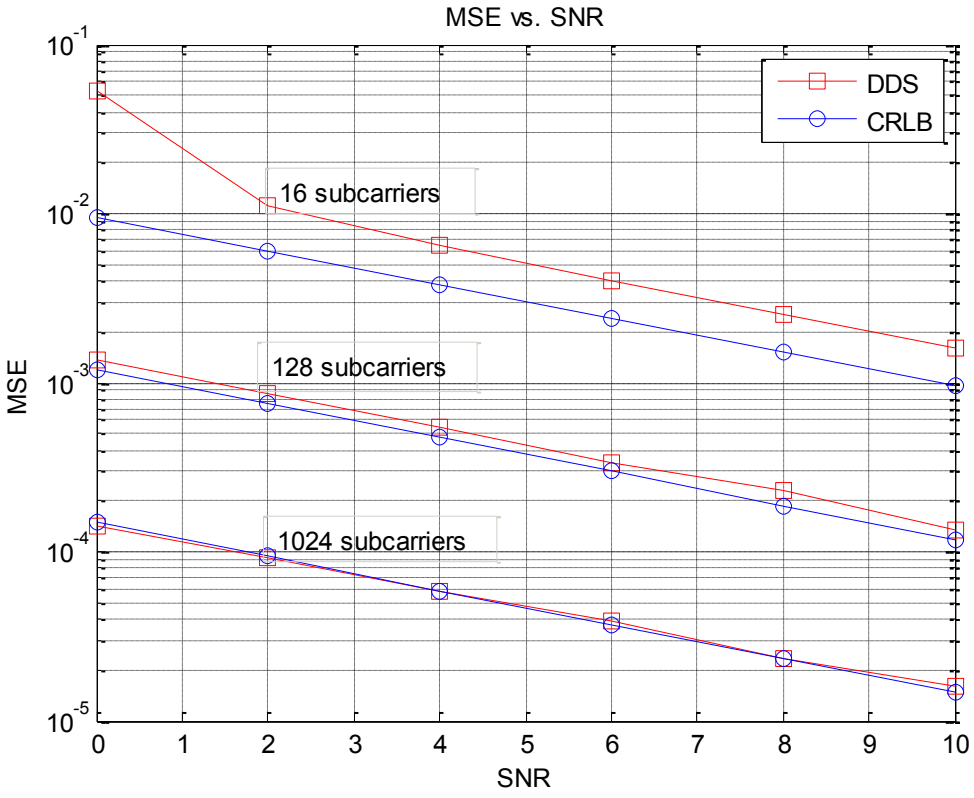

Figure 37: CRLB for different numbers of subcarriers

Chapter 5: Performance Evaluation under Fading Channel Conditions

In this chapter, simulations are performed for the proposed scheme under flat Rayleigh fading channel conditions. The results obtained are compared to the AWGN results under similar conditions to show the impact of fading on the system performance. A perfectly synchronized system is first simulated to ensure that the simulation model matches the theoretical performance. Frequency offset is then introduced to the system and the SDS and DDS performance is evaluated and compared. The effect of all the parameters is thoroughly investigated to enhance the overall performance. Synchronization tasks are more challenging in fading channels because of the significant reduction in SNR and Doppler shift.

Averaging the correlation results is necessary for fading channels since a wrong estimate when the channel is under deep fade conditions causes a large bias in the estimated offset, resulting in large degradation in the MSE performance. To overcome this problem, the correlation results of the first stage are averaged over a number of iterations to reduce the impact of these outliers. The DDS performance shows significant improvement in the MSE by more than one-order of magnitude when averaging is used. Averaging is then added to the SDS to compare both systems under similar conditions, DDS still gives better performance but both systems performance get closer. It is important to note that for AWGN channel, the DDS always gives better performance than the SDS without the need for averaging.

Simulations are then run to study the effect of interference for a perfectly synchronized OFDM system and both SDS and DDS by adding another OFDM transmitting block at different power levels. The obtained results are presented in Section 5.4. Section 5.5 considers the effect of pilot subcarriers, variations of the number of pilot subcarriers as well as the used pilot sequence are simulated for different number of pilot subcarriers and different sequences like m-sequence and complex-valued pilot symbols.

Unless otherwise specified, BPSK is the modulation level used in all simulations, 100 total correlations with N_1=30 and N_2 =70, Doppler frequency of 2

Hz, 32 subcarriers, averaging of $Q = 2$, and the experiment is repeated 1000 times for each SNR value. The effect of the following parameters is investigated:

- Value of the introduced offset
- Number of subcarriers
- Estimation range/step size
- Total number of performed searches and number of performed searches in each stage
- Doppler frequency
- Averaging window

Simulations are run to test the effect of each of the above mentioned parameters on the MSE and SER performance and the obtained results are presented in the following sections.

5.1. Flat Fading Channel with No Offset

A perfectly synchronized OFDM system is first simulated for flat fading channel conditions. At the receiver, channel correction is performed in the frequency domain after the FFT. The obtained SER results are shown in Figure 38 in which a perfect match is observed between the simulated and the theoretical curve indicating the accuracy of the simulation model.

Simulations are run to compare the SER performance for flat fading and AWGN channels with no frequency offset. Figure 39 illustrates the obtained SER for both channels. Large degradation in the SER performance is noticed due to fading. For instance, about 4 dB of SNR is required to achieve a SER of $(1 * 10^{-2})$ in AWGN channel, while about 15 dB is needed to achieve the same SER for fading channel, i.e., 12 dB more is needed for fading channel conditions for a perfectly synchronized system.

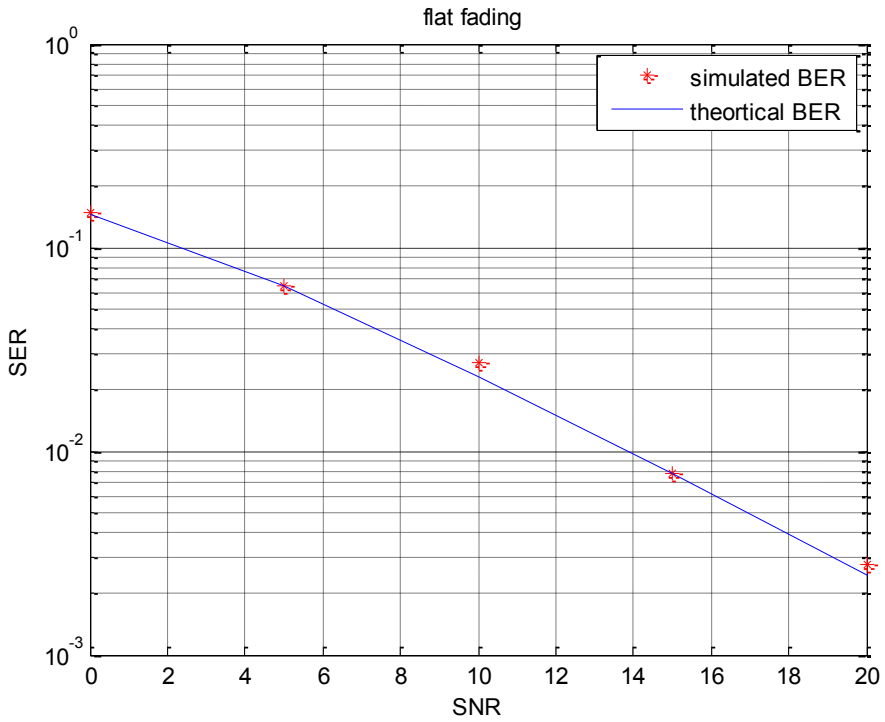

Figure 38: Simulated and theoretical SER with perfect synchronization for fading channel

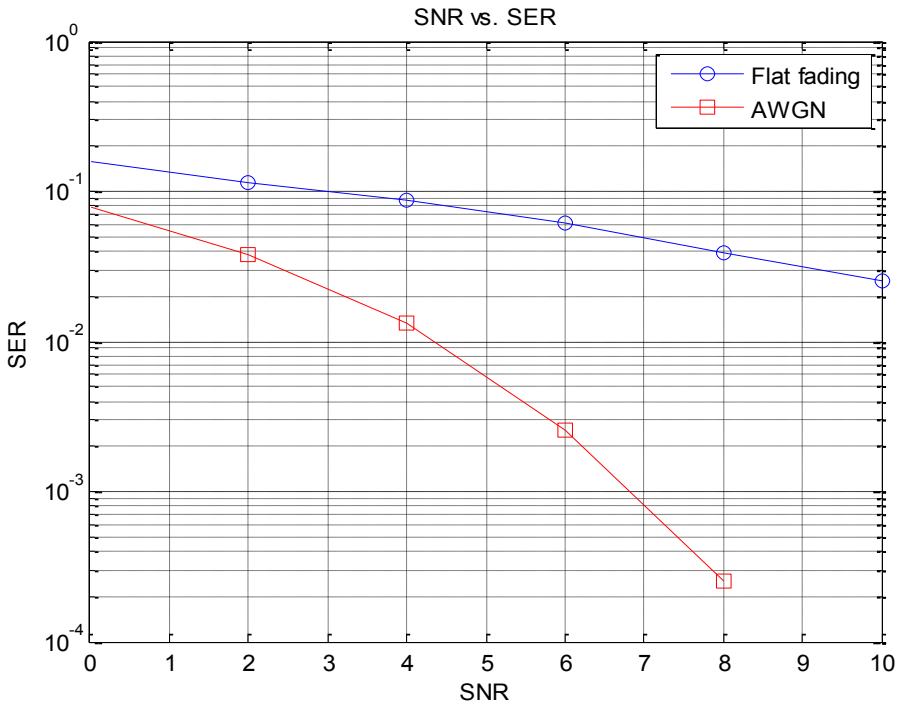

Figure 39: Comparison between AWGN and fading channel with perfect synchronization

5.2. Frequency Synchronization

In this section, simulations are run to evaluate the performance of the SDS and the DDS under flat fading channel conditions and to compare both systems' performance for different estimation ranges and offset values. Two estimation ranges (the range of normalized frequency offsets to be searched for the correct offset) are tested ($ER = 10$ and $ER = 3$) with the offset value fixed to 1.6 for both ranges, 50 total correlations are used and 10 averaging of the first stage correlation. Figures 40 to 43 show the MSE and the SER results for both ranges. It is clear that the proposed DDS shows significant improvement in the MSE performance over the conventional SDS for the two ranges. Both systems show better performance for the smaller range. For instant, to achieve MSE of (10^{-3}) for DDS, 14 dB is needed when $ER = 10$. However, this is reduced to 10 dB for $ER = 3$. On the other hand, to achieve a MSE of (10^{-1}) for SDS, 14 dB is needed when ER=10 which decreases to 5 dB for $ER = 3$. Hence, SDS shows more improvement by decreasing the estimation range and its performance approaches the DDS at higher SNR values. Nevertheless, DDS can still achieve much better accuracy. The SER for both systems is compared with the theoretical curve and a very similar performance was noted for both systems as shown in Figure 41.

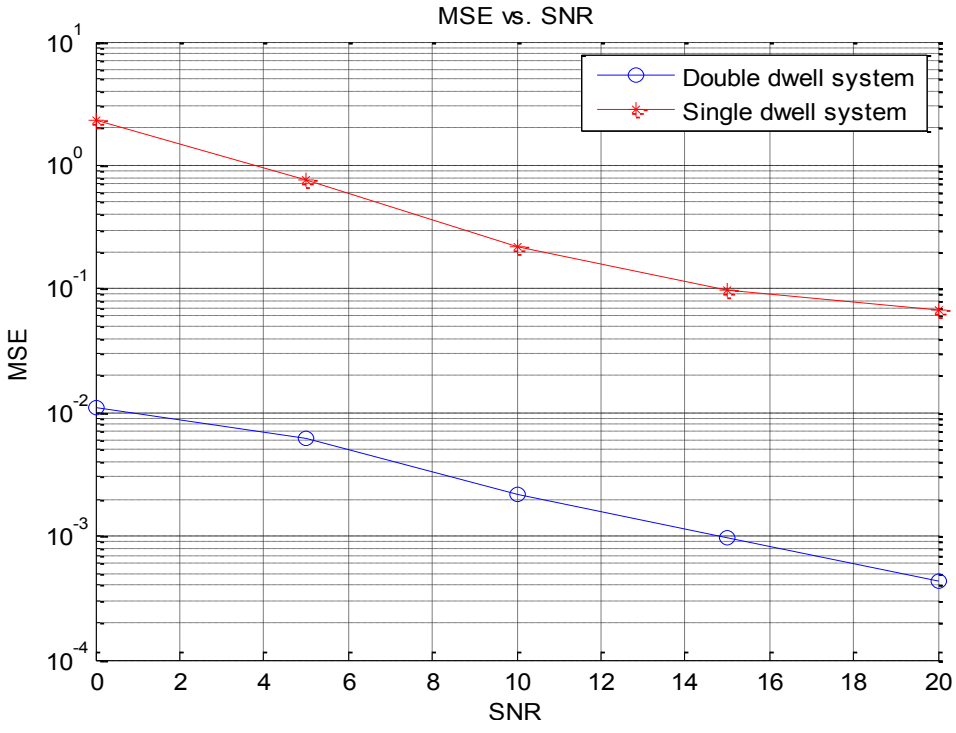

Figure 40: MSE for SDS and DDS under fading channel conditions with ER=10

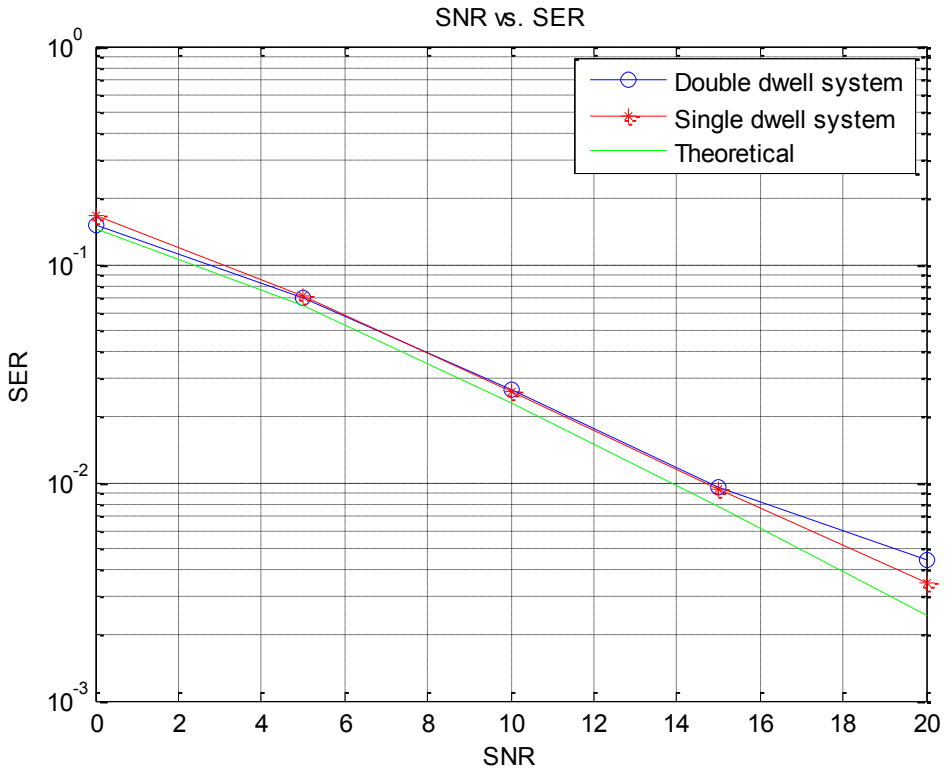

Figure 41: SER for SDS and DDS under fading channel conditions with ER=10

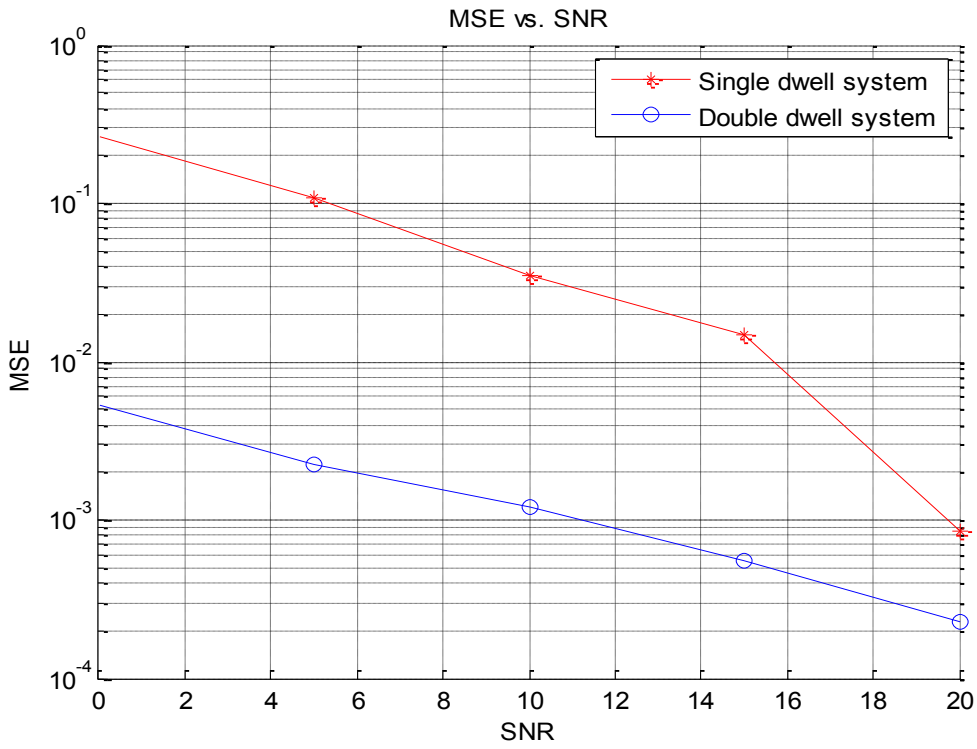

Figure 42: MSE for SDS and DDS under fading channel conditions with ER=3

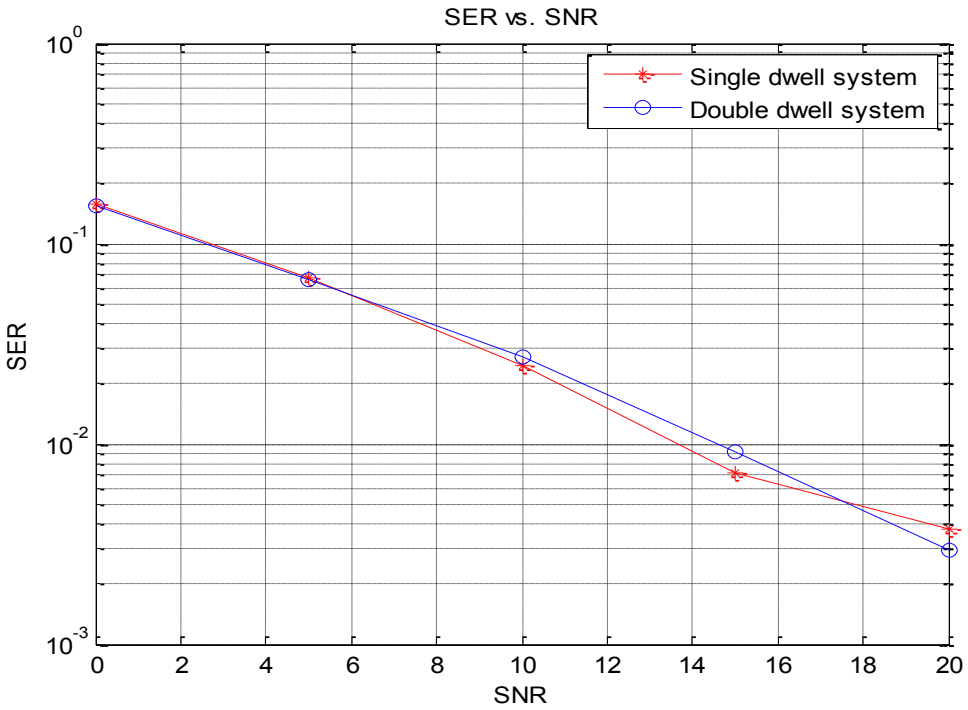

Figure 43: SER for SDS and DDS under fading channel conditions for ER=3

Simulations are then repeated for $ER = 10$, with 50 correlations but for different offset values, to test the worst case scenario in which the offset value is chosen to be in the middle of two searching offsets (e.g., f_{sn}= 0.2 for a step size of 0.4). Figures 44 and 45 illustrate the obtained results in which DDS shows improvement in both MSE and SER performance

Further, simulations are run to compare DDS with SDS under AWGN and fading channel condition using the same parameters. Similar results were noted as for the perfectly synchronized system where large degradation is noticed in both the MSE and the SER performance for fading channel conditions. Figures 46 and 47 illustrate the results obtained for both systems. The used parameters are: offset value=1.25, 50 correlations ($N_1 = 30$, $N_2 = 20$) and $ER = 5$.

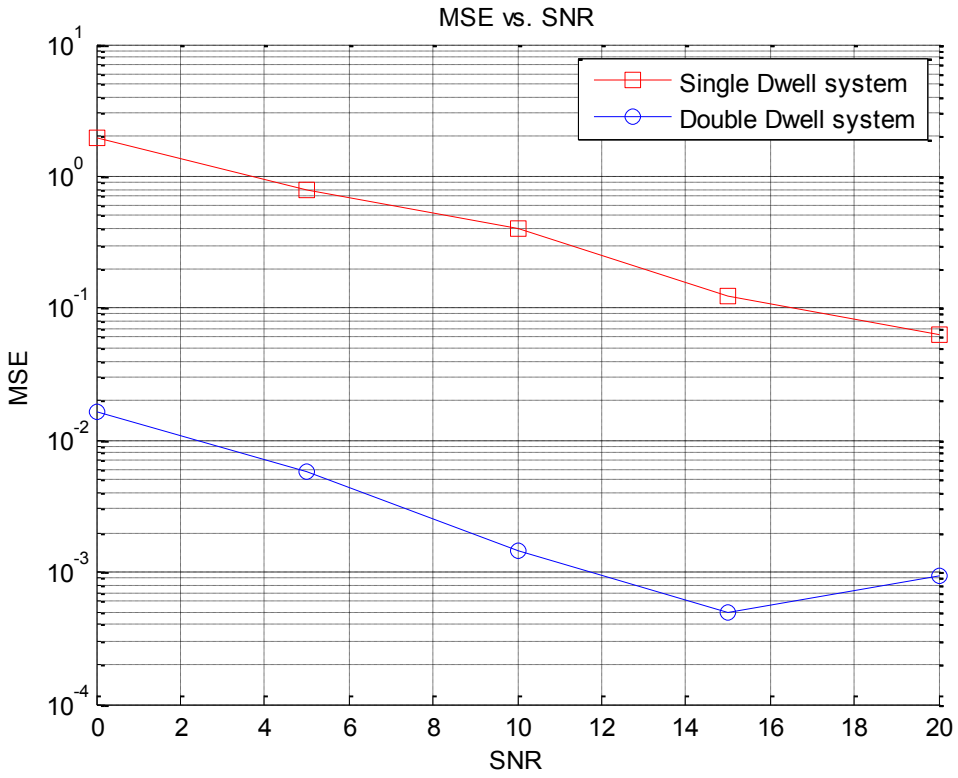

Figure 44: MSE for SDS and DDS for the worst SDS performance

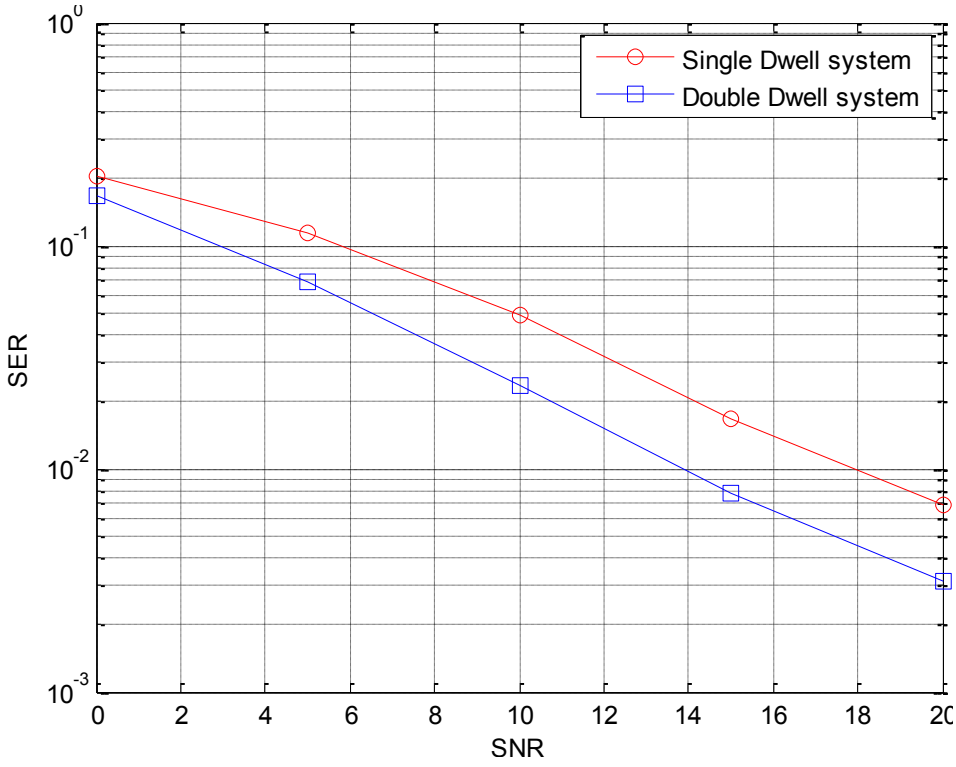

Figure 45: SER for SDS and DDS for the worst SDS performance

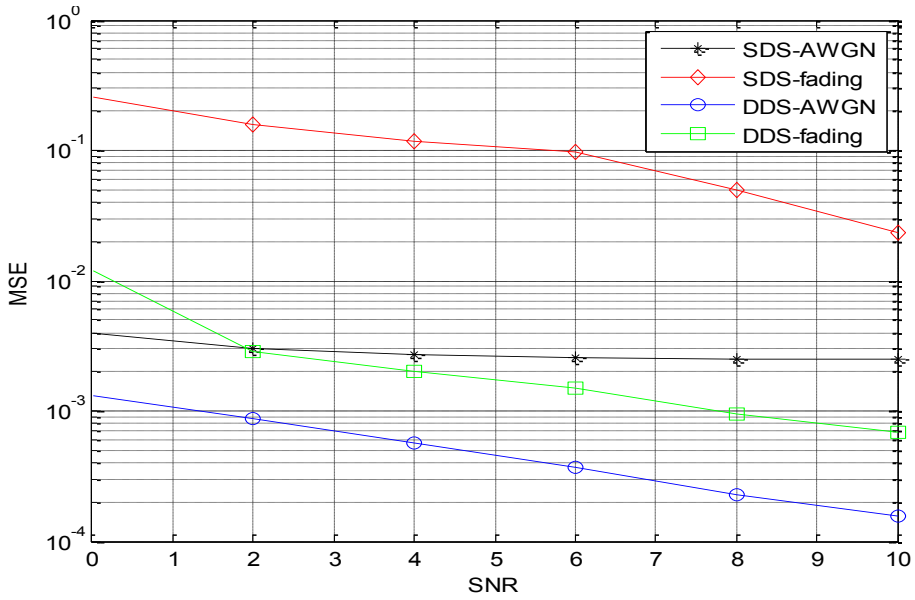

Figure 46: SDS and DDS MSE performance in AWGN and fading

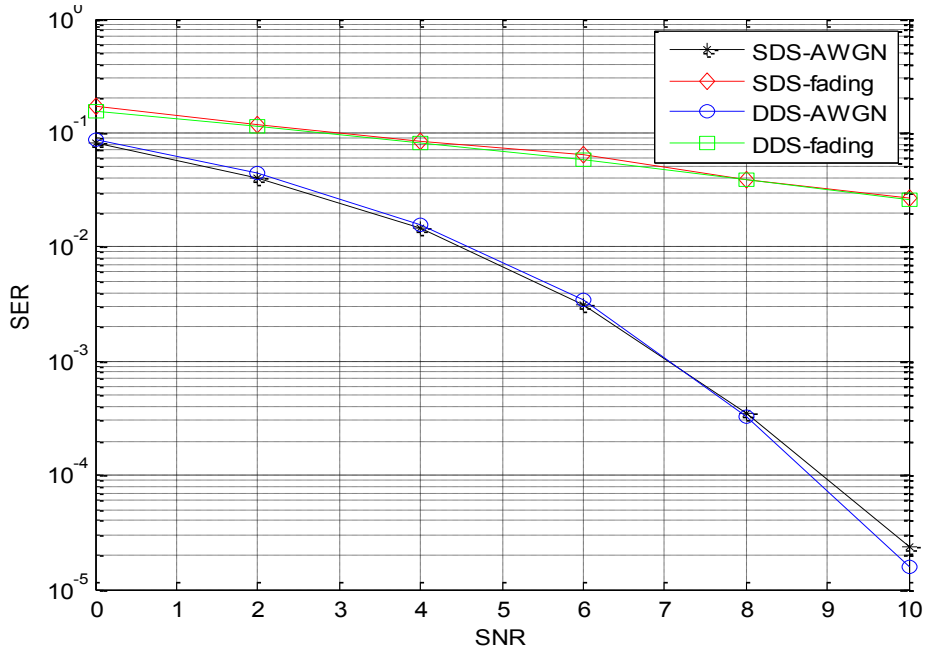

Figure 47: SDS and DDS SER performance in AWGN and fading.

5.3. Investigating the Effect of Simulation Parameters

5.3.1. Frequency Offset Value

By introducing frequency offset without correction at the receiver, SER shows large degradation where a normalized offset value of 0.5 can cause the SER to reach 0.5 as illustrated in Figure 48. Comparing the obtained results with the results for the AWGN case, it was noted that the MSE is more sensitive to frequency errors under

fading channel conditions. For instance, 9 dB of SNR are needed to achieve a SER of (10^{-1}) at an offset value of 0.2, while only 2 dB are needed to achieve the same SER for the AWGN case.

The MSE and the SER performance for DDS at different offset values are then tested. The obtained results are shown in Figures 49 and 50 where it is noticed that the system is able to track and correct for different offset values with high accuracy provided that the introduced offset is within the specified estimation range. The offset values are chosen considering different scenarios as follows:

- The introduced offset matches one of the searching offsets (best performance)
- The introduced offset is in the middle of two searching offsets (worst performance)
- The introduced offset value is randomly generated within the specified offset range (average performance)

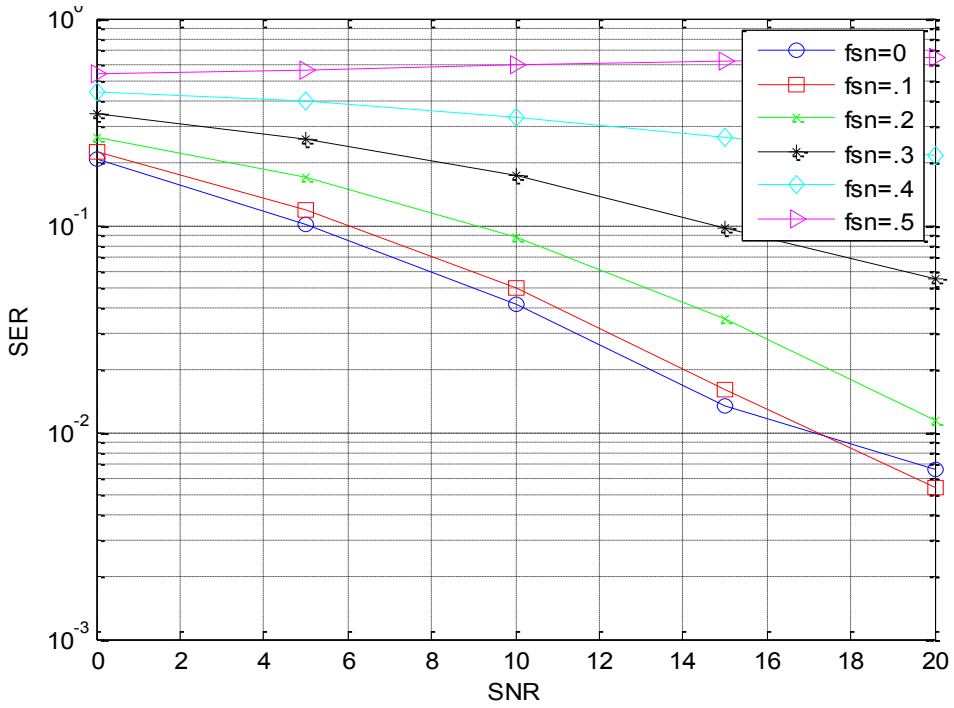

Figure 48: SER degradation for different offsets without correction at the receiver

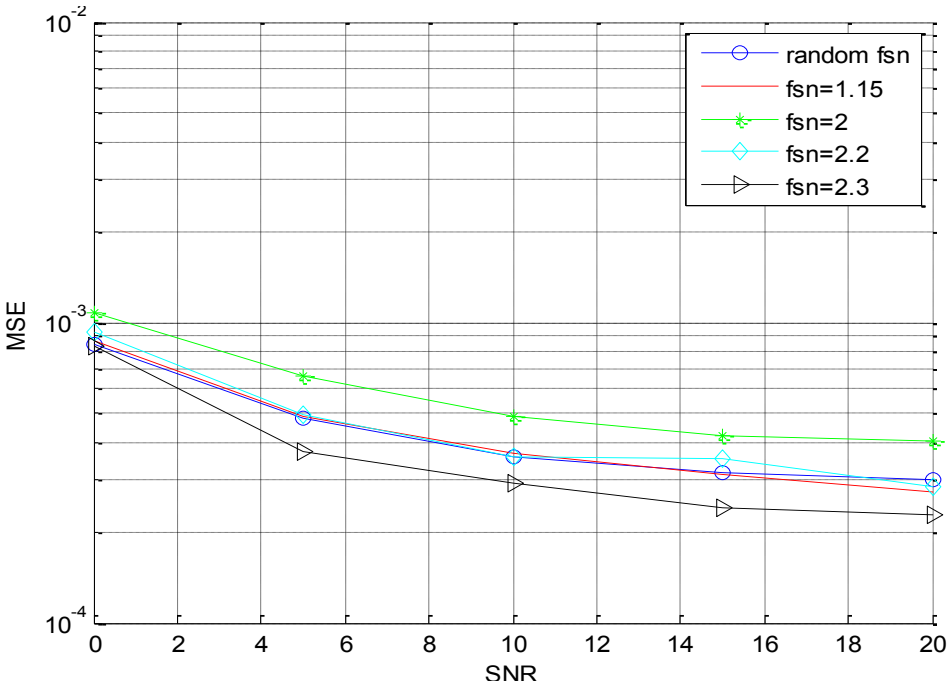

Figure 49: MSE for DDS with different offsets values

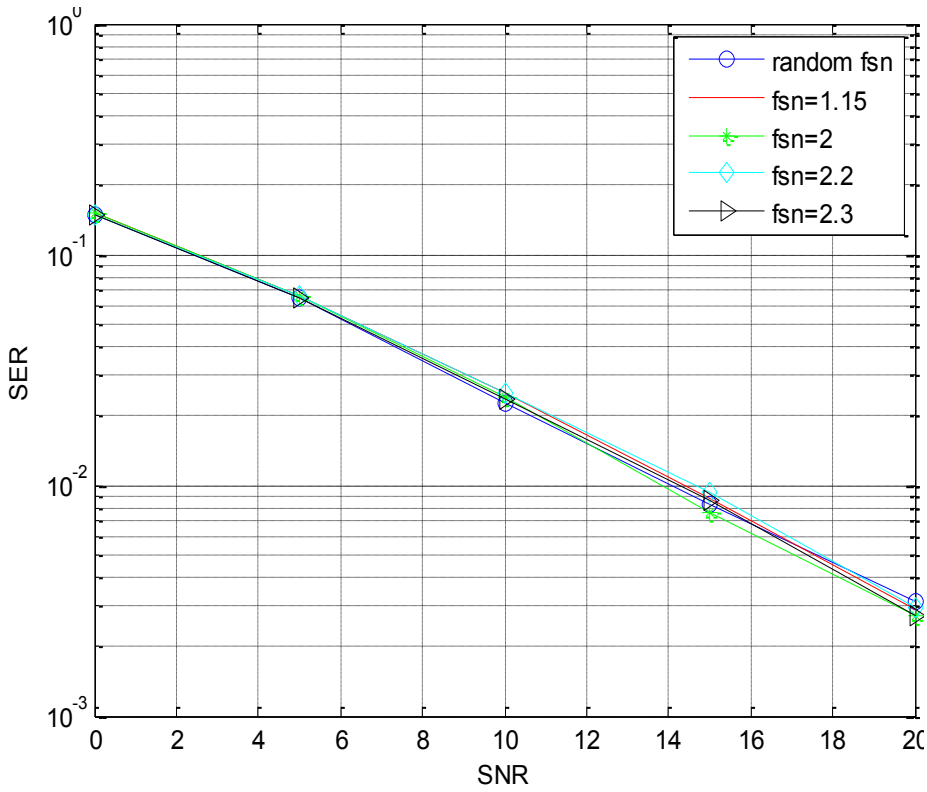

Figure 50: SER for different offsets values

5.3.2. Number of Subcarriers

In this section, the effect of the number of subcarriers is tested. Simulations are run for 16, 32, 64, and 128 subcarriers while fixing all other parameters as before. The obtained MSE and SER results are shown in Figures 51 and 52, respectively. It is noted that the higher the number of the subcarriers the better the MSE performance, as the correlation period gets longer for larger numbers of subcarriers, which improves the estimation accuracy.

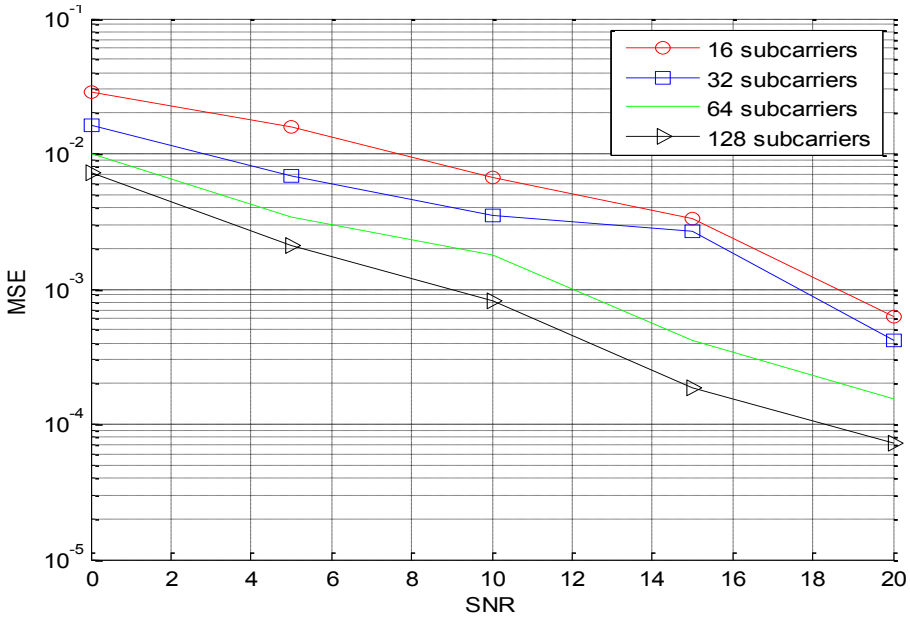

Figure 51: MSE for different numbers of subcarriers

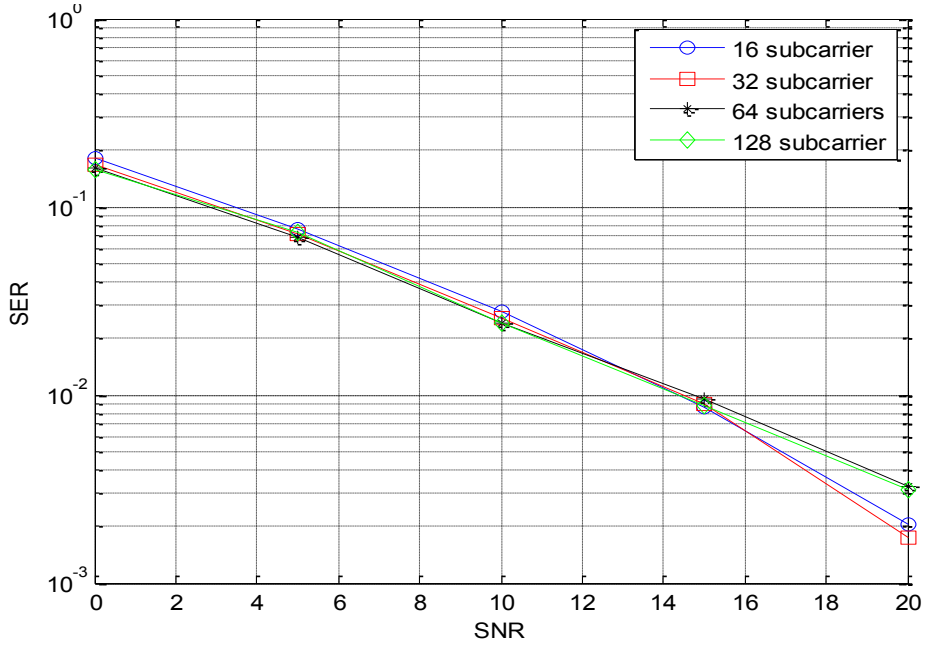

Figure 52: SER for different numbers of subcarriers

5.3.3. Total Number of Correlations and Estimation Range

The step size on both stages is affected by the estimation range (ER) and the total number of performed searches (N_{tot}). Improved performance can be achieved using smaller step size, which may be achieved either by increasing N_{tot} or decreasing ER. However, increasing N_{tot} increases the complexity of the system and adds more delay, while decreasing ER reduces the system capability to track larger offset values. In this section, simulations are run to demonstrate the effect of each of these parameters on the estimation accuracy searching for the optimum choice that leads to the best performance. The number of searches performed in each stage in DDS greatly affects the estimator accuracy, given that wrong first stage estimates cause estimation failure as the second stage range will be wrongly specified. Hence, the number of performed searches in the first stage should be enough to ensure correct estimation in the first stage.

Simulations are run for ER=5 and 10, with N_{tot} = 50 and 100. The MSE and SER results are shown in Figures 53 and 54, respectively. The best performance happens when ER=5 with N_{tot}=100. The total number of performed searches is then fixed to 100 but the number of performed searches in each stage is varied as shown in Figures 55 and 56. The best performance is obtained when N_1=80 and $N_2 = 20$, while the opposite (N_1=20 and $N_2 = 80$) gives the worst performance. This may be explained given that increasing N_1 decreases the first stage step size leading to a better first stage estimate, which facilitates the search on the second stage as the searching range will be closer to the actual offset.

The number of performed searches is then decreased to 50 with different first and second stage searches and for different estimation ranges. Simulations are repeated for ER =5, 10, and 20. The SDS is also simulated to compare both systems using different parameters. Figures 57 to 62 show the obtained MSE and SER results for the three ranges with different N_1 and N_2 combinations. Figure 57 shows the MSE for ER=5, from which it is clear that the DDS system shows better performance by more than one order of magnitude for all different combinations. However, SDS shows better performance than DDS when the ER increases to 20 with a small N_1value (N_1=10). The DDS estimate is completely wrong causing large degradation in SER as well. The first search cannot achieve an accurate estimate for a wide range

with a small N_1 value, causing large degradation in the DDS performance. Thus, the best performance happens using the largest N_{tot} and smallest ER with a larger N_1value.

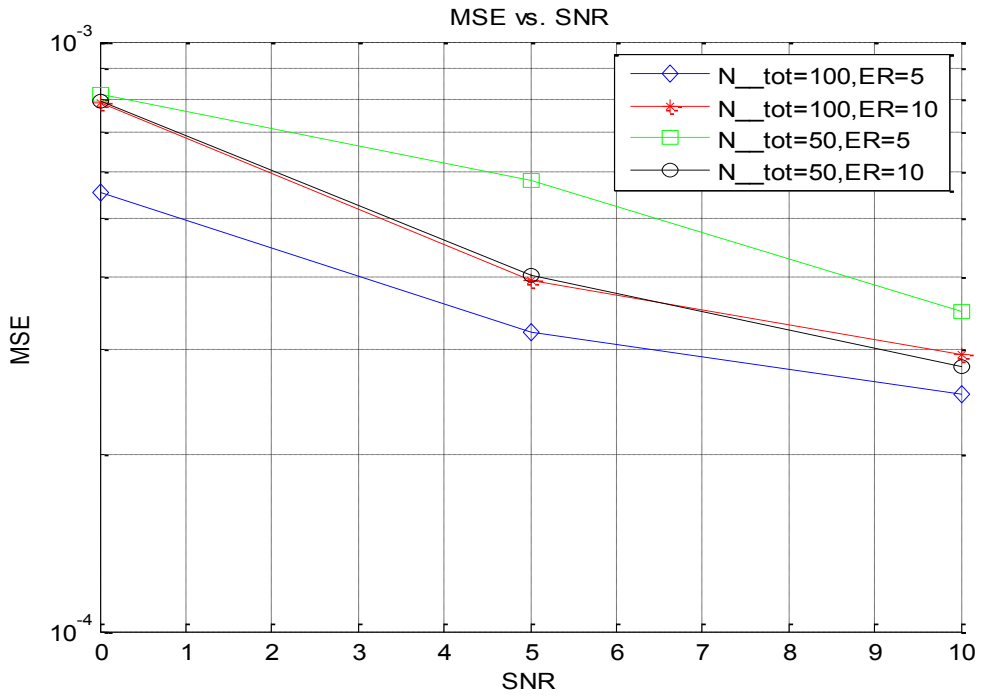

Figure 53: MSE for DDS with different ER and total searches

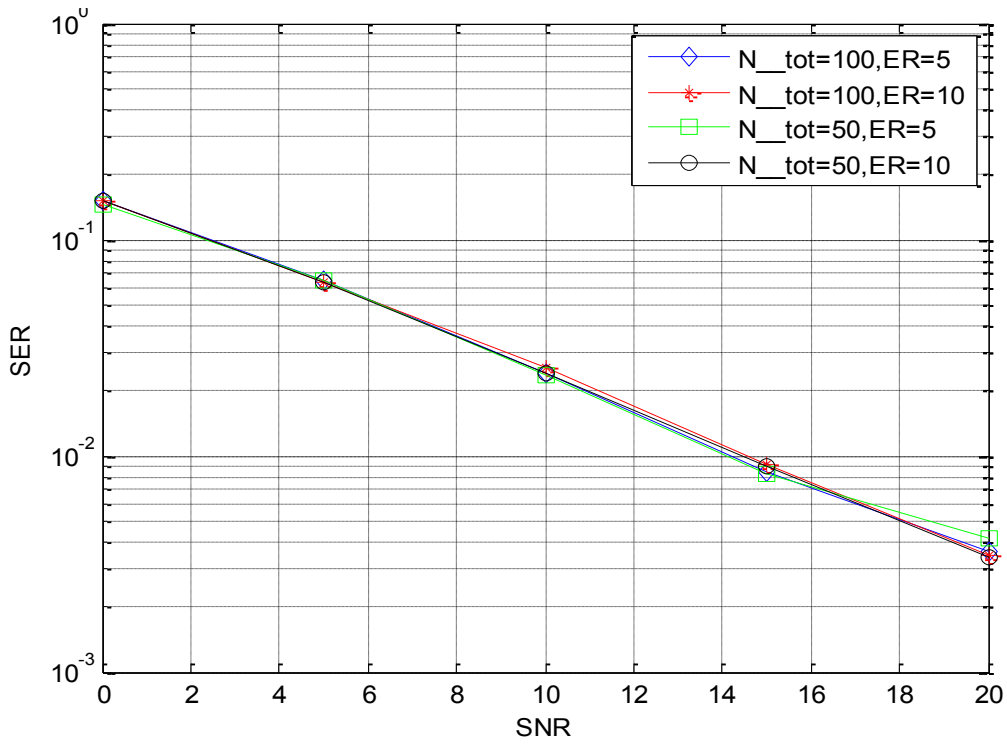

Figure 54: SER for DDS with different ER and total searches

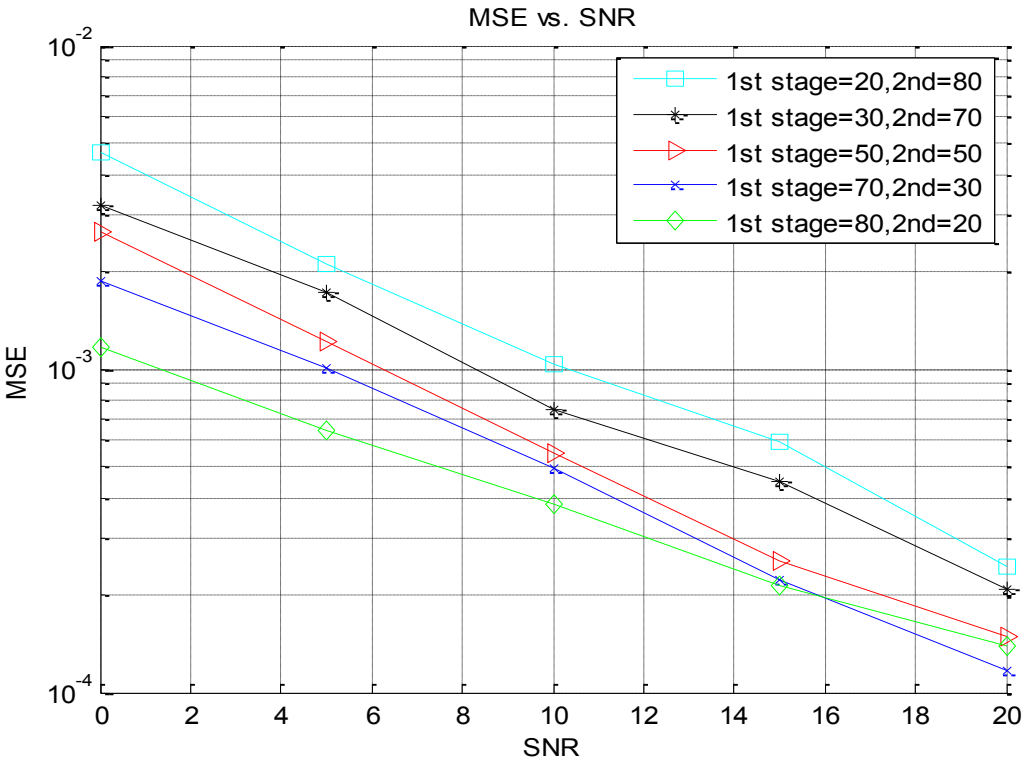

Figure 55: Impact of correlation windows on MSE with 100 correlations

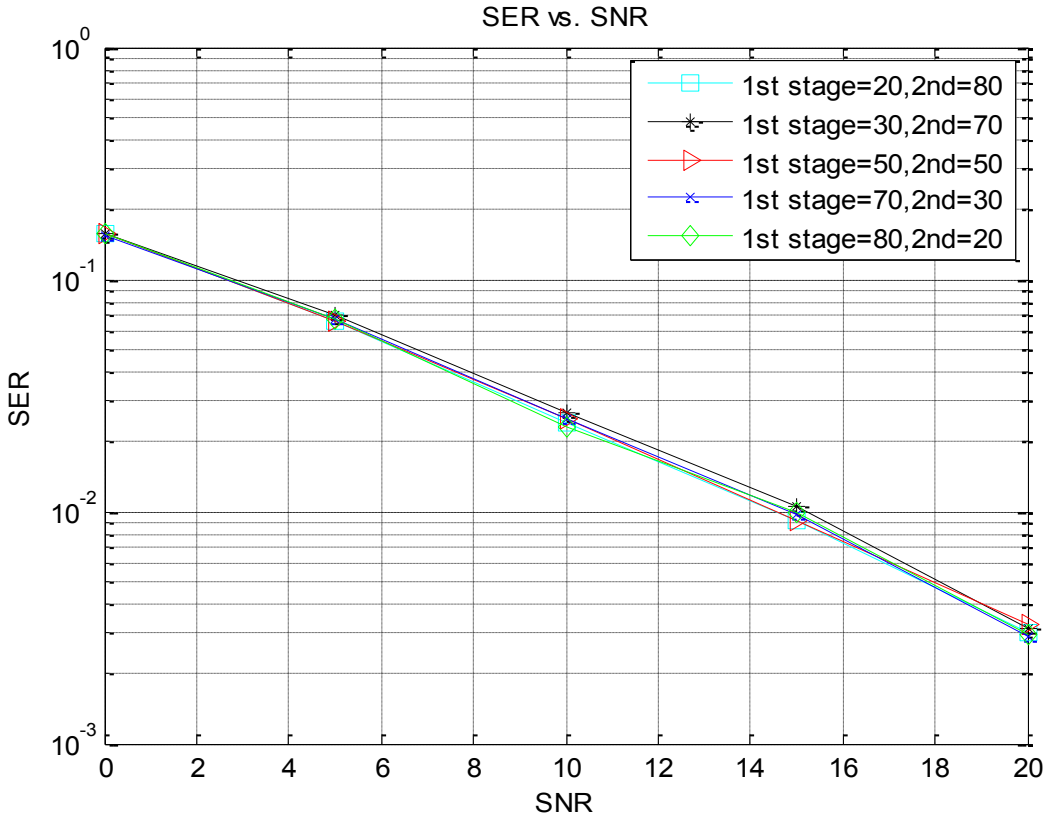

Figure 56: Impact of correlation windows on SER with 100 correlations

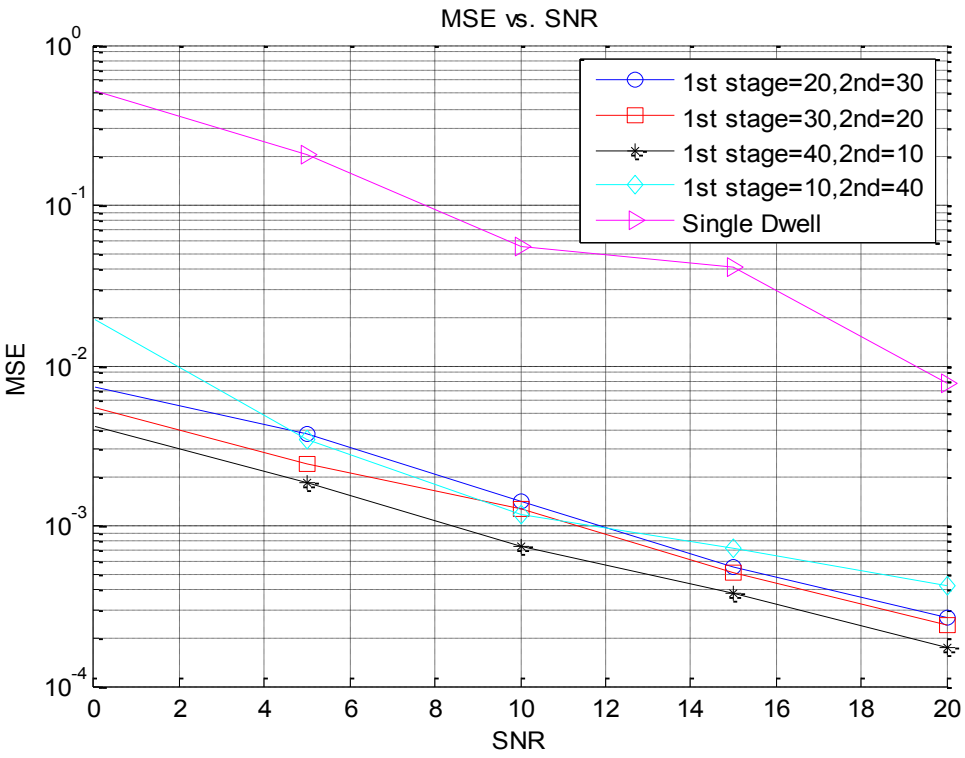

Figure **57: Impact of correlation windows on MSE with 50 correlations and ER=5**

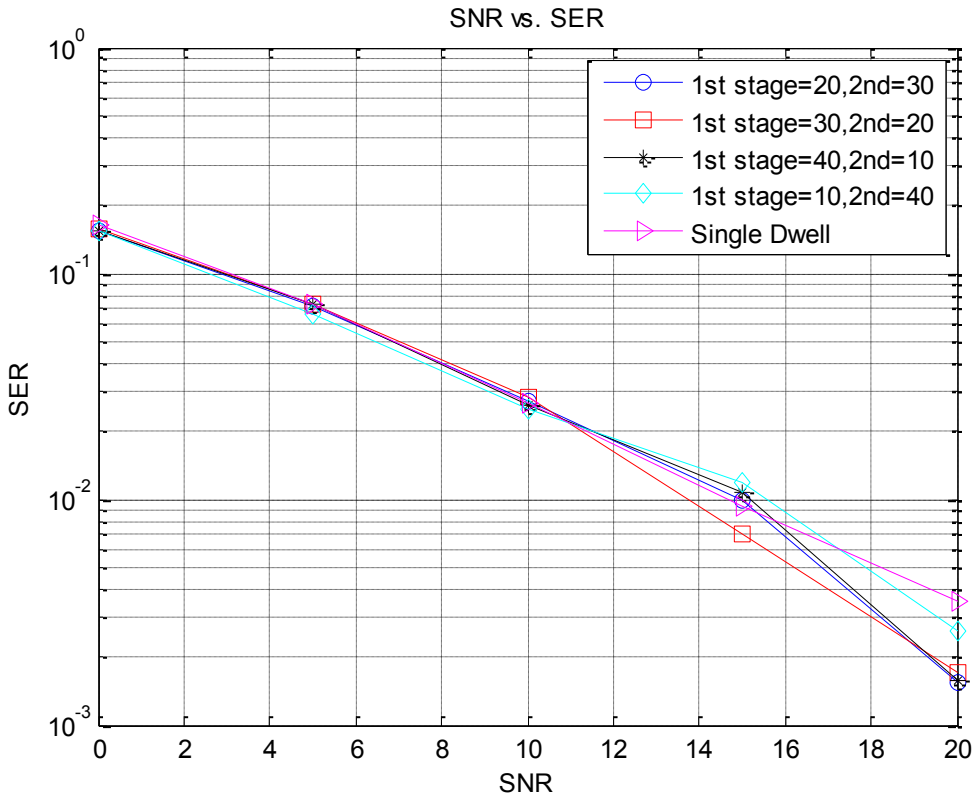

Figure 58: Impact of correlation windows on SER with 50 correlations and ER=5

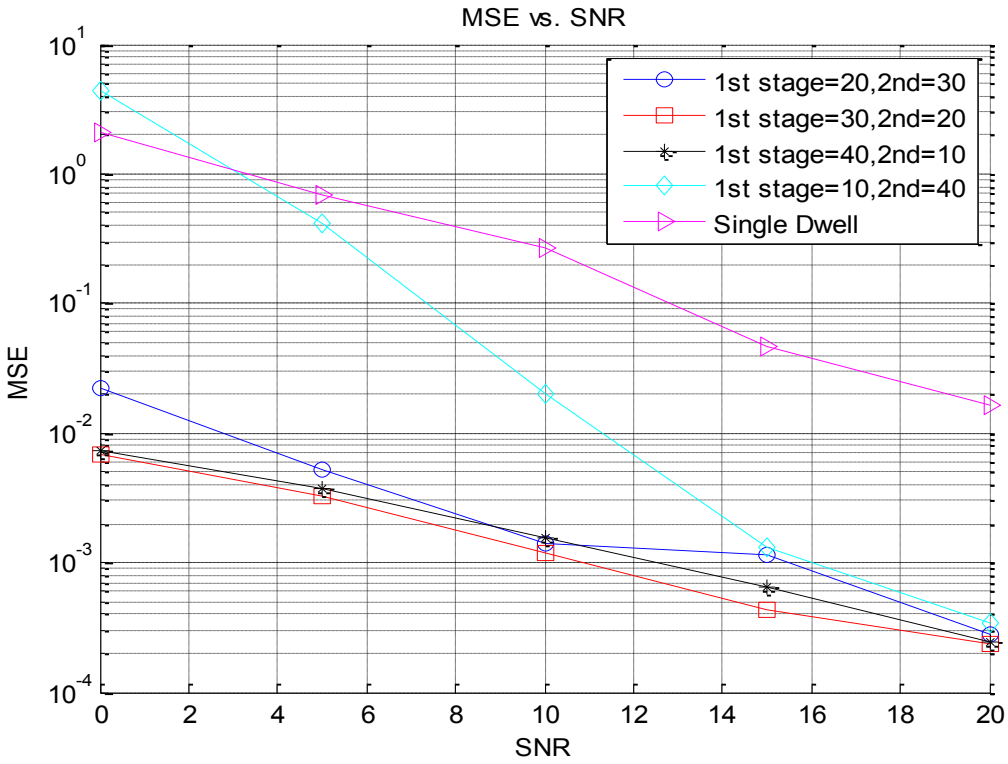

Figure 59: Impact of correlation windows on MSE with 50 correlations and ER=10

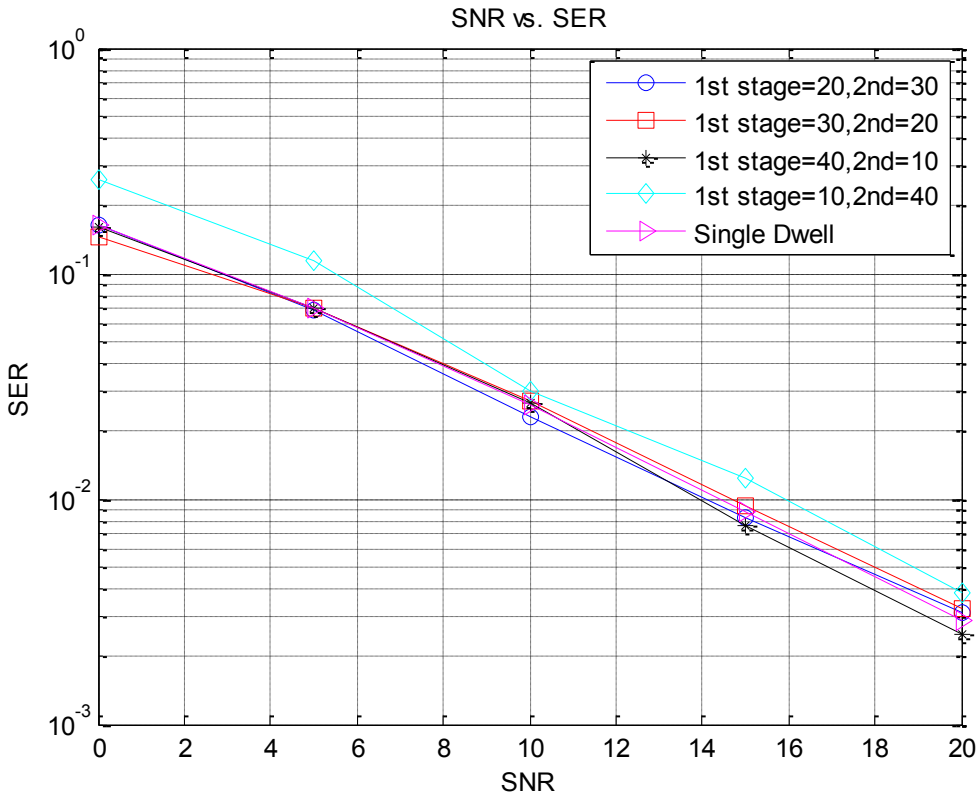

Figure 60: Impact of correlation windows on SER with 50 correlations and ER=10

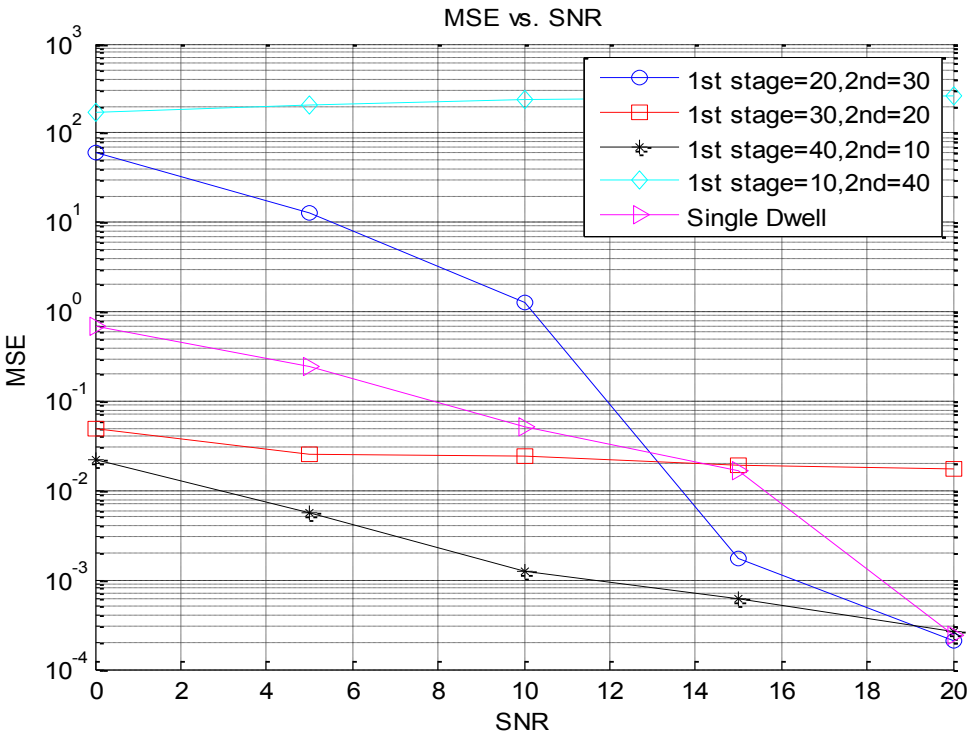

Figure 61: Impact of correlation windows on MSE with 50 correlations and ER=20

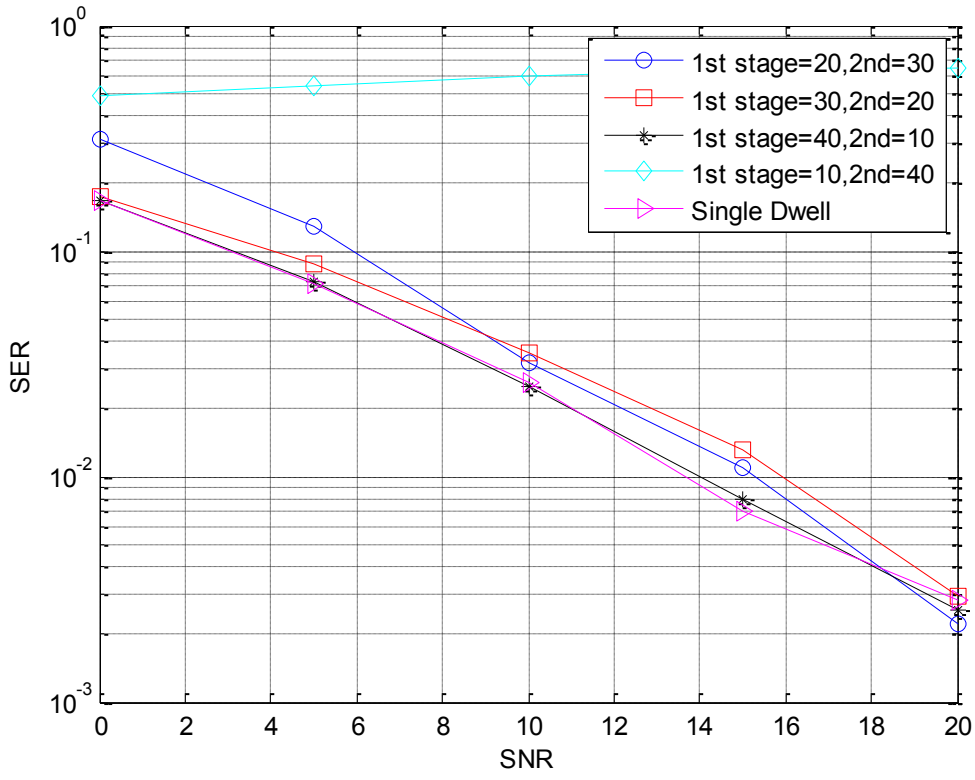

Figure 62: Impact of correlation windows on SER with 50 correlations and ER=20

5.3.4. Doppler Frequency

In all previous simulations, the Doppler frequency was set to 2 Hz. In this section, variation of the Doppler frequency is investigated. Simulations are run for a Doppler frequency of 2, 20, or 50 Hz, indicating slow, medium, and fast channel conditions, respectively. The simulations are run with ER=3, f_{sn}=1.7 and 10 averages. The obtained MSE and SER results show large degradation for higher Doppler frequency as shown in Figure 63 and Figure 64 for the MSE and the SER results, respectively. It should be noted that as the Doppler frequency increases, channel variation becomes faster and more difficult to be tracked causing more frequency offset and hence, more degradation.

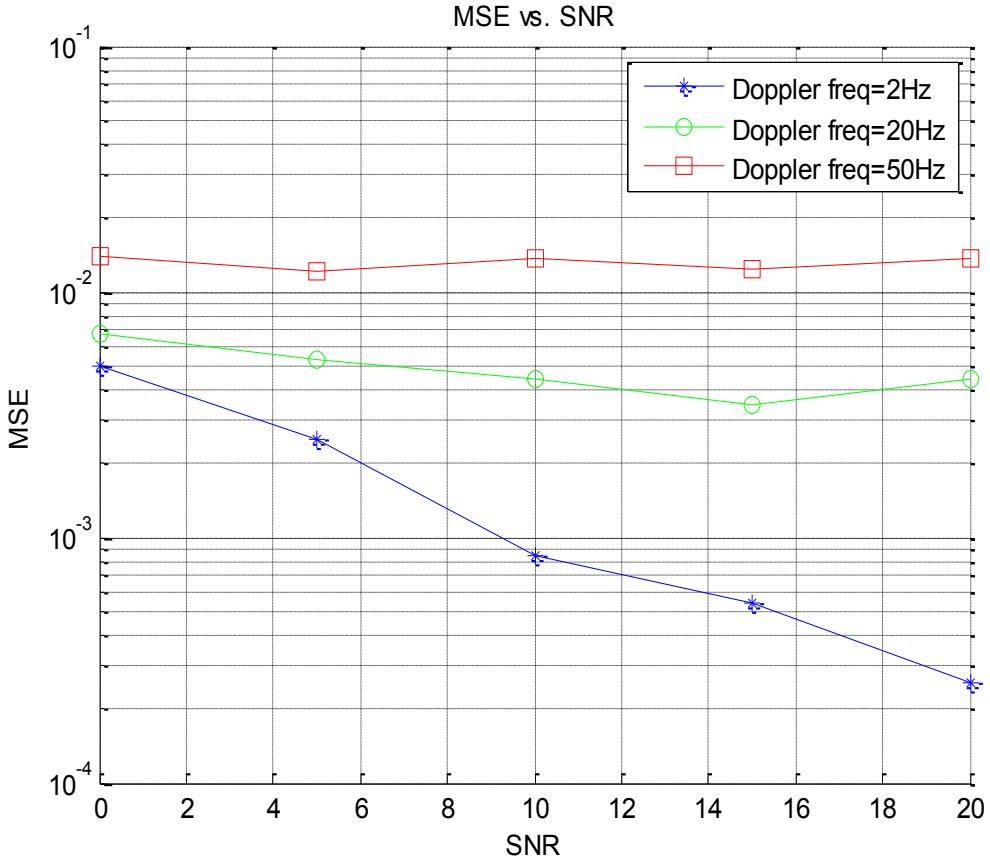

Figure 63: Impact of channel variation on MSE performance

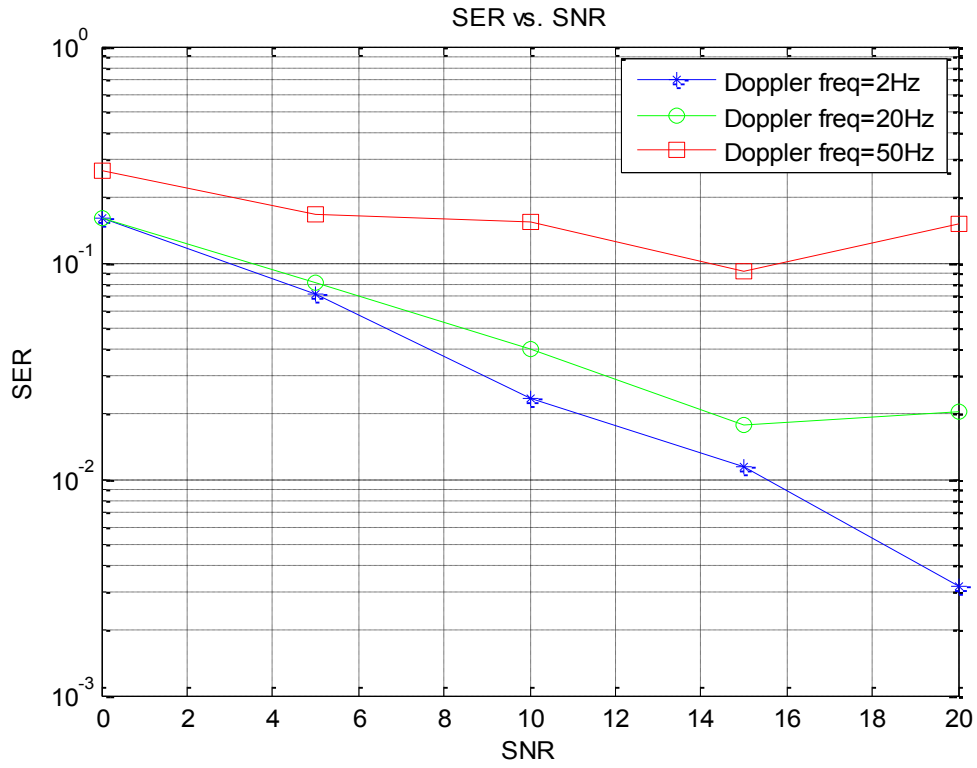

Figure 64: Impact of channel variation on SER performance

5.3.5. Averaging Window

In this section, the effect of averaging is illustrated by adding an averaging operation to the correlation results. Simulations are run for different averaging windows and the normalized offset is set to 1.2 and the estimation range is set to 5 with N_1=40 and N_2=60. Figure 65 shows the improvement in the MSE performance at different averaging windows. For instance, 4 dB SNR is needed to achieve MSE of (10^{-2}) with 2 averages while 17 dB SNR is needed to achieve the same MSE without averages. It was also noted that 5 averages are sufficient to improve the performance by almost two orders of magnitude and adding more averages would add more delay without adding any extra performance gain.

Next, simulations are run to investigate the effect of averaging at different Doppler frequencies. The results show that averaging has less effect for higher Doppler frequencies as channel variation becomes faster and more difficult to track. Figures 67 to 70 illustrate the results for Doppler frequencies of 20 and 50 Hz.

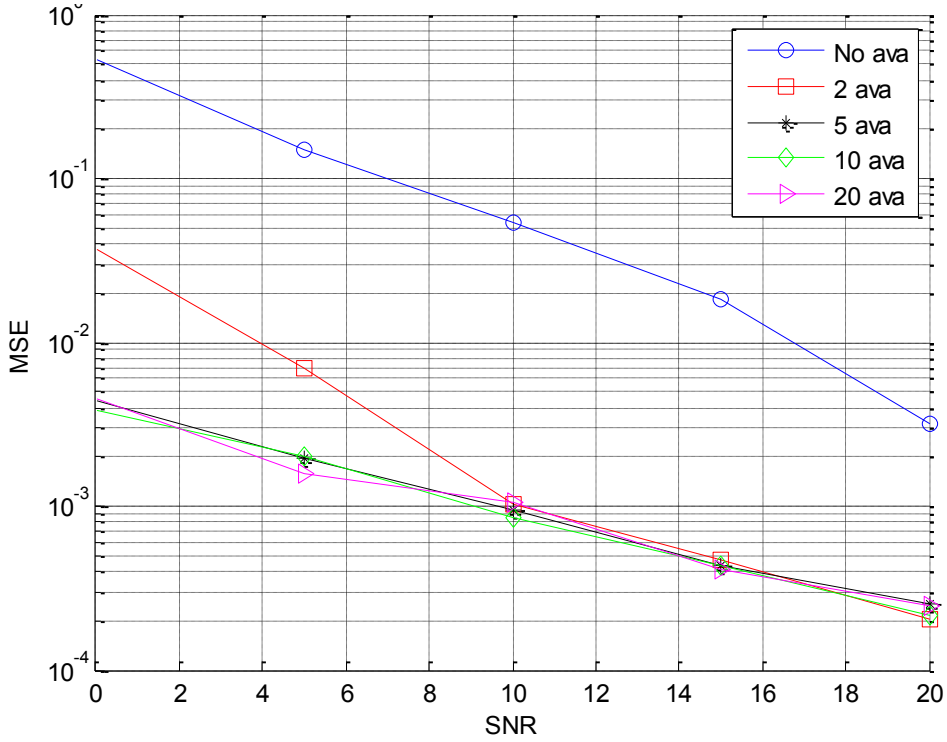

Figure 65: Variation of MSE with number of averaged correlations for Doppler =2 Hz

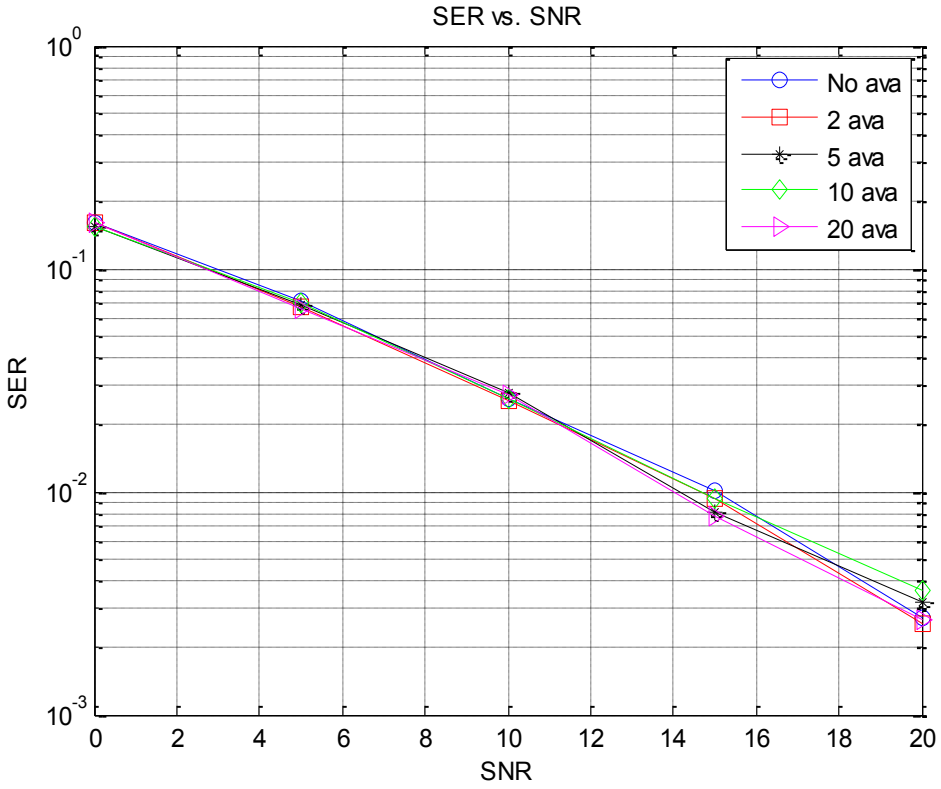

Figure 66: SER performance with number of averaged correlations for Doppler=2 Hz

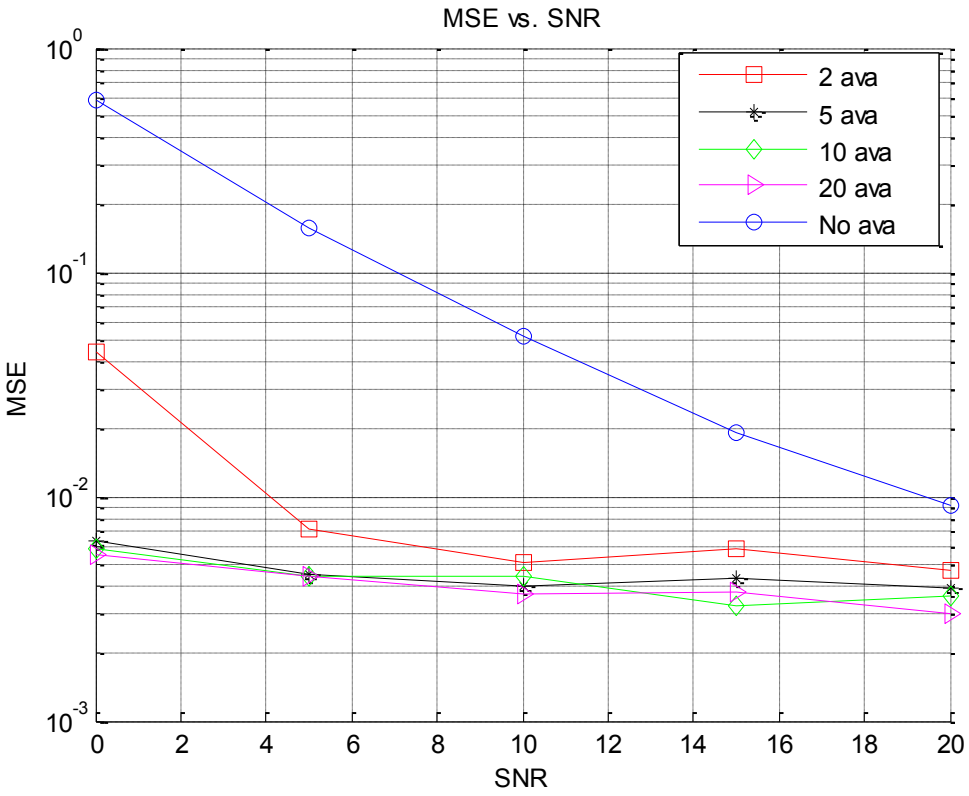

Figure 67: Variation of MSE with number of averaged correlations for Doppler =20 Hz

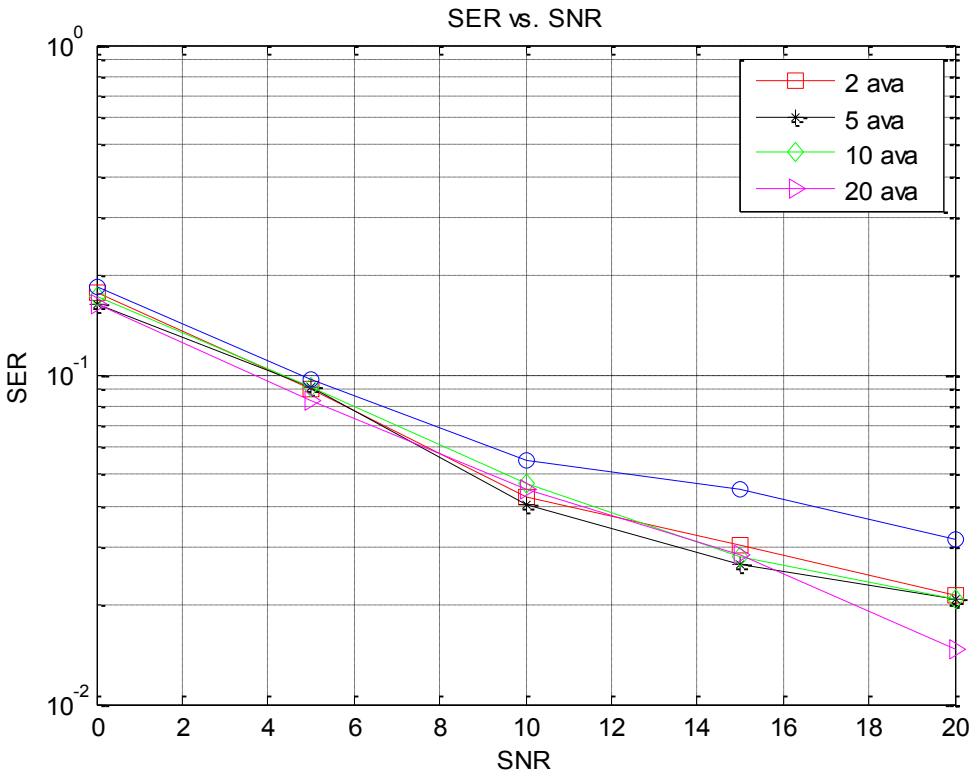

Figure 68: Variation of SER with number of averaged correlations for Doppler=20 Hz

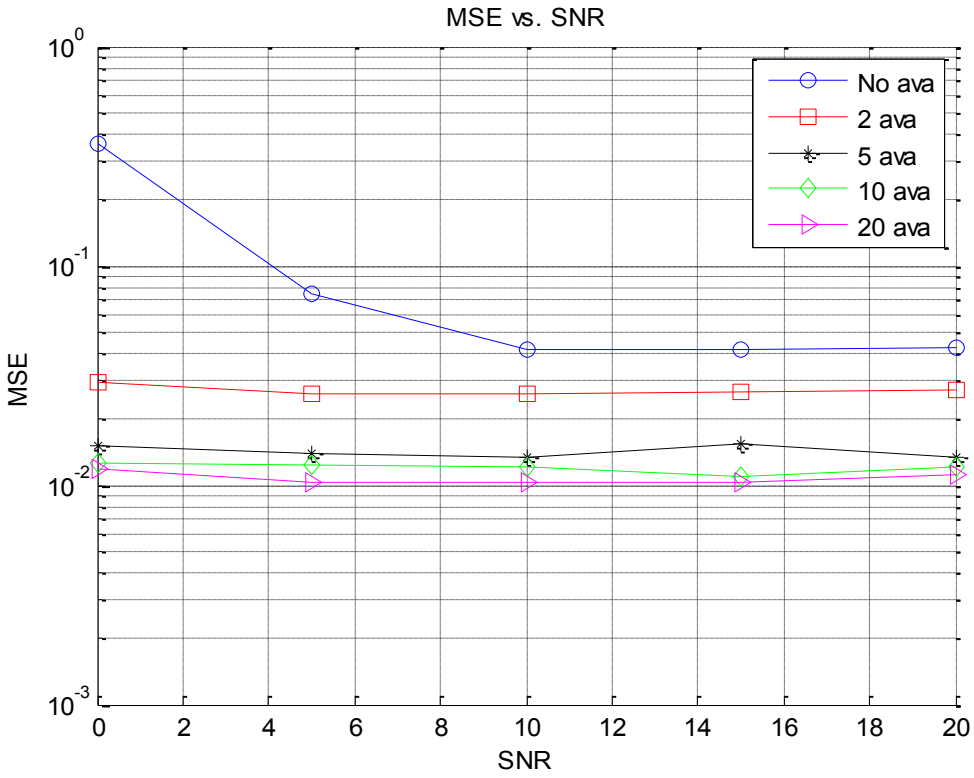

Figure 69: Variation of MSE with number of averaged correlations for Doppler =50 Hz

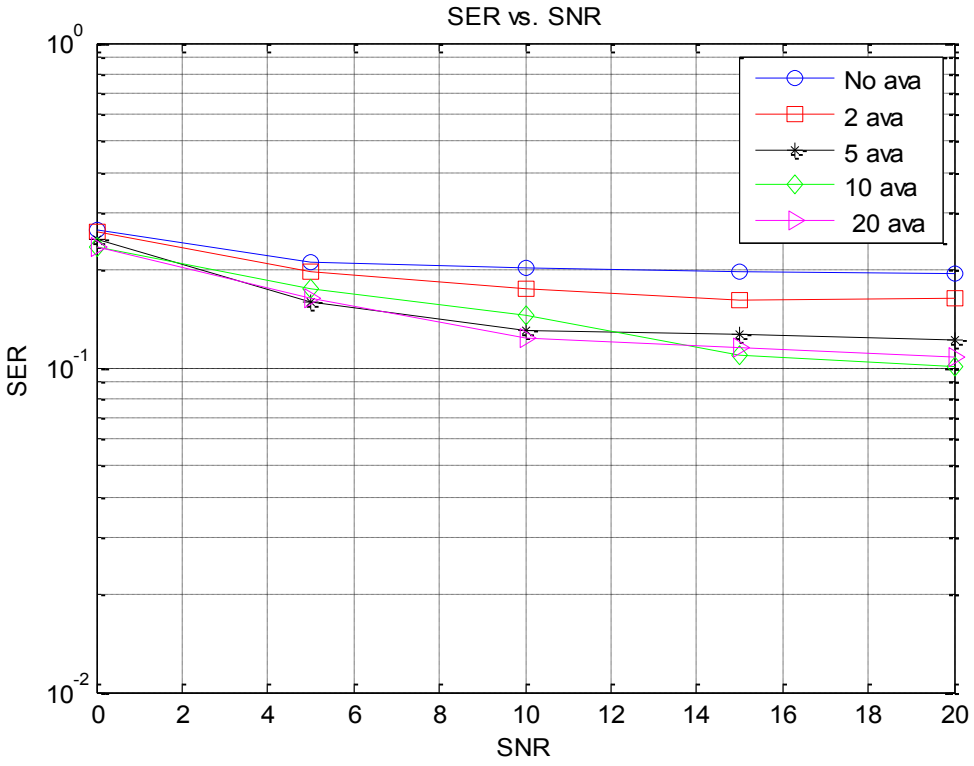

Figure 70: Variation of SER with number of averaged correlations for Doppler=50 Hz

Further, averaging is added to the SDS and simulations are run to compare both DDS and SDS performance at different averaging windows. The MSE and the SER results are shown in Figure 71 and Figure 72, respectively. The performance of both systems is evaluated with and without averaging. In these simulations, the offset value is set to 1.4, *ER*=10, 50 correlation with $N_1 = 40$ and $N_2 = 10$. The MSE results for the SDS do not show any improvement after 2 averages at which the system shows steady performance even for large SNR values. On the other hand, the DDS performance continues to improve for higher SNR values. It is important to note that averaging in SDS is more complex and requires more computations as it is applied to the total length of the correlation window while in the DDS averaging is applied after the first stage correlation which requires a fewer number of computations. For instance, the total needed computation using 5 averages in SDS with 100 correlations is 500 (5*100) but in DDS with $N_1 = 50$ and $N_2 = 50$, the computations needed reduces to 300(5*50+50). Therefore, averaging in SDS adds more delay to complete the estimation process as compared to the DDS.

Simulations are then run to investigate the effect of averaging with random generation of the offset values. The MSE results are shown in Figure 73 showing slight degradation when compared with the case of deterministic offset. However, the SER is similar for both cases as shown in Figure 74.

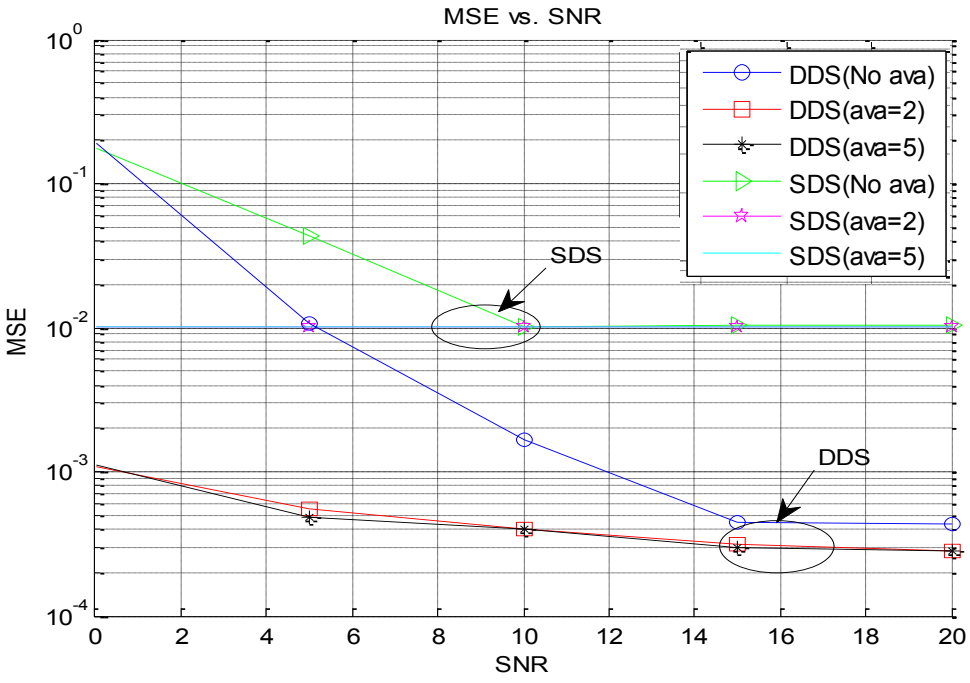

Figure 71: MSE for SDS and DDS for different averaging windows at deterministic offset

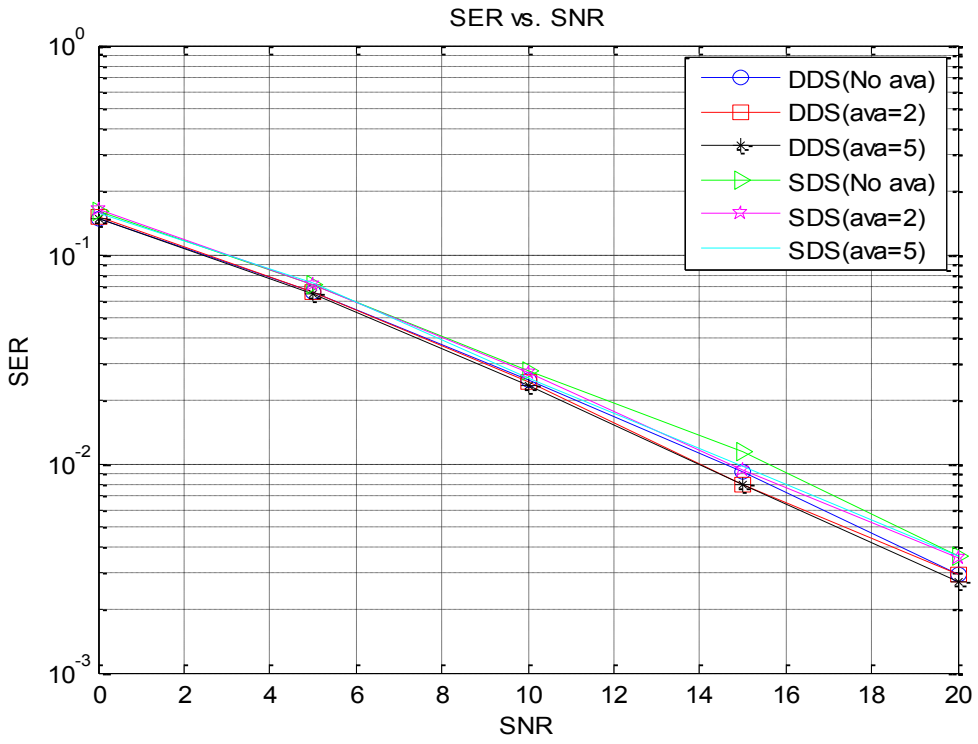

Figure 72: SER for SDS and DDS for different averaging windows for deterministic offset

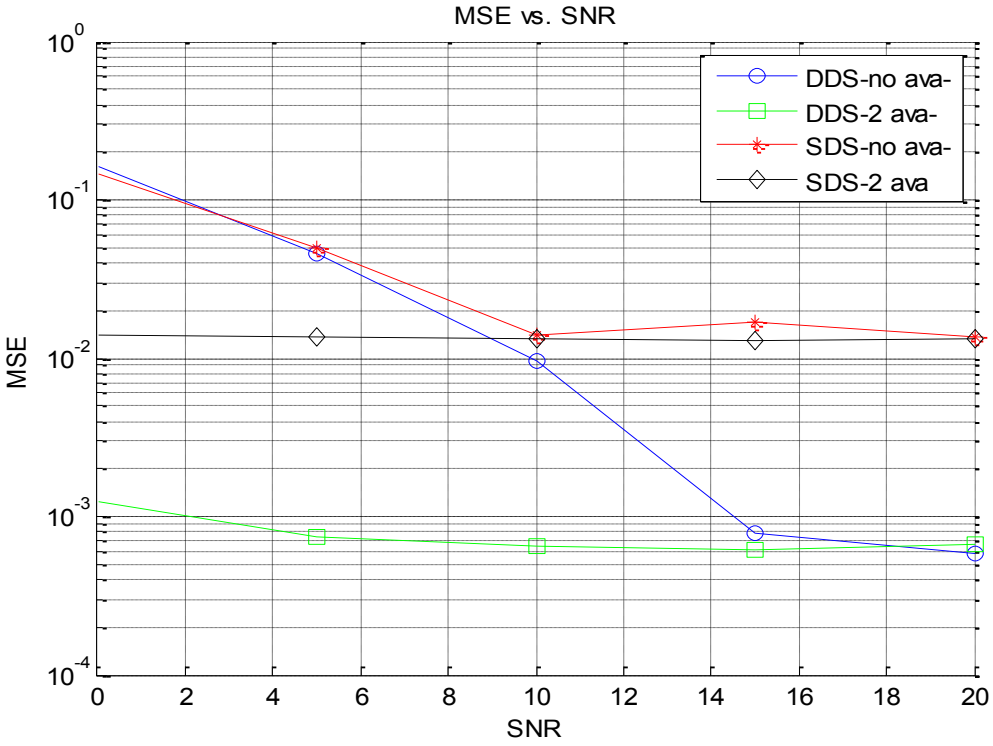

Figure 73: MSE for different averaging windows for random offset

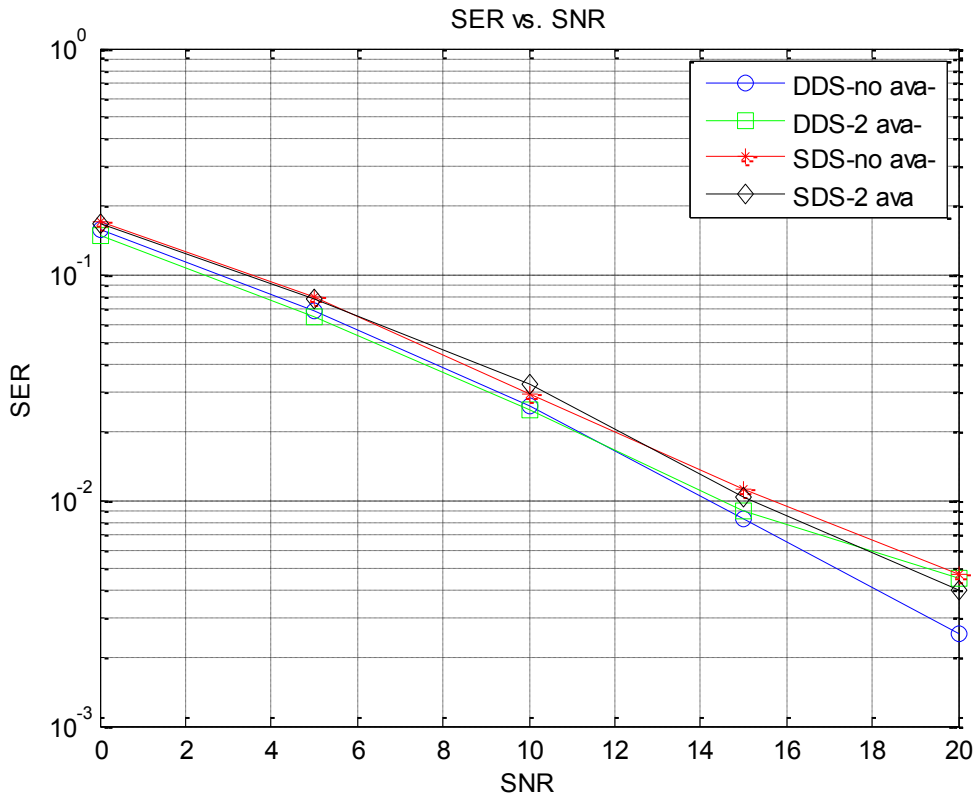

Figure 74: SER for different averaging windows for random offset value

5.4. Effect of Interference

In this section, the effect of interference is examined by adding another OFDM transmitter sending simultaneously with the desired user. Simulations are run to examine the effect of interference on the perfectly synchronized system and both SDS and DDS. Figure 75 shows the obtained results at different signal-to-interference ratios (SIR) assuming perfect synchronization (no offset) where more degradation is noticed for lower SIR (higher power of the interfering block). For example, 13 dB of SNR is required to achieve a SER of (10^{-2}) in the no interference case, which increases to 15 dB for SIR=20 dB, while this SER cannot be achieved for SIR=0 dB.

Simulations are then run to examine the performance of SDS and the DDS under interference conditions. Simulation parameters are set as follows: f_{sn}=0.75, *ER*=10, and 100 total correlations. The MSE and SER results for both systems are shown in Figures 76 to 79. Finally, a comparison between the two systems is illustrated in Figures 80 and 81. The same conclusion can be drawn in all cases in

which the higher the power of the interfering, the more the degradation in the MSE and SER performance.

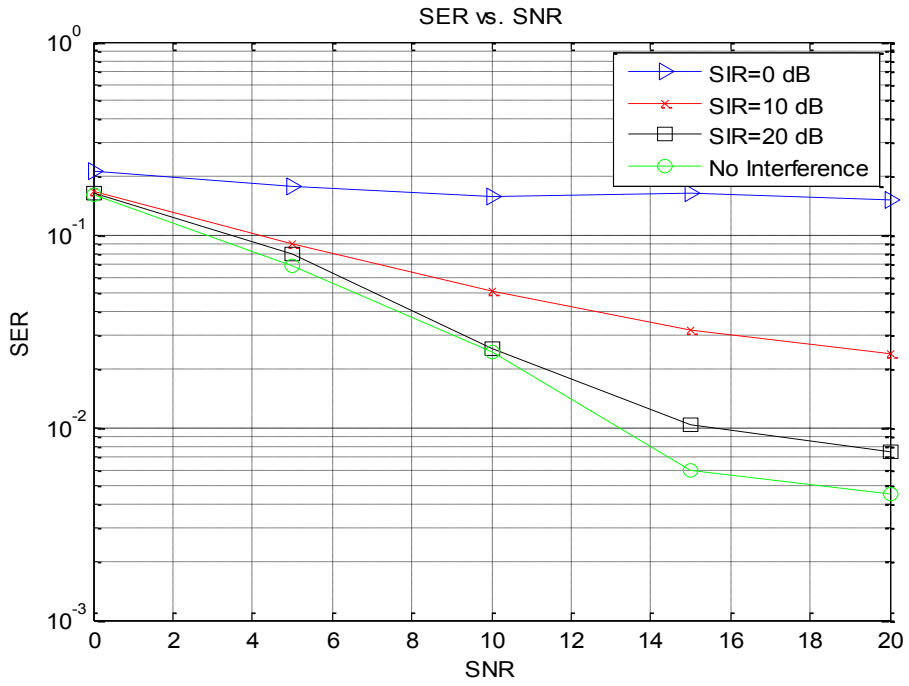

Figure 75: Effect of interference on OFDM system with no frequency offset

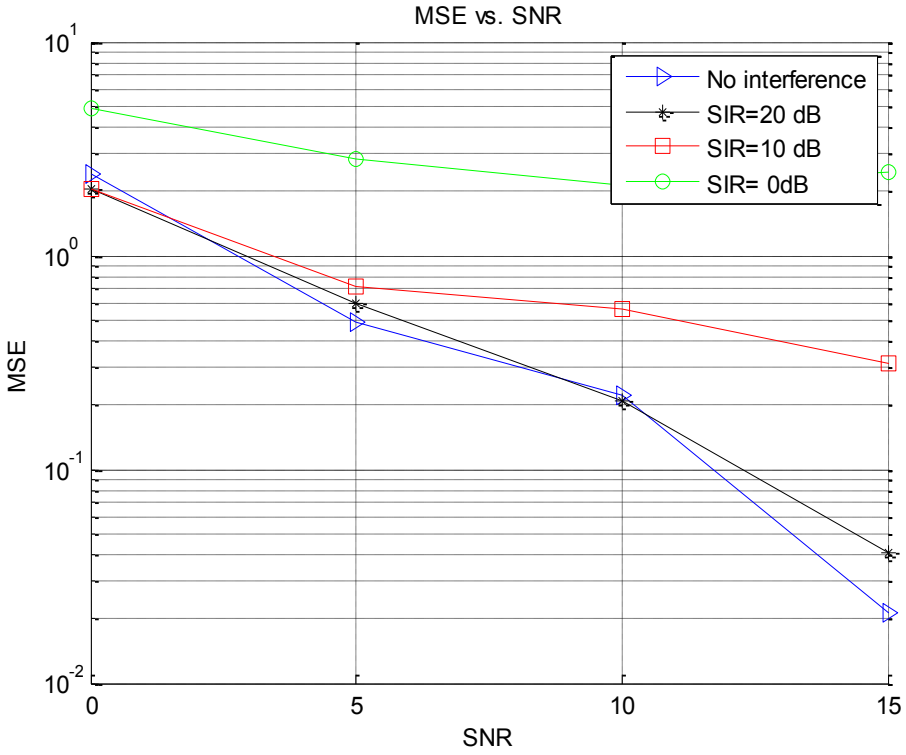

Figure 76: MSE for SDS at different SIR

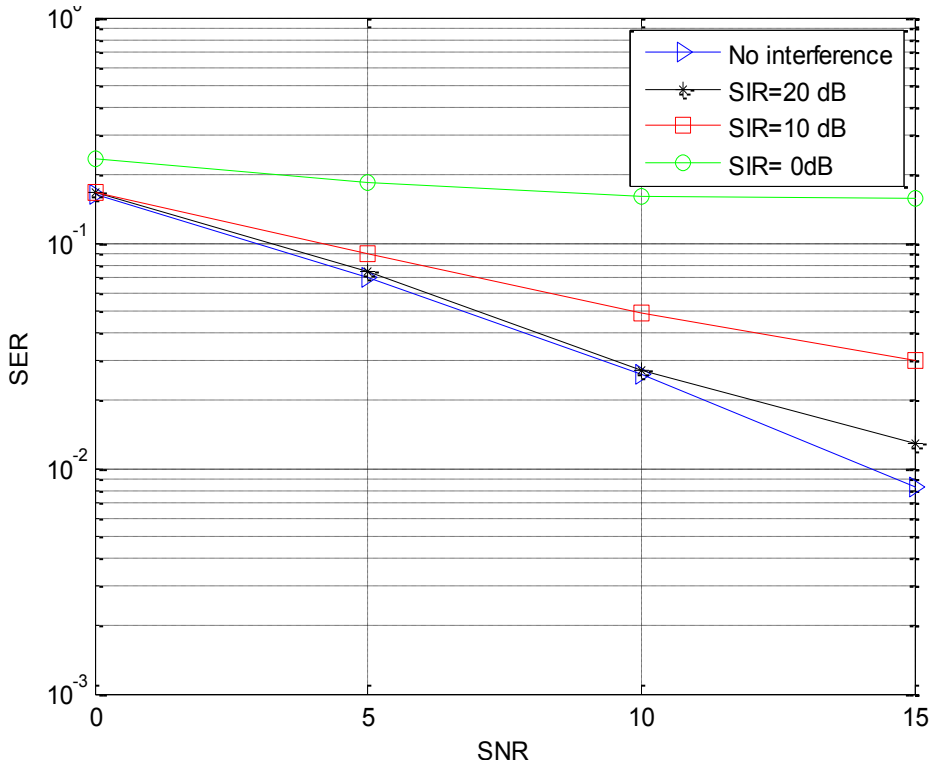

Figure 77: SER for SDS at different SIR

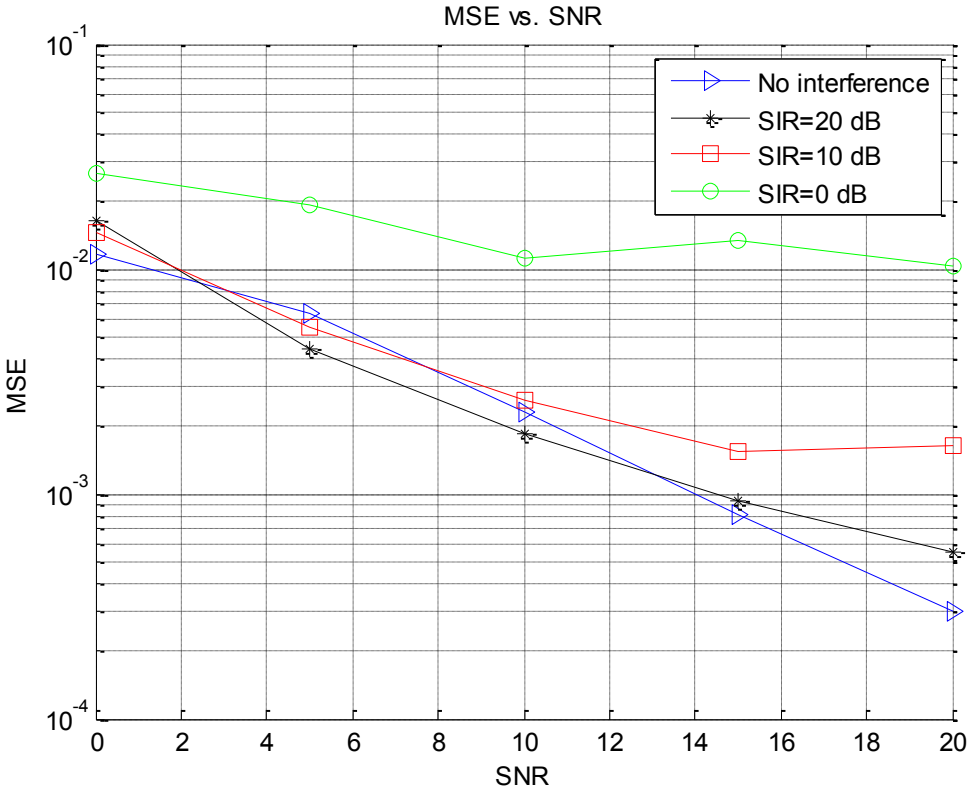

Figure 78: MSE for DDS at different SIR

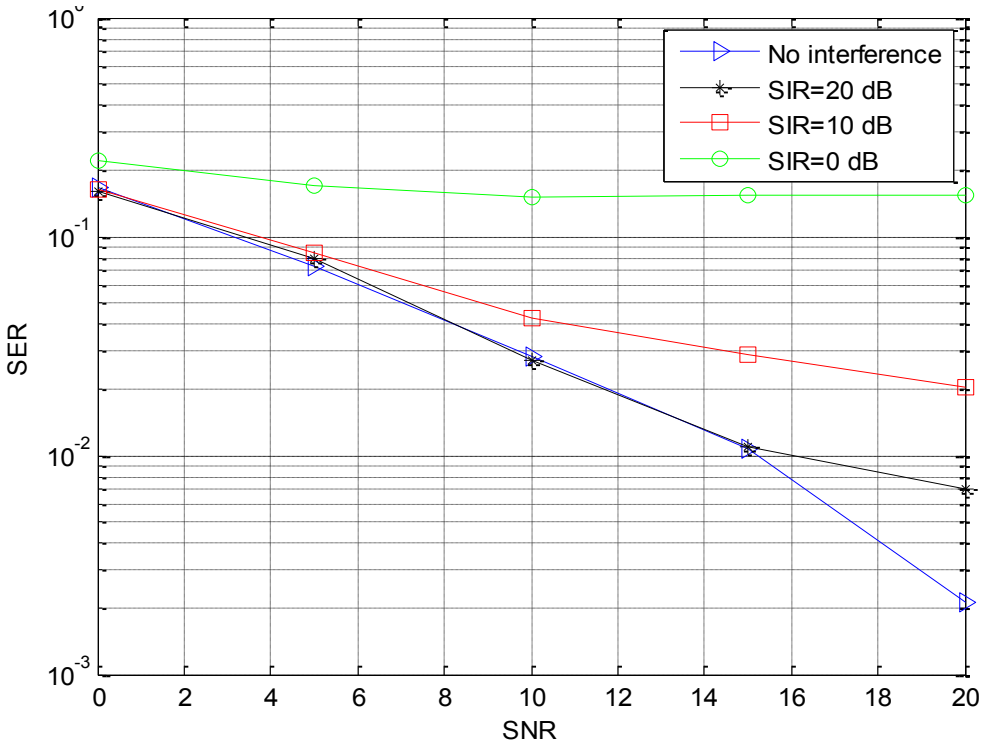

Figure 79: SER for DDS at different SIR

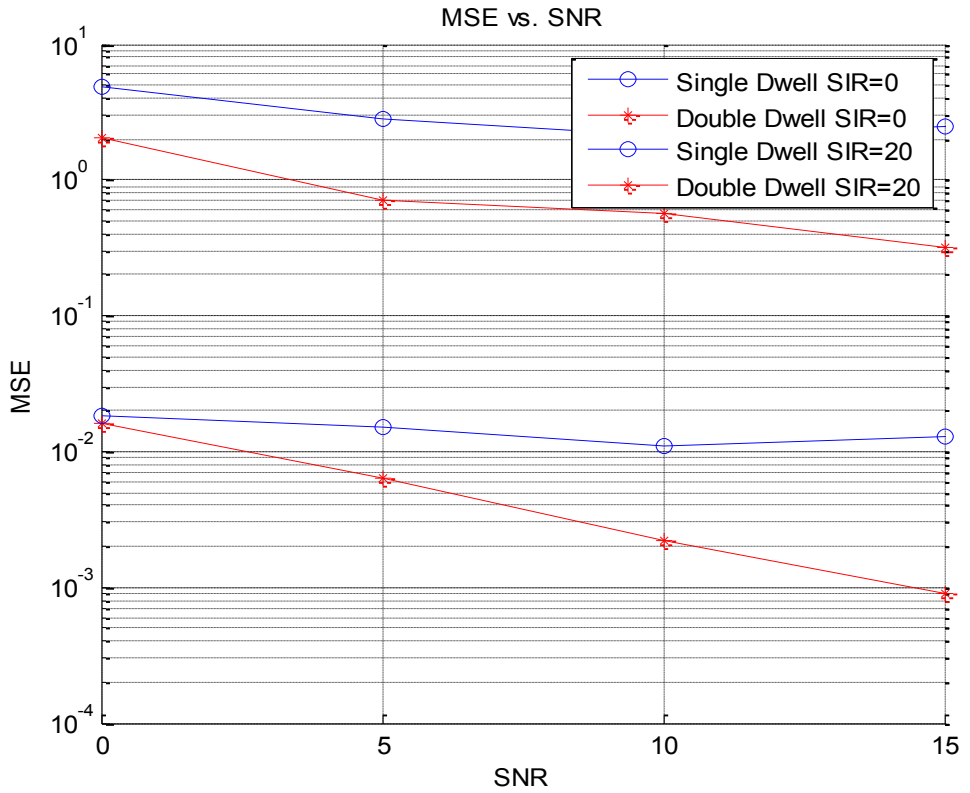

Figure 80: Comparison between MSE performance for SDS and DDS at different SIR

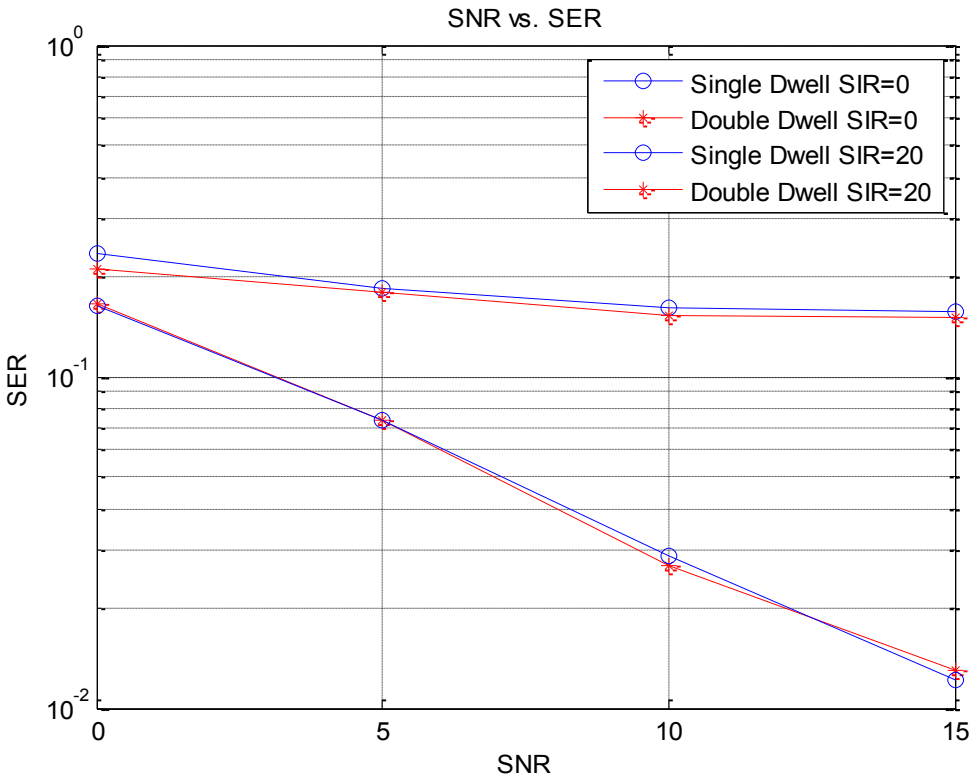

Figure 81: Comparison between SER performance for SDS and DDS at different SIR

5.5. Design of Pilot Symbols

In this section, the effect of pilot symbols is investigated from two perspectives; first the impact of the number of used pilot subcarriers and second the choice of pilot sequence. Simulations are run for both AWGN and fading channels with f_{sn} = 1.7, *ER*=5, and 100 total correlations in a 64 subcarriers system with the experiment repeated 5000 times. The pilots are inserted at the transmitter before performing the IFFT. At the receiver, the pilots are first extracted and the carrier offset estimation is performed using the pilot subcarriers only.

5.5.1. Number of Pilot Subcarriers

Simulations were run for the DDS in an AWGN channel using 32, 16, 8, and 4 pilot subcarriers. Figure 82 shows the pilot subcarriers arrangement assuming 16 pilots in a 64 subcarriers system.

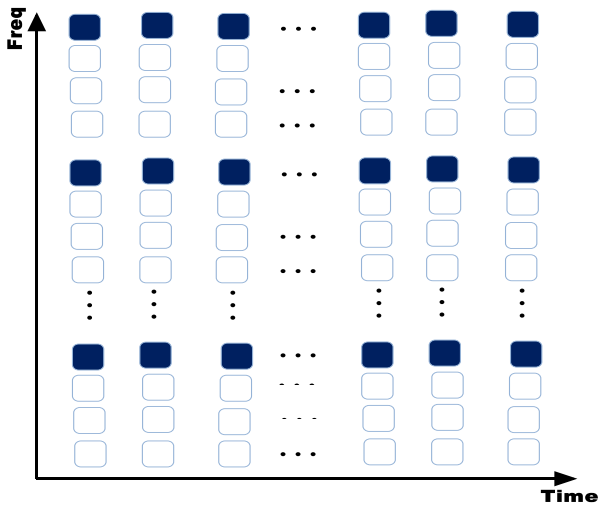

Figure 82 :pilot subcarrier arrangement using 16 pilots

Figure 83 shows the obtained MSE results, as expected, increasing the number of pilot subcarriers improves the MSE performance. For instance, about 6 dB of SNR is needed to achieve MSE of (10^{-4}) using 32 pilots, while 9 dB is needed to achieve the same MSE using 16 pilots. The SER performance is shown in Figure 84 with the larger number of subcarriers resulting in a slightly better performance. However, increasing the number of pilots reduces the number of subcarriers used for actual data transmission, hence reducing the bandwidth efficiency of the system. Similar results are obtained for fading channel as shown in Figure 85 and 86 for the MSE and SER performance.

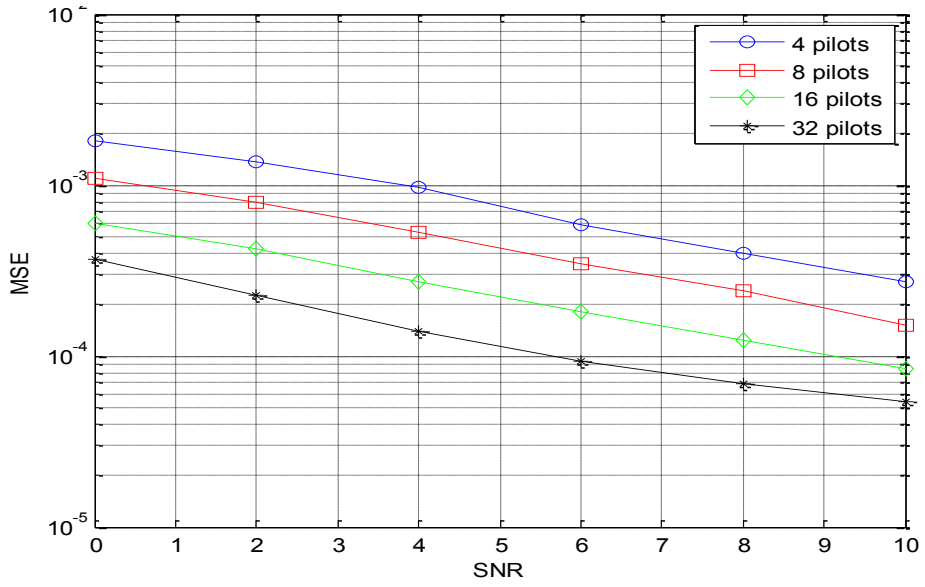

Figure 83: MSE performance using different number of pilot subcarriers in AWGN

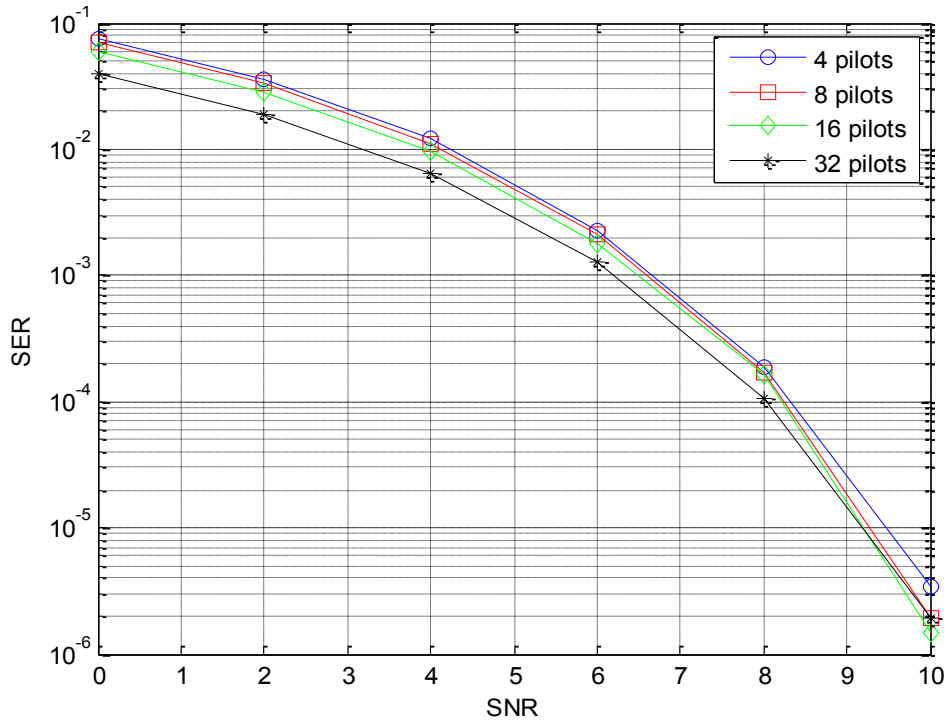

Figure 84 : SER performance using different number of pilot subcarries in AWGN

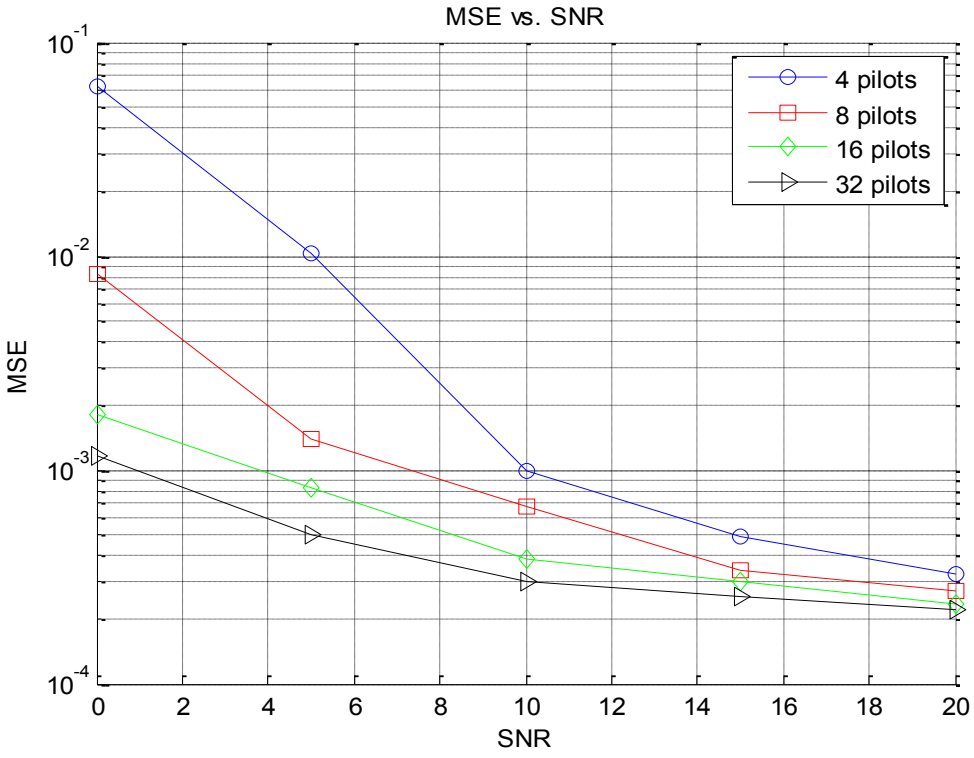

Figure 85: MSE performance using different number of pilot subcarriers in fading channel

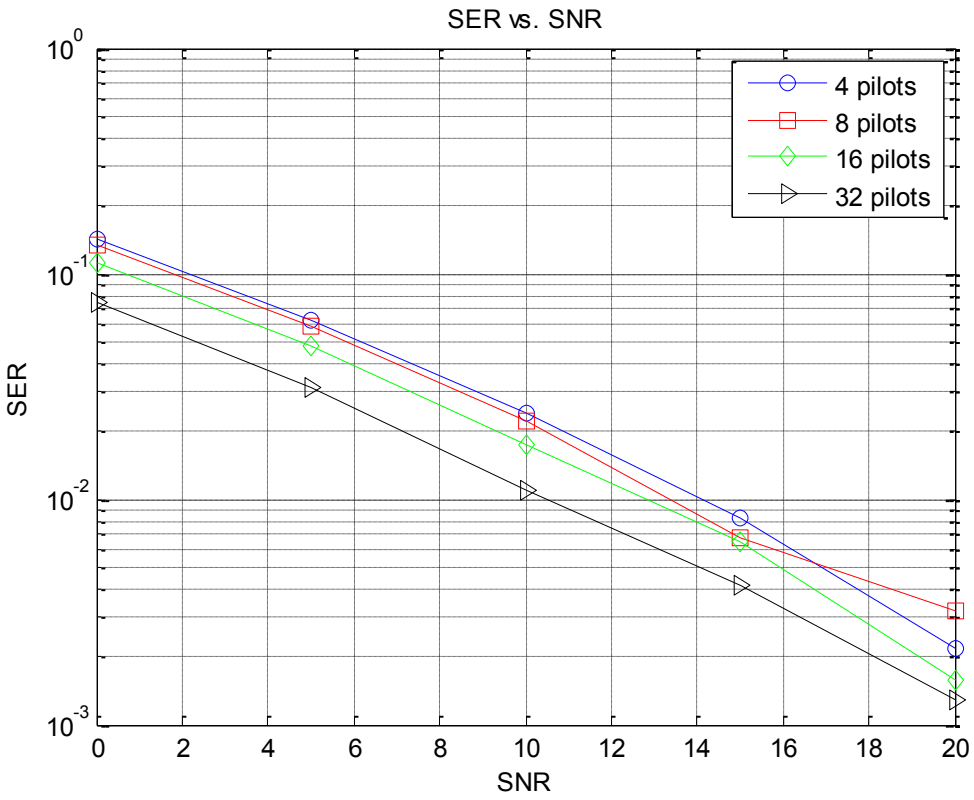

Figure 86: SER performance using different number of pilot subcarriers in fading channel

5.5.2. Pilots Sequence

Three commonly used pilot sequences are investigated to search for the best sequence to minimize the MSE for the DDS, namely: complex–valued sequence, antipodal randomly generated sequence, and pseudo noise (PN) or m-sequence. Simulations are repeated for both AWGN and fading using 16 pilot subcarriers with the same simulation parameters as in the previous section. The results show that the performance is not affected by the type of sequence in AWGN channel conditions, as illustrated in Figure 87 and 88 for MSE and SER, respectively. However, the use of m-sequence for fading channel results in some improvement in the MSE performance as shown in Figure 89, while it does effect the SER performance as shown in Figure 90. The results show that the proposed DDS is capable of tracking and correcting for the frequency offset even when a small number of pilots is employed.

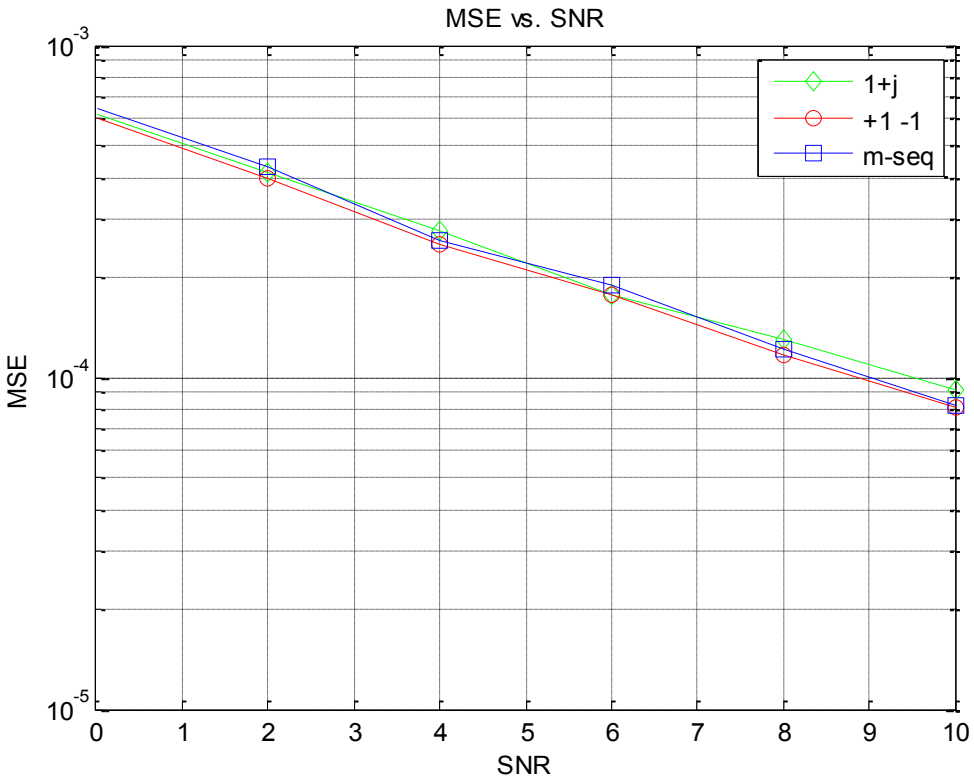

Figure 87: Effect of used pilot sequence in MSE performance for AWGN channel

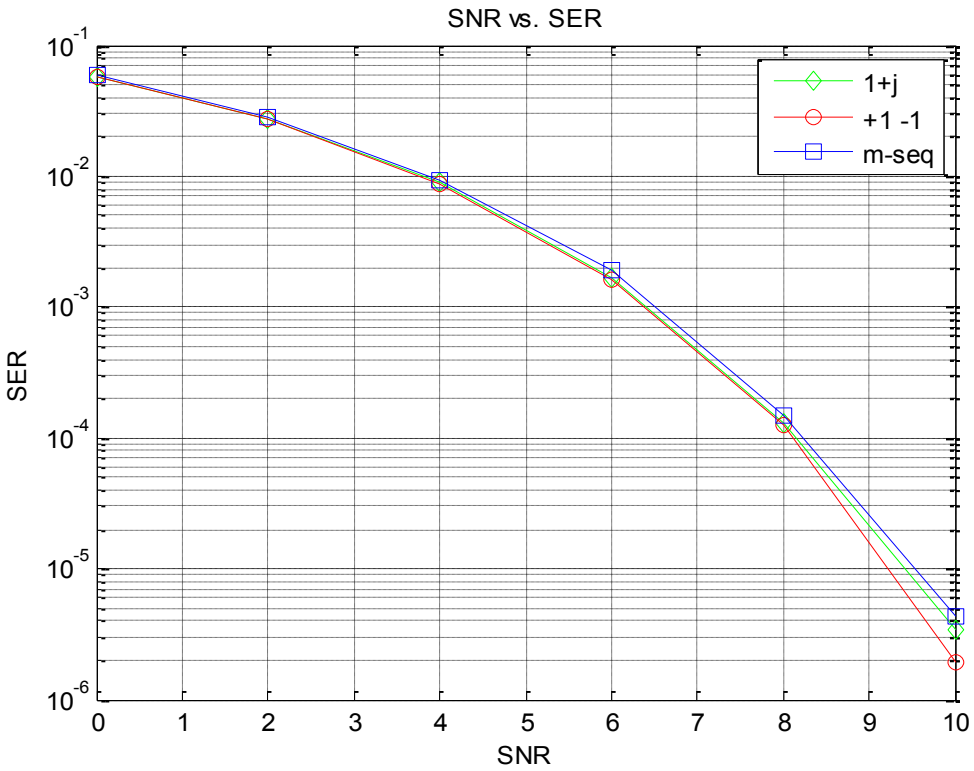

Figure 88: Effect of used pilot sequence in SER performance for AWGN channel

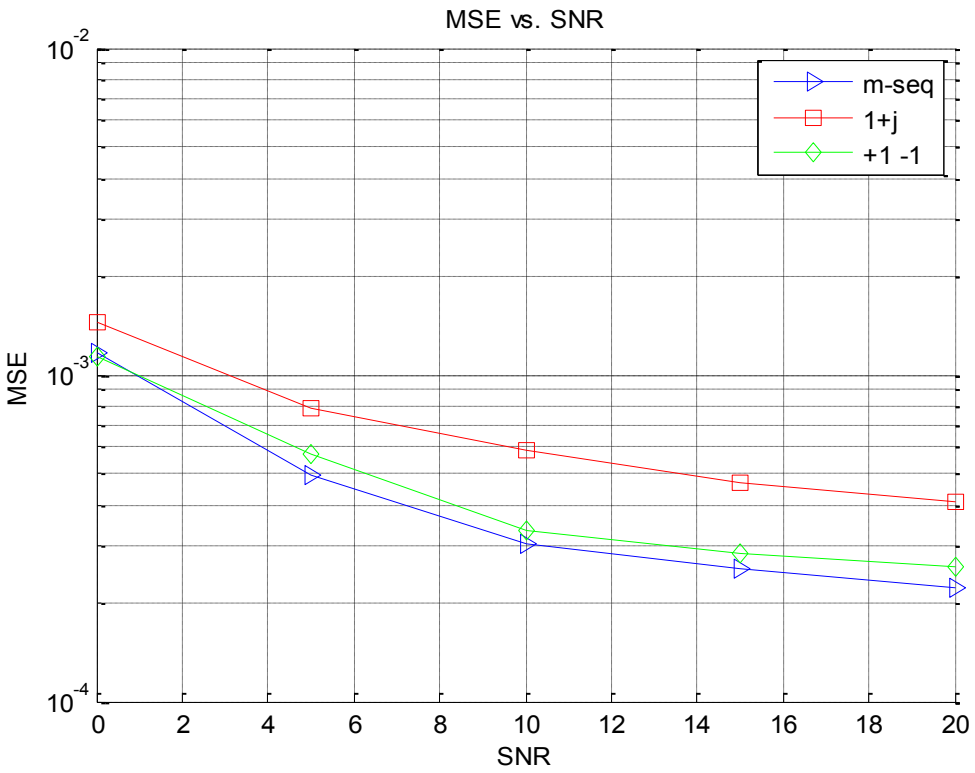

Figure 89: Effect of used pilot sequence in MSE performance for flat fading channel

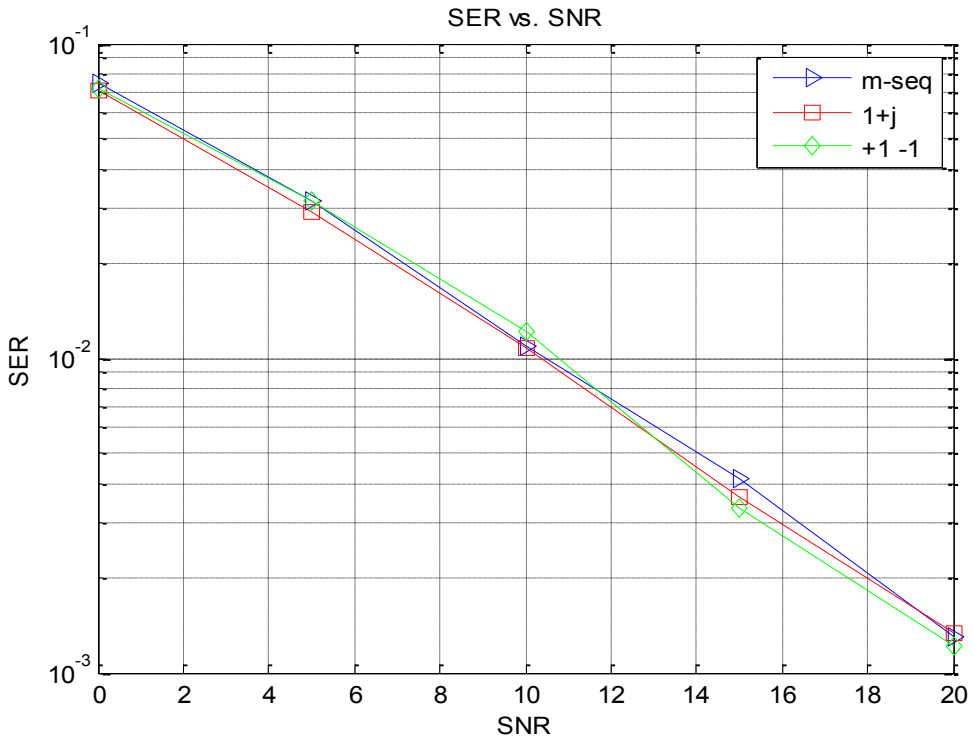

Figure 90: Effect of used pilot sequence in SER performance for flat fading channel

Chapter 6: Conclusion

OFDM has emerged in many recent communication systems as a promising technology due to its numerous advantages over traditional techniques. However, frequency synchronization is essential in OFDM systems to preserve orthogonality and maintain good performance. In this thesis, a Double-Dwell frequency synchronization algorithm for OFDM signals is presented. The proposed scheme relies on pilot data that is used to perform an initial coarse search for the carrier offset followed by a more accurate fine search. Variable step size is used to search for the frequency offset in each stage. Different design parameters are investigated to optimize the searching process such as the search step size, estimation range, number of subcarriers, and pilot symbol selection. The performance of the proposed scheme is evaluated through extensive simulations in both AWGN and flat Rayleigh fading channels.

Simulation results show that the proposed scheme provides a significant improvement in the MSE performance compared to the conventional Single-Dwell scheme without incurring any increase in complexity. It is shown that the proposed scheme can work for large frequency offset ranges but at a reduced accuracy. The effect of the estimation range as well as the total number of performed correlations and the searching step size is examined. It is noticed that the best performance is achieved for the largest number of correlations with the narrowest estimation range. However, increasing the number of correlations increases the implementation complexity and reduces the estimation range reducing the system's capability to track large offset values. The number of the used subcarriers also affects the estimation accuracy and simulation results show that increasing the number of subcarriers provides better MSE performance. In the case of fading conditions, averaging the first stage correlations is necessary to avoid large errors in estimating the offset due to deep fades. It is shown that the averaging operation improves the MSE performance by more than two orders of magnitude compared to the case without averaging. We have also discussed the performance degradation in the proposed scheme due to the presence of interference from other users. Finally, the effect of the number of employed pilot subcarriers and the impact of selecting different types of pilot symbols have been investigated, showing that higher number of pilot subcarriers improves the

system performance but reduces actual data transmission and hence the bandwidth efficiency of the system and the use of m-sequence pilots give better performance in fading channels.

Some of the research that can be investigated as a continuation of this work includes assessing the impact of frequency selective fading on the proposed synchronization scheme performance. Although an OFDM system is designed to mitigate interference due to multipath, the synchronization scheme might not cope with multipath resulting in major degradation in the system performance. This needs to be investigated and might result in the need for a modified structure to mitigate the interference, such as the use of MIMO systems. Another extension to this work might include investigation of joint timing and frequency synchronization using the proposed scheme.

.

References

[1] M. Jiang and L. Hanzo, "Multiuser MIMO-OFDM for Next-Generation Wireless Systems," *Proceedings of the IEEE,* vol. 95, no. 7, pp. 1430-1469, 2007.

[2] R. VanNee and R. Prasad, *OFDM for Wireless Multimedia Communication,* Bosten: Artech house publishers, 2000.

[3] J.Faezah and K.Sabira, "Adaptive Modulation for OFDM Systems," *International Journal of Communication Networks and Information Security (IJCNIS),* vol. 1, no. 2, 2009.

[4] B. Ballal, A. Chadha and N. Satam, "Orthogonal Frequency Division Multiplexing and its Applications," *International Journal of Science and Research (IJSR),* vol. 2, no. 1, pp. 325-328, 2013.

[5] K. Fazel and S. Kaiser, *Multi-Carrier and Spread Spectrum Systems*, England: WILEY, 2003.

[6] N. Pathak, "OFDM (Orthogonal Frequency Division Multiplexing) SIMULATION USING MATLAB," *International Journal of Engineering Research & Technology,* vol. 1, no. 6, pp. 1-6, 2012.

[7] T. Keller, L. Piazzo, P. Mandarini and L. Hanzo, "Orthogonal Frequency Division Multiplex Synchronization Techniques for Frequency-Selective Fading Channels," *IEEE Journal on Selected Areas in Communications,* vol. 19, no. 6, pp. 999-1008, 2001.

[8] J.Proakis and M. Salehi, *Digital Communication*, New York: McGraw Hill, *5th edition*, 2008.

[9] N. LaSorte, W. Barnes and H. Refai, "The History of Orthogonal Frequency Division Multiplexing," in *Global Communications Conference* , New Orleans, 2008.

[10 C. Langton, 2005. [Online]. Available: http://complextoreal.com/wp-content/uploads/2013/01/ofdm2.pdf. [Accessed 16 December 2014].

[11] M. Viswanathan, 27 June 2001. [Online]. Available: http://www.gaussianwaves.com/2011/06/introduction-to-ofdm-orthogonal-frequency-division-multiplexing-part-3/. [Accessed 16 December 2014].

[12] A. Cortés, I. Vélez, M. Turrillas and J. Sevillano, "Fast Fourier Transform Processors: Implementing FFT and IFFT Cores for OFDM Communication Systems," in *Fourier Transform - Signal Processing*, InTech, 2012, pp. 953-978.

[13] Lecture Notes [Online]. Available http://www.cs.nccu.edu.tw/~lien/NIIslide/WirelessTech/propage.htm. [Accessed 16

December 2014].

[14] N. Marchetti, M. Rahman, S. Kumar and R. Prasad, "OFDM: Principles and Challenges," in *New Directions in Wireless Communications Research*, New York, Springer US, 2009, pp. 29-62.

[15] V. Ramasami, "Orthogonal Frequency Division Multiplexing," [Online]. Available: https://www.cresis.ku.edu/~rvc/documents/862/862_ofdmreport.pdf. [Accessed 1 May 2013].

[16] R. Prasad, *OFDM for Wireless Communication*, Bosten: Artech House, 2004.

[17] M. Ghogho and A. Swami, "Carrier Frequency Synchronization for OFDM Systems," in *Signal Processing for Mobile Communications Handbook*, CRC Press, 2005.

[18] T. Pollet and M. Moeneclaey, "Synchronizability of OFDM Signals," in *Global Telecommunications Conference*, St.Louis, 1995.

[19] A. AI-Dweik, A. Hazmi and M. Renfors, "Joint Symbol Timing and Frequency Offset Estimation for Wireless OFDM Systems," in *Personal Indoor and Mobile Radio Communications(PIMRC)*, Cannes, 2008.

[20] B. Ai, Z.-x. Yang, C.-y. Pan, J.-h. Ge, Y. Wang and Z. Lu, "On the Synchronization Techniques for Wireless OFDM Systems," *IEEE Transactions on Broadcasting,* vol. 52, no. 2, pp. 236-244, 2006.

[21] H. Zhou, A. Malipatil and Y. Huang, "Synchronization Issues in OFDM systems," in *Asia Pacific Conference on Circuits and Systems (APCCAS)*, Singapore, 2006.

[22] M. Sandell, J. Beak and P. Borjesson, "Time and Frequency Synchronization in OFDM Systems Using the Cyclic Prefix," *In Proceedings of International Symmposium on Synchronization*, Germany, 1995.

[23] B. Ai, J. Ge, Y. Wang, S. Yang, P. Liu and G. Liu, "Frequency Offset Estimation for OFDM in Wireless Communications," *IEEE Transactions on Consumer Electronics,* vol. 50, no. 1, pp. 73-77, 2004.

[24] C. Shaw and M. Rice, "Optimum Pilot Sequences for Data-Aided Synchronization," *IEEE Transactions on Communications,* vol. 61, no. 6, pp. 2546 - 2556, 2013.

[25] F. Wu and M. Abu-Rgheff, "Time and Frequency Synchronization Techniques for OFDM Systems Operating in Gaussian and Fading Channels: A Tutorial," in *Postgraduate Symposium on the Convergence of Telecommunications, Networking and Broadcasting*, Liverpool, 2008.

[26] Y. Abdelkader and E. Jamal, "Optimal Spacing Design for Pilots in OFDM Systems over Multipath Fading Channels," in *IEEE Transactions on Communications,* vol. 61, no. 6, pp. 2546-2556, 2010.

[27] A. Khatter and P. Goyal, "Design and Analyze the Various m-sequences Codes in Matlab," *International Journal of Emerging Technology and Advanced Engineering,* vol. 2, no. 11, pp. 125-129, 2010.

[28] [Online].Available:http://www.gaussianwaves.com/2010/09/maximum-length sequences-m-sequences-2/. [Accessed 16 December 2014].

[29] M. Mansour, "Optimized Architecture for Computing Zadoff-Chu Sequences with Application to LTE," in *Global Telecommunications Conference*, Honolulu, 2009.

[30] S. Budisin, "Decimation Generator of Zadoff-Chu Sequences," in *Sequences and Their Applications (SETA)*, Paris, 2010.

[31] P. Moose, "A Technique for Orthogonal Frequency Division Multiplexing Frequency Offset Correction," *IEEE Transactions on Communicaions,* vol. 42, no. 10, pp. 2908-2914, 1994.

[32] T. Schmidl and D.Cox, "Robust Frequency and Timing Synchronization for OFDM," *IEEE Transactions on Communications,* vol. 45, no. 12, pp. 1613-1621, 1997.

[33] M. Morelli and U. Mengali, "An Improved Frequency Offset Estimator for OFDM Applications," *IEEE Communications Letters,* vol. 3, no. 3, pp. 75-77, 1999.

[34] H. Minn, P. Tarasak and V. Bhargava, "OFDM Frequency Offset Estimation Based on BLUE Principle," in *Vehicular Technology Conference*, Vancouver, 2002.

[35] Z. Cvetkovic, V. Tarokh and S. Yoon, "On Frequency Offset Estimation for OFDM," *IEEE Transactions on Wireless Communications,* vol. 12, no. 3, pp. 1062-1072, 2013.

[36] D. Huang and K. Letaief, "Carrier Frequency Offset Estimation for OFDM Systems Using Null Subcarriers," *IEEE Transactions on Communications,* vol. 54, no. 5, pp. 813-823, 2006.

[37] S. Kandeepan and S. Reisenfeld, "Frequency Error Correction for OFDM based Multicarrier Systems and Performance Analysis," in *International Conference on Information and Communication Systems (ICICS)*, Bangkok, 2005.

[38] H. Abdzadeh-Ziabari and M.Shayesteh, "Integer Frequency Offset Recovery in OFDM Systems," in *Asia-Pacific Conference on Communications (APCC)*, Jeju Island, 2012.

[39] D. Toumpakaris, J. Lee and H.Lou, "Estimation of Integer Carrier Frequency Offset in OFDM Systems Based on the Maximum Likelihood Principle," *IEEE Transactions on Broadcasting,* vol. 55, no. 1, pp. 95-108, 2009.

[40] M. Ghogho, A. Swami and P. Ciblat, "Training Design for CFO Estimation in OFDM over Correlated Multipath Fading Channels," in *Global Telecommunications Conference*, Washington, 2007.

[41] A. Pelinković, S. Djukanović, I. Djurović and M. Simeunović, "A Frequency Domain Method for the Carrier Frequency Offset Estimation in OFDM Systems," in *8th International Symposium on Image and Signal Processing and Analysis (ISPA)* , Trieste, 2013.

[42] S. Yi, L. Ming-ming, G. Ya-nan, C. Jia-fu and W. Guang-xing, "Joint OFDM Synchronization Algorithm Based on Special Training Symbol," in *International Conference on Communications and Mobile Computing*, Shenzhen, 2010.

[43] L. Nasraoui, L. Atallah and M. Siala, "An Efficient Reduced-Complexity Two-Stage Differential Sliding Correlation Approach for OFDM Synchronization in the AWGN Channel," in *Vehicular Technology Conference*, San Francisco, 2011.

[44] L. Nasraoui, L. Atallah and M. Siala, "An Efficient Reduced-Complexity Two-Stage Differential Sliding Correlation Approach for OFDM Synchronization in the Multipath Channel," in *IEEE Wireless Communications and Networking Conference*, 2012.

[45] Omar R. Al-Sammarraie and Mohamed G. El-Tarhuni, "Double-dwell frequency synchronization in OFDM signals," in *Communications, ACTA Press*, 2012.

[46] W. Chin, "Blind Symbol Synchronization for OFDM Systems Using Cyclic Prefix in Time-Variant and Long-Echo Fading Channels," *IEEE Transactions on Vehicular Technology,* vol. 61, no. 1, pp. 185-195, 2012.

[47] X. Ma, C. Tepdelenliglu and G. Giannakis, "Consistent Blind Synchronization of OFDM Transmissions using Null Sub-carriers with Distinct Spacings," in *Third IEEE Signal Processing Workshop on Signal Processing Advanceces in Wireless Communications*, Taiwan, 2001.

[48] S. Sameer and R. Kumar, "A Low Complexity Null Subcarrier Aided Frequency Offset Estimation Technique for OFDM," in *Vehicular Technology Conference (VTC)*, Singapore, 2008.

[49] Y. Liu and Z. Tan, "Carrier Frequency Offset Estimation for OFDM Systems using Repetitive Patterns," *Radio Engineering,* vol. 21, no. 3, pp. 823-830, 2012.

Vita

Nour Kousa was born in November 1988 in Fujairah, UAE. She received a Bachelor of Science degree (honors list) in Electrical Engineering from Ajman University of Science & Technology in 2010. She then received a graduate teaching assistantship to join the Master of Science in Electrical Engineering program at the American University of Sharjah. She was involved in lab supervision and conducting research in the area of frequency synchronization for OFDM systems. Her work has been accepted for publication in the 2015 International Conference on Communications, Signal Processing, and Their Applications (ICCSPA15) to be held in Feb. 2015 in Sharjah, UAE.